Effects of microstimulation and ketamine anesthesia on neural responses in somatosensory system: a case for pairwise correlation method for data analysis

A thesis submitted to the faculty of
The School of Graduate Studies,
State University of New York,
Downstate Medical Center,
In partial fulfillment of the requirements
For the degree of Doctor of Philosophy
by

Anna Rozenboym

Research Sponsor: John K. Chapin, PhD

February 12, 2009

Program in Neural and Behavioral Science
Department of Physiology and Pharmacology
School of Graduate Studies
State University of New York

The thesis submitted in partial fulfillment of the degree of Doctor of Philosophy

by **Anna Rozenboym**

is accepted by this Examination Committee of the Faculty

of the School of Graduate Studies

February 12, 2009

Mark G. Stewart

John K. Chapin

Robert K.S. Wong

Stephen T. Onesti

Jeremy D. Coplan

Contents

List of Figures and Illustrations

List of Figures and Illustrations

List of Abbreviations

BMI – brain machine interface
CPS – central pain syndrome
CPSP – central post stroke pain
ERP – event related potential
fMRI – functional magnetic resonance imaging
HFO – high frequency oscillation
ISI – interspike interval
LFP – local field potential
LIP – lateral interparietal area
LT – low threshold
MEG – magnetoencephalograph
MIP – medial interparietal area
MR – multireceptive
MU – multiunit
MUA – multiunit activity
NS – nociceptive specific
PF – projection field
PV – parietal ventral area
PR – parietal rostral area
PSTH – poststimulus time histogram
RF – receptive field
RA – rapidly adapting fibers
SI – primary somatosensory cortex
SII – secondary somatosensory cortex
SA – slowly adapting fibers
SEF – somatosensory evoked magnetic field potentials
SEP – (somato)sensory evoked potentials
SSEP – somatosensory evoked potential
SU – ingle unit
VIP – ventral interparietal area
VP – ventroposterior nucleus of thalamus
VPI – ventroposterior inferior nucleus of thalamus
VPL – ventroposterior lateral nucleus of thalamus
VPM- ventroposterior medial nucleus of thalamus
VMpo – posterior ventral medial nucleus
VPS - ventroposterior superior nucleus of thalamus
VS – ventral somatosensory area

Abstract

The neurophysiology of the somatosensory system has been under investigation for decades. The coding properties of neural populations and single units in cortical and subcortical regions have been characterized extensively using electrophysiology. Tactile stimulation produces evoked responses in the thalamus and cortical regions dedicated to processing of sensory information. The ability to evoke naturalistic neural responses as well as tactile perceptual experiences by means of microstimulation in the absence of real stimulus presented to the periphery is imperative for the development of a sensory neuroprosthesis. Three specific aims were pursued in the present study: 1. The development and validation of a novel assessment technique to quantify sensory evoked responses. 2. The investigation of effects of ketamine anesthesia on the cortical evoked responses. 3. The assessment of the feasibility of microstimulation of Ventroposterior Lateral (VPL) nucleus of the thalamus as a way to produce naturalistic responses in the primary somatosensory cortex.

Brief tactile stimulation of various hand locations produces characteristic responses in both thalamic and cortical multi-neuron populations. These responses were used to create somatotopic maps of the hand regions in awake animals with chronically implanted electrode arrays in the SI cortex and in anesthetized animals during acute preparations.

In the first Aim, method based on the analysis of correlation was developed to compare the firing recorded on individual electrodes during different stimuli presentations to determine which neural populations showed most activation during an evoked response. The procedure required relatively short duration of stimulation sessions.

The effects of anesthesia on neural coding were studied in the second Aim using ketamine anesthetized monkeys. Ketamine anesthesia is easily induced, relatively short lasting, and generally safe. In awake chronically implanted monkeys properties of neural responses to tactile stimulation were assessed. Receptive fields (RF) corresponding to five digits were identified using recordings from an electrode array placed in area 1 of SI. Cortical projection fields (PF) representing signal flow from each receptive field were identified. Neural responses under ketamine anesthesia were reassessed using the same mapping techniques. The responses recorded during the maintenance phase of anesthesia were similar to responses evoked under awake condition. Most changes in the neural responses occurred during induction and recovery phases. Overall, ketamine produced responses of shorter duration compared to the awake condition.

In the final Aim, isofluorane/fentanyl anesthetized monkeys had microelectrode arrays acutely implanted in the VPL thalamus and area1, 3b, and 2 of SI. Recordings were used to estimate the sizes of PFs in the thalamus and cortex. Thalamic neural representations were associated with RFs that typically spanned several digits, while cortical recordings were associated with smaller RFs. Microstimulation of the VPL (1ms single pulses, 50μA) resulted in the activation of somatotopically appropriate cortical neural ensembles. The responses in the VPL and cortex were characterized by the presence of High Frequency Oscillations (HFO) (up to 800Hz). The presence of the HFOs was observed following both tactile and electrical stimulation.

In summary, techniques for analyzing evoked multiunit responses were developed and used to explore cortical and thalamic responses to tactile stimulation, the effects of

ketamine anesthesia on such responses, and parameters for thalamic stimulation to simulate tactile “sensation” in cortex.

Introduction

The sense of touch is imperative for the development of adaptive capabilities of any animal. From the early stages of the development humans experience their environment through interactive tactile sensations: from feeding to walking, to object recognition. By constantly experiencing various objects and surfaces with their appendages humans are building a database of most things that are contained in their proximal environment. The more objects are experienced through the touch the greater facilitation of the subsequent interactions with the same objects is obtained. Using this learning experience humans are able to be visually guided in their interactions with the environment: by looking at the object or a surface necessary associations or expectations are evoked and most of the computations are made before the execution of the motor command.

Once the information flow transmitting tactile sensory data is disrupted this life experience of sensing becomes hindered. People with the severe injury to the spinal cord or the periphery loose both motor control of the limbs and the sensory feedback. Studies conducted under the umbrella of Brain Machine Interface (BMI) research aim at utilization of motor commands produced by spared brain regions in order to reinstate mobility in otherwise paralyzed patients. If the motor regions in the brain are intact, the neural recordings of the activity underlying motor planning and execution become obtainable. These motor commands generated in the motor cortex could be decoded into a trajectory of movement of a robotic arm or a neuroprosthetic device.

The information relevant to the position or location in space should be relayed back to the brain in order to keep track of the limb and also to facilitate further movement

execution (error correction, learning). In healthy individuals proprioceptive system deals with this on and offline analysis. Further, if one is to reach and grasp an object, the object has to be detected and forces exerted on this object need to be assessed. This sensory tactile feedback is abolished in most paralyzed patients and so far none of the assistive devices were made to reinstate this ability to perceive through the sense of touch. This gap in the development of the neurprosthesis has to be filled in order to create a fully functioning complete system. The present study delineates issues pertaining to the investigation of a possibility of reinstatement of tactile perception by means of electrical microstimulation of the somatosensory brain regions. The overall goal is to provide sensory information by means of electrical intracranial stimulation such as it will be perceived as a normal touch.

The advances in the field of BMI research (Chapin, et al., 1999, Wessberg et al., 2000; Carmena et al, 2003, Lebedev and Nicolelis, 2006) make construction of a fully integrated neuroprosthetic system more feasible. The electrical stimulation of the cortical brain regions has been known to evoke sensory percepts in humans (Penfield and Boldrey, 1937). The microstimulation of human sensory cortex is possible during neurosurgery such as a placement of Deep Brain Stimulator for treatment of symptoms of Parkinson's disease. Current reports indicate that microstimulation in patients produces parasthesias, such as tingling sensation (Kiss et al., 2003) and in some cases more naturalistic tactile and pressure sensation (Dostrovsky et al., 1993; Ohara et al., 2004). Following amputation microstimulation has been known to generate phantom sensations (Davis et al., 1998).

Perceptual characteristics associated with microstimulation are more difficult to ascertain from animal studies. On the other hand, in animals responses to electrical stimulation could be recorded from various levels of the somatosensory pathway through chronically or acutely implanted electrodes. The characterization of such responses of neural populations transmitting sensory information could aid in identification of optimal target stimulation sites and in assessment of feasibility of development of a sensory neuroprosthesis. Animal species with the somatosensory system architecture similar to humans are sought after by researchers. Nonhuman primates are known for their advanced motor and sensory capabilities. Their participation in such studies is of great value.

Aims

The ultimate goal of the present study was to assess the usefulness and effectiveness of electrical microstimulation of subcortical regions for the development of a sensory neuroprosthesis. The main idea was to investigate whether electrical stimulation in the brain could activate neural circuitry implicated in the processing of naturally occurring tactile stimuli.

Cortical evoked responses following tactile and microstimulation were compared. This analysis involved investigation of spatiotemporal characteristics of neural responses. One of the goals of the present study was to develop a novel and relatively simple methodology for analysis of neural recordings, specifically a method that would include assessment of both temporal and spatial components. Further, this analysis had to be shown to be both reliable and valid.

Work with live animals, especially, nonhuman primates requires many man hours invested into habituation and training of the animals. Certain experiments do not require animals to be fully awake. These experiments could be conducted on temporarily sedated or anesthetized animals. For example, experiments involving electrical stimulation that might produce aversive reaction or studies examining integrity of newly developed technology, such as multielectrode arrays. The sedation or anesthesia used for such experiments should be easily administered, relatively short lasting, and associated with minimal risks and side effects. For anesthetic agents to be utilized efficiently their effect on information processing has to be established. The optimal type of anesthetic agent would produce minimal changes in activation properties of neurons.

Three specific research questions were addressed in the present study.

1. Does analysis of correlation help to define neural populations responding to specific stimuli? In order to answer this question both reliability and validity of this method were assessed on several unrelated data sets. Experiments involving comparison of neural recordings during tactile stimulation in awake and anesthetized animals were used as well as sessions investigating effects of microstimulation on cortical responses. This method of analysis was shown to be useful and easily applied to various experimental conditions. The results of this investigation are summarized in Results I section.

2. Does Ketamine anesthesia induce changes in somatosensory evoked responses? This set of experiments was conducted on chronically implanted animals. Evoked responses to tactile stimuli administered to various hand locations were analyzed. Different states of anesthesia such as induction, maintenance, and recovery were identified using behavioral measures (changes in motor responses, eye movements, and withdrawal reflexes). These states were characterized by specific patterns of neural responses. These activation patterns were compared to awake condition in the same animal. The similarity or dissimilarity of responses between states was assessed using correlation analysis. Further, investigation concentrated on closer examination of specific temporal patterns of responses. An early response (15-17ms latency) reflected activation of the basic somatosensory pathway and a later response (220ms latency) may reflect more complex processing. The findings are summarized in Results II section.

3. Does microstimulation of the thalamus produce naturalistic responses in cortical neural populations? This series of experiments aimed at comparison of the patterns of neural responses elicited by natural tactile stimulation on the skin and microstimulation

of VPL thalamus (to a lesser extend SI cortex). The experiments were conducted on acutely implanted animals. The neural responses to cutaneous stimuli delivered to hand and arm regions were recorded simultaneously from thalamus and SI cortex using microelectrode arrays. The characteristic spatiotemporal patterns of these responses were analyzed. Upon assessment of the neural responses to natural stimulation, electrical microstimulation of the VPL and/or SI was delivered. The intensity of stimulation was optimized to elicit neural responses in the cortex comparable to those obtained under natural stimulation conditions. This was assessed through comparison of both spatial and temporal characteristics of neural activity for both conditions.

Background

Somatosensory system: structure

The organization of the somatosensory system of mammalian brain follows a general scheme characterized by the afferents originating in the peripheral receptors and terminating on neurons in the spinal cord or brain stem that continue to transmit information to the relay nuclei in the thalamus which in their order project to different areas of neocortex. The cortical somatosensory areas are heavily interconnected and are known to project to motor cortex and other cortical areas (for example, representing other sensory modalities) as well as to subcortical structures (Mountcastle, 2005). Somatosensory system as any developed (in this case throughout the course of evolution) and fully integrated system includes mechanisms of feedback communication. These feedback loops are numerous and constitute a large proportion of projections within somatosensory system (Kaas et al., 2002).

Afferent projections include those from several types of mechanoreceptors found in the skin that register and transmit information pertinent to detection and discrimination of tactile stimuli, muscle-spindles and joint receptor that signal movement and position, and receptors specializing in transduction of pain and temperature signals (Mountcastle, 2005). On all levels of the somatosensory pathway somatotopic representation of the skin is conserved. Density of innervation determines the size of the area and neural volume allocated to the representation (projection field – PF) of a particular skin location. For example, glabrous skin of the fingers in primates is known for high receptor density therefore it is not surprising that the afferents from those receptors converge on numerous cell populations in the brain stem, thalamic, and cortical somatic regions. This type of

organization relates to the issue of acuity of sensory processing (for example, two point discrimination). It is the functional relevance of the skin location that determines the extent of neural representation. In human and non-human primates most of the tactile information related to the processing of the surroundings requires some contact with a hand. In animals that are not capable of extensive manual manipulations, mouth and lips are more involved in the exploratory behavior. The following overview of the somatosensory system will concentrate on pathways involved in sensory tactile discrimination.

Glabrous skin is innervated by three classes of receptors: mechanoreceptors, thermoreceptors, and nociceptors corresponding to the processing of tactile, temperature, and pain properties of a stimulus (Mountcastle, 2005). The receptors within each class are distinguished based on their anatomical and functional characteristics. In the mechanoreceptor class Merkel cells and Ruffini endings are associated with the slowly adapting (SA) afferents SAI and SAII while Meissner corpuscles and Parcininian corpuscles are associated with the rapidly adapting (RA) fibers RAI and RAII (Kaas et al., 2002). Currently, there is no support in the literature for the presence of Ruffini endings in the monkey glabrous skin. Hairy skin also houses hair follicle mechanoreceptors. The SA and RA afferents ascend in parallel and tend to terminate in segregated zones throughout dorsal column-medial lemniscal system. The axons of mechanoreceptors are of a large diameter, heavily myelinated, and are characterized by high conducting velocities of up to 75m/sec. On the other hand, afferents carrying information on pain are of smaller diameter, show little or no myelination and have much

lower conducting velocities in the range of 0.5 (C-fibers) to 40m/sec (A-delta fibers) (Mountcastle, 2005).

In monkeys, afferents from the mechanoreceptors in the skin enter the spinal cord and project in the somatotopic manner to the dorsal column nuclei in the lower brain stem (Florence et al., 1989; Coq et al., 2000). SA and RA inputs to gracile, cuneate, and trigeminal nuclei are relayed to the ventroposterior nucleus (VP) of the thalamus. Separate groups of neurons in the VP thalamus are activated by SA and RA fibers (Dykes, 1982; Dykes et al., 1981). Afferents originating from the face regions terminate in the VPM –medial subnucleus of VP and those representing the rest of the body terminate in the VPL- lateral subnucleus. Separation of VPL from VPM is identified by the presence of a fiber septum with sparse neuronal representation (Kaas et al., 2002). VPL and VPM project to the primary somatosensory (SI) cortex to area 3b, less strongly to area 1, and in lesser degree to area 2. In squirrel and owl monkeys as much as 20% of the VP neurons were found to project to both area 3b and area 1 (Lin et al., 1979; Cusick et al., 1985). In squirrel monkeys, projections from area 3b terminate in layer IV of the cortical area 1 while projections from VPL synapse on the cells in more superficial layers (Jones et al., 1975).

Muscle spindle receptor inputs of the dorsal column nuclei – external cuneate nucleus - are relayed to the ventroposterior superior nucleus (VPS) located dorsal to VP (Kaas et al., 2002). VPS projects to area 3a and area 2 of SI. Spinothalamic terminals relay to the ventroposterior inferior nucleus (VPI). VPI is located ventral to VP. VPI projects mostly to secondary somatosensory cortex SII and parietal ventral area (PV) (Krubitzer and Kaas, 1992). The projections from VPI terminate in the superficial rather

than in middle cortical layers as do projections from VP (Raussell and Jones, 1991b) which might point to different mechanisms of activation and signal processing. Spinothalamic inputs responsive to pain and temperature are also found in the posterior ventral medial nucleus – VMpo which is located more caudally in the thalamus (Craig et al., 1994).

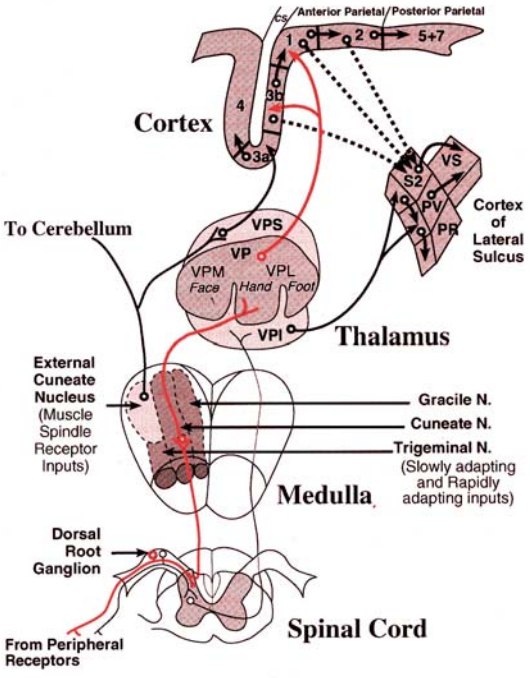

Illustration 1. Somatosensory pathway.
Modified from Kaas et al., 2002, p.9, Fig. 1.4

The anterior parietal cortex of monkeys – the primary somatosensory cortex (SI)- contains 4 areas that extend mediolaterally: area 3a, 3b, 1 and 2. These are strips of variable widths that contain somatotopic representations of the body (Merzenich et al., 1978; Kaas et al 1979). In monkeys, area 3b is confined to posterior aspect of the wall of central sulcus and the most rostral area of the post central gyrus. Area 3b was found to be the most homologous (based on staining procedures and electrophysiological recordings) to the SI cortex in lower animals such as rats (Kaas, 1983). Jain et al (1998) report area

3b to be densely myelinated and subdivided by narrow myelin-light septa into digit and pad representations. In the hand representation of area 3b of monkeys, segregation of SA and RA inputs is observed (Sur et al., 1984).

Area 1 is located caudally to area 3b and also contains body representation (Kaas et al., 1979; Sur et al., 1982; Felleman et al., 1983b). Cutaneous information is delivered through connections from both VPL and area 3b (Cusick et al., 1985).

Area 3a lies rostrally to area 3b in the central sulcus. It receives mostly proprioceptive inputs from the VPS (Cusick et al., 1985). Some cutaneous receptor information is transmitted to area 3a from area 3b (Krubitzer and Kaas, 1990). Some of the area 3a outputs terminate in primary motor and premotor areas (Huerta and Pons, 1990; Darian-Smith et al., 1993; Huffman and Krubitzer, 2001) indicating integration of proprioceptive and cutaneous information into the motor processing.

Area 2 neurons generally respond to light touch and manipulations involving activation of deep receptors (Pons et al., 1985). Area 2 is interconnected with area 3a and receives inputs from area 1 (Pons and Kaas, 1985). Most proprioceptive inputs to area 2 ascend from VPS. Area 2, in its turn, projects to posterior parietal cortical regions: area 5 and area 7.

Other areas involved in the processing of somatosensory information are localized to the parietal cortex of the lateral sulcus and are subdivided into areas SII, PV, ventral somatosensory area (VS), and parietal rostral area (PR). All areas of SI project to areas SII and PV (Krubitzer and Kaas, 1990). In posterior parietal cortex areas 5, 7, medial, (MIP), lateral (LIP), and ventral (VIP) areas of interparietal sulcus are associated with the

multimodal processing and integration involving visuomotor coordination (Andersen et al., 1990, 1997; Lewis and Van Essen, 2000).

Somatosensory system: function

Somatosensory processing involves both serial and parallel arrangements. The high degree of cortical as well as subcortical interconnections adds to the complexity of the system. There are various mechanisms of activation and modulation of responses. Due to the high volume of feed-forward and feedback projections the neural activity in each of the brain areas undergoes multiple transformations. This exceedingly regulated network is integrated with other systems which add on another dimension of complexity.

The mechanoreceptors specialize in the identification of particular types of stimuli and when stimulated are associated with a particular sensory experience. The afferents originating from RAI Meissner corpuscle carry information on movement, displacement, and velocity and respond the most to flutter stimulation of 20-30 Hz (Mountcastle, 2005). RAII fibers transmit signals pertaining to the contact, vibration (250Hz), and movement of the stimulus. SAI afferents are implicated in conduction of signals relating to contact, pressure, and movement characteristics of a stimulus.

Generally, VP maps a systematic representation of the contralateral part of the body with some representation of ipsilateral oral cavity (Rausell and Jones, 1991a). VPS contains a separate representation of the body. VPI was shown to map contralateral body although the representation is not as fine as seen in VP (Apkarian and Shi, 1994). Neurons in VPI are responsive to both noxious and innocuous (cutaneous) stimuli.

Both primary and secondary somatosensory cortical regions possess map-like topographical organization (Woolsey et al., 1958). Neighboring receptors from the

periphery project to neighboring cortical locations, so that the spatial position of the neural activation represents or is involved in encoding of certain features or nature of a stimulus (Peterson and Diamond, 2001). Using electrophysiological methods, namely single-electrode recordings, highly organized representations of individual digits and pads has been documented in SI regions of the primates (Kaas, 1997). In humans, fMRI studies were employed to observe distinct representations in SI (Maldjiian, et al., 1999).

Area 3b has been reported to be the only somatic cortical area responding well to the cutaneous stimulation in all primates (Kaas et al., 2002). Light tapping of body parts is usually required in order to activate area 3a cells (Huffman and Krubitzer, 2001). Somatotopic representation of the deep receptors is observed in area 3a.

The body map of the receptor representation in area 1 is a mirror image of the map in area 3b (Merzenich et al., 1978; Nelson et al., 1980). For example, in area 3b digit representation from D1 (thumb) to D5 (pinkie) is organized mediolaterally and digit to pad (palm) representation lies rostro-caudally. At the junction of area 3b and area 1, pad representations from area 3b would neighbor with pad representations of area 1. Digits in area 3b would be found more rostral to the junction and digit representations in area 1 more caudally to the junction. In electrophysiological studies this feature of cortical maps aids in guidance of electrode placements to the correct cortical areas of interest.

In monkeys lateral somatosensory cortex in the lateral sulcus has been divided in at least 2 regions: SII and PV (parietal ventral area) based on anatomical (Burton et al., 1995) and electrophysiological (Krubitzer and Kass, 1990; Krubitzer et al., 1995; Qi et al., 2002) evidence. Each region contains a complete representation of the body surface (Krubitzer and Kass, 1990). In humans this subdivision is supported by the surface

(Mima et al., 1997), intracortical (Frot and Mauguiere, 1999, Barba et al., 2002) somatosensory evoked potentials (SEP) and fMRI (Disbrow et al, 2000) findings.

The study of the RF size variability among somatosensory cortical areas was pioneered by Duffy and Burchfiel (1971) and Sakata et al (1873). They found that RFs of area 5 neurons were larger and more complex than the RFs in SI. These results led to extensive investigation into the interregional difference of RF representation. Up to date literature confirms a progressive increase in complexity of RFs along rostro-caudal axis in the postcentral gyrus. Area 3b is characterized by rather small Receptive Fields (RF) (skin representations in the form of neural signals). Receptive fields in area 1 tend to be larger than in area 3b. In area 3a the RFs are large spanning multiple digits. Area 2 RFs tend to be larger than in area 1 and area 3b and often span several digits. The complexity of the RF properties increases from area 3b to 1, 2 and 5 (Hyvarinen and Poranen, 1978; Iwamura et al, 1980, 1983, 1994, Sur 1980; Sur et al., 1985).

The comparative analysis of temporal relationship of activation among somatosensory cortical areas has been employed as a mechanism of elucidation of direction of the information flow in the somatosensory system. Specifically, it is widely utilized as a tool for distinguishing between serial and parallel modes of somatosensory processing.

It has been shown that transection of afferents in the dorsal columns of the spinal cord, sparing spinothalamic tract with relay localized to the VPI, eliminates firing by neurons in all SI cortical areas (Jain et al., 1997, 1998, 2001a). Based on this evidence, it has been concluded that VPI is not capable of activation of SI but is rather implicated in the modulation of the activity in these areas. Both human (Wood et al., 1985; Allison et

al., 1989) and monkey (McCarthy et al, 1991) studies report that the earliest response to median-nerve stimulation takes place in area 3b as recorded by somatosensory evoked potentials (SEPs) and somatosensory evoked magnetic field potentials (SEFs). Anatomically it has been established that in monkeys area 3 projects predominantly to area 1 (Vogt and Pandya, 1978). Electrophysiologcal studies in monkeys showed lack of responsivity in area 1 following ablation of area 3b (Garraghty et al, 1990a). Intracranial SEP (Allison et al, 1989) and magnetoencephalographic (MEG) recordings (Inui, et al, 2004) indicate that area 1 (18ms) activation follows area 3b (14ms) activation by about 4 ms. There are sparse projections from thalamus to area 1 (Jones and Powell, 1970; Nelson and Kaas, 1981). Studies indicate that lesion to area 3b abolishes evoked responses in area 1 in squirrel and owl monkeys (Garraghty et al., 1990b). These findings suggest that inputs from VPL might play a rather modulatory function, while area 3b inputs would be implicated in the activation of area 1 (Kaas et al., 2002). Some MEG studies (Forss et al., 1994; Hoshiyama et al., 1997) report activation of area 5 to have long latency (50-100ms) while others (Inui, et al 2004) report much earlier onset of the activity (22ms). These finding are consistent with the serial processing of information.

Inui et al, 2004 report simultaneous activation of area 4 (primary motor area) and area 3b following electrical stimulation to the periphery in humans. These results illustrate that area 4 receives separate thalamic inputs and does not require inputs from area 3b to get activated. Later responses in area 4 are proposed to be modulated by area 3b, 1 and 2. There are only very weak projections from area 3 b to area 4 (Vogt and Pandya, 1978; Darian-Smith et al., 1993; Burton and Fabri, 1995). Area 4 is mainly driven by the thalamic inputs (Ghosh et al., 1987; Stepniewska et al 2003) although it is

also receiving projections from areas 1 and 2 (Ghosh et al, 1987; Darian-Smith et al, 1993; Burton and Fabri 1995).

Area 3a receives inputs mostly from the deep tissues (Heath et al, 1976). The theory of hierarchical cortical somatosensory processing posits that serial intercortical connection of the increasingly complex representations result from convergence of multiple inputs to single neurons in the more caudal regions (Review Iwamura, 1998). Both anatomical (Vogt and Pandya, 1978; Burton and Sinclair, 1996; Burton et al, 1995) and physiological (Pons et al., 1987, 1992) studies have provided support for serial intercortical processing between areas within SI and between SI and SII.

Serial processing between SI and SII in monkeys is supported by some anatomical (Jones and Powell, 1970, Friedman et al, 1980) and electrophysiological (Pons et al, 1987, 1992; Garraghty et al, 1990b) studies. However studies in marmosets indicate parallel processing of tactile signals by SI and SII (Zhang, et al., 2001a,b). In humans the results of MEG studies present conflicting results with some reports landing support for the serial (Hari et al., 1984., Elbert et al, 1995., Disbrow et al., 2001; Inui, et al., 2004) processing in SI and SII and others documenting simultaneous activation in these regions (Karhu and Tesche, 1999). MEG recordings enable analysis of activity from many sensory cortical areas. According to Inui, et al, 2004 differences in response latencies between areas 3b, 1, 5, SII, and posterior parietal cortex support a hypothesis of serial processing in the somatosensory cortex in human.

Neural responses: VPL

High initial population firing synchrony is reported in the sensory thalamus in rats (Pinto et al, 1996; Muthuswamy, et al, 1999; Temereanca and Simons, 2003). These reports propose that synchronous thalamic firing enhances transmission of relevant information to the sensory cortex. In rat and cat VPL, nearby thalamo-cortical neurons show correlated firing (in response to cutaneous stimulation of common regions of their receptive fields) over time intervals less than 5ms (Alloway et al 1995). Synchronization of thalamic outputs has been reported to produce enhancement in cortical responsiveness (Roy and Alloway 2001). The activity of the layer IV cortical neurons appears to be determined by the firing rates of populations of thalamic neurons at least during the early response phase (Pinto et al 2000). Using single unit recordings stimulus amplitudes and periods were shown to influence the pattern of neural responses in the VPL (Muthuswamy et al 1999).

The early component of the thalamic response showed consistent variations with stimulus parameters (Temereanca and Simons 2003). Such stimulus parameters as location, direction of movement, and velocity are differentially encoded by the synchronous thalamic activity in thalamic barreloids as evidenced from the Local Field Potential (LFPs) and multiunit activity (MUA) recordings. Further, the firing synchrony is concluded to serve as a mechanism for encoding information in the thalamus.

Later components of the thalamic responses are thought to coincide with arrival of inhibitory inputs from thalamic reticular nucleus and excitatory inputs from the cortex as concluded from the studies on rat whisker thalamic representation (Temereanca and Simons 2003). These later responses were reported to be variable and poorly predicted by

stimulus parameters such as location, direction, and velocity. Facilitation of corticothalamic activity has been shown to affect the later component of the thalamic LFP. Therefore, thalamic firing synchrony evoked by lemniscal inputs might be modulated by cortical feedback.

Ergenzinger et al. (1998) manipulated corticofugal projections transmission by injecting the NMDA receptor antagonist D-APV to the area 3b hand region in monkeys. Chronic (lasting up to 5 months) and acute injection produced suppression of activity in area 3b and enlargement of RFs in the VPL. Thalamic RF enlargement indicates a 'top-down' modulation of signal processing. The authors propose the mechanism leading to enlargement of VPL RFs to be mediated through a loss of excitatory corticothalamic inputs on inhibitory neurons in the VPL or thalamic reticular nucleus.

Neural responses: Synchrony and Oscillations

Tactile stimuli tend to produce tight time-locked responses throughout somatosensory system. There is a high degree of correlation of neural responses between stimulus- induced activity in PNS and CNS as well as between brain regions encoding somatosensory stimuli: brainstem, thalamus, SI, and SII (Lee and Ebner 1992; Alloway et al., 1993, 1994; Johnson and Alloway 1994;1996; Vickery et al., 1994; Gynthler et al., 1995; Swadlow 1995; Nicolelis et al., 1998; Zacharian et al., 2001; Roy and Alloway 2001). Furthermore, simultaneous multiunit recordings in the brainstem, ventrobasal thalamus, SI and SII cortex have indicated that neighboring neurons with similar RF and submodality properties are firing simultaneously for short periods following tactile stimulation onto periphery (Metherate and Dykes 1985; Alloway et al, 1995; Swadlow et

al, 1998; Roy and Alloway 1999, 2001; Nunez et al 2000; Alloway et al, 2002). The synchronization appears to be more prevalent in cat SII cortex than in SI (Alloway et al, 2002). The higher degree of synchronization in SII could be explained in terms of greater overlap in the RFs or in terms of the functional specificity of SII namely detection of moving stimuli (Alloway et al 2002). Alloway et al (2002) concluded that local pairs of neurons in SII with similar properties such as directional preference and RF representation exhibit tight synchronization. The degree of this synchronization depends on cortical proximity and RF overlap among these neurons.

Stimulus induced simultaneous firing in cortical areas is consistently reported in several sensory systems. It brings out a question whether oscillations are necessary for mediating such synchronization (Shadlen and Movshon, 1999). Some studies implicate gamma frequency oscillation in the synchronization (Murphy and Fetz 1996a,b) of responses– temporal binding hypothesis, while others report only marginal oscillatory activity evident in the cortical responses (Bair et al., 1994; Nowak et al, 1995, Roy et al 2001).

The function of oscillations in the sensory system has generated much debate. Gamma frequency (35-45Hz) oscillations in particular have been proposed to be necessary for synchronization of distinct cortical areas involved in sensory processing (Singer, 1999). However, Roy et al. (2001) argue that the gamma range oscillations observed in the cat SI and SII cortices is not necessary for the synchronized activation of these areas. The authors report high degree of the synchronization (within < 5 ms) between these areas upon light cutaneous stimulation in the absence of underlying unifying oscillations.

Valencia et al. (2006) explain appearance of high frequency oscillations (HFOs) in the somatosensory evoked potentials (SSEPs) following median nerve electrical stimulation as having a phase-resetting function. HFOs are believed to serve as a time-locking mechanism enhancing signal detection (Valencia et al., 2006). HFOs could be thought of as marking the firing of neurons responding to the stimulation (Hanajima et al., 2004) or as providing time-locked framework for these neurons. There is no need to change frequency and amplitude of the HFOs – phase shift alone could account for the signal synchronization (Kazantsev et al., 2004). HFO's themselves functionally might not transmit any qualitative information about the stimulus but act as a time-resetter or count mechanism in order for the sensory event to be registered and/or to provide synchronizing mechanism for functional interaction or integration of information between various brain regions (Varela, et al., 2001). Furthermore authors propose that these HFOs do not lead to the emergence of new responses but serve as resetters of ongoing activity so that to time-lock the stimulus and evoked response (Valencia et al., 2006).

Ploner et al. (2006) investigated the dynamics of alpha and beta oscillations during presentation of painful laser and subsequent non-painful electrical stimuli to the periphery in humans. Alpha (8-14Hz) and beta (15-33Hz) rhythms constitute mu –rhythm which shows suppression after presentation of painful stimulus. This suppression was accompanied by an increase in the excitability measured by the response amplitude following presentation of non-painful stimulus. The presentation of painful stimulus is hypothesized to serve alerting function i.e. it modulates cortical activity so that to make sure the successive stimulus is registered properly.

Noradrenergic (NA) locus coeruleus (LC) system has been shown to suppress oscillatory activity in both thalamus and cortex; enhance excitability at thalamic and cortical levels, and to be involved in attentive processes (McCormick et al, 1991; Aston-Jones et al, 2000; Berridge and Waterhouse, 2003) as well as detection of behaviorally relevant stimuli (Downar et al., 2000; Corbetta and Shulman, 2002).

Neural responses: Inhibitory interactions

Multisite stimulation was found to produce both excitatory and inhibitory interactions in barrel cortex of rats. In extracellular and intracellular studies it has been shown that at interstimulus interval of 10 to 20 ms between the presentations of stimulus to the neighboring whiskers produces mostly inhibitory interactions (Simons 1985; Brumberg et al 1996; Higley and Contreas 2003). In awake rats multiple unilateral electrical stimulation of the facial afferent infraorbital nerve produced greatest suppression at ISI of 25 to 50 ms (Fanselow and Nicolelis, 1999). On the other hand synchronous stimuli presentation results in linear and sublinear summation as reported by Simons and Carvell 1989 and Mirabella et al. 2001. The surround inhibition in layer IV, i.e. the inhibition of surrounding cortical regions by the most active cortical region is proposed to facilitate an enhancement of the signal for the principle whisker (Brumberg et al, 1996). The inhibitory interactions could be also viewed as a mechanism for preventing response saturation and maintenance of a dynamic response range under active whisking (Mirabella et al 2001).

In awake rats the behavioral state of the organism was found to influence spatio-temporal characteristics of the neural response. For example, according to Krupa et al.

(2004b) the inhibitory response modes in all layers of barrel cortex were more predominant in actively discriminating animals compared to passively stimulated group. Furthermore, it has been suggested that greater activity during quiet waking state is implicated in the detection of a stimulus, while inhibitory interactions are more important for active discrimination tasks (Moore et al 1999; Fanselow and Nicolelis 1999, Nicolelis and Fanselow 2002; Moore 2004; Castro-Alamancos 2004). Accordingly, the state dependant neural responses exemplify the dynamic nature of sensory information processing.

Neural responses: Ipsilateral and bilateral activation

Sensory information integration plays a crucial role in the processing of tasks requiring bilateral manipulations. There is an increasing volume of generated research on the bilateral integration and ipsilateral representation in the somatosensory cortex. In rats, specifically, neural responses from barrel cortex indicate a cross talk between hemispheres (Pidoux and Varley, 1979). The existence of the interhemispheric connection between rat SI regions has been well documented (Cauller et al. 1998; Koralek et al. 1990; Olavarria et al. 1984; White and DeAmicis 1977). Studies in the rat sensory cortex have shown that inactivation of contralateral hemisphere abolishes responses that would normally be relayed to the ipsilateral hemisphere (Pidoux and Verley 1979; Shuler et al. 2001). Hayama and Ogawa (1997) showed that callosal projections terminate predominantly in the infra-and supra-granular layers of the barrels. These layers are known to have larger – multiwhisker receptive fields than the layer IV and the intercolumnar connections in these layers are more prevalent (Armstrong-James

et al. 1992; Ghazanfar et al. 2000; Schubert et al. 2001). The studies have demonstrated that in anesthetized rats whisker stimulation on either contra- or ipsilateral side evokes responses in the same neuron of layer V – major output path of SI (Shuler et al. 2001) and that in awake animals signals are integrated from both sides - bilaterally in order to perform a tactile discrimination task (Krupa et al., 2001b). Weist, et al (2005) found support for the bilateral integration in layer V of the barrel cortex (SI) in awake rats. In this study, the same single unit (SU) or multiunit (MU) clusters responded to multiwhisker stimulation applied contra, ipsi, or bilaterally. They showed that the bilateral integration extended over 100 ms and that both excitatory and inhibitory interactions were pronounced. The latency of ipsilateral stimulation was around 24msec compared to the contralateral 14 ms while the magnitude of response was largest after bilateral stimulation. When the delay between asynchronously presented bilateral stimuli is around 30 ms the magnitude of excitatory response decreases causing response suppression. The results of the recent study by Rema and Ebner (2005) indicate that following muscimol (selective GABAa receptor agonist – suppresses activity) injection in the ipsilateral barrel cortex of rats responses to the whisker stimulation were diminished in layers II III and IV while levels of spontaneous activity stayed unchanged. This finding was surprising as layer IV has not been shown to have dense calossal projections. Both fast spiking (inhibitory) and regular spiking cells exhibited decreases in activity. Based on the data it was concluded that inactivation of ipsilateral (to the site of stimulation) cortex induces changes in magnitude and latencies of response in the contralateral barrel cortical field. This points to the relative importance of the contribution of the ipsilateral processing in bilateral integration. The authors also note

that clinical literature describes bilateral neurological impairments following unilateral stroke.

Sensorimotor Integration

Human studies on sensorimotor integration tend to employ noninvasive methodology such as: EEG recordings, and event related potentials (SEP, MEG studies). The literature suggests that sensorimotor events involving somatosensory stimuli modulate centro-parietal areas during both execution of these events and during the anticipatory period. In humans cortical events associated with the anticipatory period are investigated using noninvasive methodology such as EEG recordings, event related potentials (SEP, MEG). Negative ERPs (event related potentials) were reported over posterior midline and bilateral central areas during expectation period in a Go/NoGo task involving painful and non-painful stimulations of the left arm cuing right hand movement (Babiloni et al., 2004b, 2005a).

EEG recordings indicate that sensorimotor processing modulates cortical slow delta-theta (2-7Hz), alpha (8-14Hz), beta (15 -33Hz), and gamma (34-45Hz) rhythms (Pfurtscheller and Lopes da Silva 1999). It has been documented that there is a selective increase in the amplitude of alpha event-related desynchronization during anticipatory period preceding only painful sensorimotor events but not non-painful sensorimotor events or pain anticipation lacking motor component (Babiloni et al., 2005a). Studies on expectancy of cognitive and visuomotor events also indicate modulation of alpha rhythms (Babiloni et al., 2004a,; Gomez et al., 2004; Klimesch, 1996,1997; Klimesch et al., 1996, 1998).

Babiloni et al. (2006) showed that functional coupling of EEG rhythms in central and parietal cortical areas increases during anticipatory period preceding both contralateral somatosensory stimulation and motor events. The extent of functional cooperation among brain areas was assessed using the EEG coherence: a normalized measure of the coupling between two signals at any given frequency (Rappelsberger and Petsche, 1988). In their task somatosensory nonpainful electrical stimulation was applied to the index finger (left hand) preceding or simultaneously with the visually cued Go/NoGo motor command (to be executed by the right hand). Sensory stimulation was disassociated from the motor event i.e. it didn't serve as a cue. Anticipatory period was marked by visual presentations to enhance attentive processes. When the somatosensory stimulation was delivered simultaneously with the motor command cue, bilateral centro-parietal activation during but not after the expectation period was observed. On the other hand, on trials involving delayed task, anticipation of somatosensory and visiomotor events increased contralateral – hemisphere specific centro-parietal coupling during their respective anticipation periods. These results suggest that centro-parietal coupling persists not only before presentation of the stimulus leading to an action but also before a "noninformative" sensory stimulus indicating some functional coordination of these areas during the expectation period.

Electrical Stimulation of SI: detection, discrimination

Experiments involving both electrophysiology and behavioral measures of perception, at least the ability to discriminate, serve a guiding role in the investigations into meaningfulness and validity of electrical brain stimulation as means for recreating

normal perceptual experiences. Studies by Romo, et al. (1998, 2000) address this issue in regards to vibro-tactile properties of a stimulus. In the experiments monkeys were trained to discriminate between two frequencies of vibratory stimuli applied to the finger tip using “match to sample” task paradigm. Monkeys were trained to indicate whether experimental stimulus matched the control stimulus. When no-match condition was met, they had to indicate whether experimental stimulus was of higher or lower frequency than control. The neural activity in the cortex was recorded through electrodes placed in area 3b. The neural population recordings were indicative of periodic neural firing in response to the vibratory stimulus. The same electrodes were subsequently used to electrically stimulate the same sites in area 3b. Frequency of pulses of electrical stimulation was matched to the frequency of mechanically administered stimuli. Electrical stimulation was used to substitute either control or experimental stimuli. Typically, monkeys showed accuracy of response comparable to the one obtained under conditions of vibro-tactile skin stimulation. The ability to discriminate between stimuli was retained.

Another recent study by Fitzsimmons et al. (2007) has shown that intracortical stimulation can be used in the form of guiding cues in reaching and grasping task. Owl monkeys were initially trained at the reaching task cued by vibromechanical stimulation to the arms. They were to reach to the box, open the door, and retrieve food. Later, vibromechanical stimulation was substituted by electrical stimulation (in SI) of 150microA at 100Hz. The authors indicate that although the differences in the tasks employed for electrical and mechanical stimulation were minimized, monkeys failed to generalize new stimuli (or percepts thereof) to the already successfully learned task. In the course of several months monkeys acquired new learning and were able to

discriminate between cues based on location representation and temporal order of stimulus trains. The authors further conclude that multichannel microstimulation is a viable method for integration of sensory information into the neural prosthesis.

Issues associated with electrical stimulation of VPL

Several caveats of VPL electrical stimulation are discussed in this section. These issues pertain to the clinical practice of VPL stimulation in human subjects with spinal cord injury and address characteristic features of thalamic responses namely spike bursts. Under normal circumstances, spike bursts (3-8 action potentials with short interspike interval) have been implicated in the synchronization of the activity of neurons within and between thalamic nuclei as well as between thalamus and cortex (Warren et al., 1994; Destexhe et al., 1998; Kim and McCormick, 1998; Steriade et al., 1998; Timofeev and Steriade, 1998). Some reports argue for their involvement in efficacy of thalamo-cortical signaling (Swadlow and Gusev, 2001; Sherman, 2001). For example, the low threshold (LT) calcium spike burst varies with the level of arousal and attention and can be influenced by the anesthesia (Destexhe et al., 1998).

Deafferentation in the form of spinal cord lesioning is a widely used animal model for elucidation of plastic changes in the somatosensory system. Animal models are utilized to investigate various phenomenological findings produced by the studies involving human patients. One such finding is of crucial concern for the implementation of the sensory neuroprostesis. Deafferentation in both human and animals has been reported to induce an increase in the spike burst activity in the thalamus. These bursts are characterized by the presence of high frequency (67-167Hz) spike trains of 3-8 action

potentials. The elevation of the levels of spontaneous spike bursts following lesions has been reported in both the thalamus of animals (Rodin and Kruger, 1984; Albe-Fessard et al, 1985; Weng et al., 2000; Weng et al, 2003) and in humans (Lenz et al, 1987, 1989; Jeanmonod et al, 1993). The importance of these spike bursts in thalamo-cortical processing of sensory information becomes apparent due to the numerous findings indicating their involvement in pain modulation. Human clinical studies report high concentration of spike burst activity in the VPL/VPM regions representing the "painful" part of the body in patients with the lesions (Lenz et al, 1987, 1989). On the other hand, electrical microstimulation in the areas of VPL that are associated with increased bursting is more likely to produce pain in both post-amputation and post-stroke central pain syndrome (CPS) patients than in other areas of VPL (Davis et al., 1996; Lenz et al., 1998a). Therapeutic approaches to pain relief in the patients with post-stroke central pain are aimed at surgical lesion of the medial thalamic regions of abnormal bursting (Ishijima et al., 1975; Jeanmonod et al., 1993). Further the results of studies by Lenz et al. (1987, 1989) have shown that the nature of the spike-train alterations varies with specific pain syndromes. Increase in the number of bursts with increase in the number of action potentials (principal events) is observed in patients with post-amputation pain while increase in the number of bursts with decreased principle event rates is associated with spinal cord injury pain. These findings point to the emergence of differential modulation of physiological processes occurring at the level of thalamus following spinal cord vs. peripheral injury. Additional evidence for two different activation patterns of the sensory thalamus comes from research involving positron emission topography. PET studies also subdivide central pain syndrome into two types: one associated with increased and

another with decreased metabolic activity (Cesaro et al., 1991; Hirato et al., 1994; Iadarola et al., 1995).

Findings the most relevant to the somatosensory prosthesis project (especially at the present stage) are obtained from the lesion experiments involving non-human primates. In these experiments the changes in the VPL responses to various stimuli are assessed. Usually, the neural responses to the various stimuli (noxious and innocuous) are recorded from the VPL before and after lesion. Typically cells in the VPL are divided into 4 types based on their response characteristics to mechanical stimuli (Casey and Morrow, 1983; Chung et al., 1986; Bushnell et al., 1993; Koyama et al., 1993; Sherman et al., 1997; Dougherty et al., 1997b). Low-threshold (LT) neurons respond preferentially to brushing (light touch) stimulation. Multireceptive (MR) neurons respond to both light touch and compressing (noxious) stimuli, but show no response grading to increases in stimulus intensity. Wide-dynamic-range neurons respond to both types of stimuli (as MR) but exhibit linear positive relationship between firing rate and stimulus intensity. Finally nociceptive-specific (NS) cells respond exclusively to noxious stimuli. The LT class sometimes is subdivided into 2 subgroups: RA (rapidly adapting) and SA (slowly adapting) (Tremblay et al., 1993; Dykes et al, 1981). The changes in the firing rates and patterns of these classes of neurons were investigated in primates following the lesions to the spinal cord. It has been shown (Weng et al., 2000) that the long term effects of the partially deafferenting lesion (observed after 50 weeks) mostly involve MR neurons. Increased spontaneous activity, increased responses to cutaneous stimuli, and larger receptive field sizes characterized responses from MR cells compared to the unaffected by the lesion (having intact innervation) thalamic MR neurons. The incidence and

duration of spike bursts also increased during both spontaneous and evoked responses pointing to the altered spike-train properties of the cells. These changes involving burst activity were wide spread in the thalamus, i.e. not exclusively contained within the afflicted region which might point to cortico-thalamic influences.

The results of experiments involving assessment of short-term (12 week) effects of deafferentation showed similar pattern of responses, with marked increase in the physiological activity of thalamic neurons as specified by even higher rate of responses (especially bursting) recorded during both spontaneous-baseline and stimulation experiments (Weng et al., 2003). The increasing number of high frequency spikes speaks of hyperactivity that is found in the deafferented and other areas of the thalamus. This hyperactivity subsides as the animals enter into the long-term phase following deafferentation. The functional reorganization of the sensory system following deafferentation is a long term process. Initially, lesions reduce sensitivity to pain and touch (Vierck et al, 1971; Vierck, 1998, Willis, 1985). During the mid-term period after spinothalamic lesion the pain and sensitivity returns sometimes with the exaggerated responsiveness to the nociceptive stimuli (Vierck et al 1990). Dysesthesias (changes in the sensation – painful or non-painful) are prevalent in deafferented animals: some animals develop self-mutilating behaviors indicating the presence of spontaneous pain (Levitt, 1991). In human subjects pain is most commonly reported long after (more than 6 months) the injury (Tasker, 1991). Anatomic plasticity becomes more apparent during the long-term phase. There is a marked loss of afferent terminals and decrease in the neuron density (Rausell et al., 1992). There is a decrease in size of zones of parvalbumin and cytochrome oxidase staining, characteristic of lemniscal terminals. The calbidin-positive

zones, characteristic of spinothalamic terminals show an increase. GABA circuitry is also affected as shown by reports of decreased GABA-A receptor presence without any changes in number of GABA-positive interneurons (Rausell et al., 1992).

To conclude, spinal cord injury exerts profound effects on the pain modulation. The extent of the plasticity following injury has to be assessed in order to successfully integrate sensory system into neuroprosthetic application. Both the type of cells and the timing after the injury affect outcomes of electrical stimulation of the VPL. Understanding the intricacies of the functional and anatomical reorganization following spinal cord injury would provide a basis for the optimization of the location and parameters of electrical stimulation in the thalamus. Nevertheless, the ground work based on the "uninjured" animals is necessary to establish the feasibility of targeting thalamus as a microstimulation site.

Micro Electrode Arrays:

The chronic placement of microarrays has been established as an exceedingly useful tool for the study of somatosensory processing in rats (Nicolelis and Chapin, 1994; Nicolelis et al., 1995) and monkeys (Nicoloelis et al., 1998). There are several advantages offered by such high power recordings over traditional single unit recordings. The use of microwire microarray electrodes lends an opportunity to simultaneously sample activity from a large number of neurons from several brain regions. Chronically implanted, such arrays make it possible to record neural activity for prolonged periods of time. These microarrays make it feasible to monitor neural activity in response to both externally and internally produced events in a number of brain areas at the same time. It is possible,

therefore to investigate how neurons within and between various regions relate to each other and what are the characteristic properties of such single neurons and multiunit clusters. Chronically implanted arrays also allow recordings from awake animals making it possible to look at neural activity during behavior. Furthermore, long term recordings – lasting days, weeks, years – permit studies of neural dynamics under conditions approaching naturalistic. The effects of learning, experience, sensory deprivation and enrichment, drug application, damage to the periphery or the CNS could be investigated under such a preparation.

There is a growing number of electrode configurations devised for multineuron single-unit chronic recordings. Among such are arrays of stainless steel or tungsten microwires that are anchored to the skull (Nicolelis et al., 1993). These types of arrays usually have rectangular configuration and are typically made up of two rows and several columns, although circular assembly is possible. Electrodes can have blunt or beveled tips. Utah arrays (Nordhausen et al., 1996) have ten by ten configuration allowing sampling from one hundred electrode tips. It is placed directly on the brain surface with a pneumatic gun with the flexible cables exiting through a thin groove in the skull allowing complete closure of the craniotomy by the skull bone. This type of array has been proven to be reliable over a long period of time and currently undergoing clinical evaluation in humans (House et al., 2006; Norman RA, 2007).

The Michigan system is another type of electrode system which could be fixed or floating (Drake et al., 1988). Individual floating wires that are affixed in the place on the dura are also used (Schmidt et al., 1976; Donoghue et al., 1998). Another class of arrays has gained its momentum in the past several years. These arrays are made of ceramic

materials and have several contact points throughout the shaft of each individual electrode allowing simultaneous recordings from several cortical layers (Moxon, et al, 2004).

Studies of the long-term reliability indicate that the microelectrode arrays retain ability to record from the same small clusters of neurons over long periods of time (weeks to months), although the presence of individual neurons might fluctuate. Overall RF representations stay relatively stable although small insignificant shifts do occur (in the course of a year) (Jain et al, 2001).

The damage to the surrounding tissue caused by chronically placed electrodes has been shown not to seriously compromise local circuitry (Schmidt, et al., 1976; Agnew et al., 1986). The extent of damage was localized to the immediate vicinity of the electrode tracts with fair amount of gliosis surrounding electrode (Nicolelis et al., 1998).

Ketamine

Ketamine (DL-2-(o-chlorophenyl)-2-(methylamino) cyclohexanone hydrochloride) belongs to a class of dissociative anesthetics. It is a noncompetitive NMDA antagonist (Lodge and Anis, 1982; Harrison and Simmonds, 1985MacDonald et al., 1987, 1991). Ketamine blocks NMDA receptor at the phencyclidine site. It has also been shown to modulate activity of nicotinic acetylcholine, muscarinic, and opioid receptors (Finck and Ngai, 1982; Hustveit et al., 1995; Hirota and Lambert, 1996; Scheller et al., 1996; Brau et al., 1997). Ketamine was also implicated in potentiation of $GABA_A$ receptors (Gage and Robertson, 1985; Lin et al., 1992; Irifune et al., 2000).

Specifically it was shown to selectively modulate α6 and δ subunits of $GABA_A$ receptors found in cerebellar granule cells (Hevers, et al., 2008).

Clinically Ketamine has been used as an anesthetic agent in pediatric and adult populations (2mg/kg IV). Its safety and efficacy profiles have led to its wide application in procedures on children (Greens et al., 1998). Ketamine has a short duration of action, fast rate of induction, lacks convulsive side effects, and produces low incidence of adverse reactions. Its use as an anesthetic is prevalent across different animal species. Ketamine administration induces of catalepsy, amnesia, and analgesia (Carter, 1995). The catalepsy is defined as an akinetic state and loss of the body righting reflex (Chen, 1965). The state of catalepsy typically indicates the induction of anesthesia. Ketamine can produce psychotomimetic and euphoric effects in humans (Zarate et al., 2007). Transient behavioral and cognitive deficits associated with psychotic episodes present in schizophrenia (mostly positive symptoms) have been reported following ketamine administration (Catrer, 1995). On the other hand, there is no evidence that ketamine causes physical dependence in humans (Britt and McCance-Katz, 2005). Several studies report that repeated ketamine administration does not increase the risk of more severe psychosis, long term perceptual changes, and severe emotional distress in both psychiatric and healthy populations (Carpenter, 1999; Perry et al., 2005).

The new trend in the psychopharmacolgy research led to investigations of potential beneficial application of ketamine for treatment of psychopathology. Specifically, ketamine was shown to alleviate symptoms of major depression in treatment resistant populations (Salvadore et al, 2008). Major depression is typically treated by conventional antidepressants that exert their effect on the monoaminergic systems

(serotonergic, dopaminergic, and noradrenergic) by increasing the intrasynaptic levels of the neurotransmitters (Sanacora, 2008). Medications targeting these systems do not induce rapid improvements in the symptomatology. Furthermore, many patients do not respond to these treatment options. According to Trivedi et al. (2006) only 50% of the patients with major depression achieved remission following 24 weeks of treatment. These findings support evidence for involvement of other pathways in psychopathology and treatment of mood disorders (Manji et al., 2000). Abnormal activity of the glutamatergic system has been implicated in impairments in synaptic plasticity observed in patients with mood disorders (Sanacora, 2008). Ketamine is known to affect glutamatergic system by blocking NMDA ionotropic receptors. It has been proposed that it enhances the firing rate of glutamatergic neurons, increasing presynaptic release of glutamate and therefore, leading to increased extracellular level of glutamate Mogghadam et al., 1997). This increase in extracellular glutamate produces selective activation of AMPA receptors. Selective activation of AMPA receptors has been linked to ketamine's antidepressant effects (Maeng and Zarate, 2007). AMPA antagonists block ketamine effects (Maeng et al., 2008).

Animal studies provided evidence for ketamine's anxiolytic and antidepressant effects (Zarate et al, 2002; Zarate et al., 2003). Antidepressant effects of ketamine have been also documented in humans (Zarate et al., 2006, Berman et al, 2000). Study by Berman et al., 2000 showed improvement in treatment resistant subjects with Major Depression Disorder (MDD) following Ketamine treatment. Another study by Zarate et al. (2003) found rapid antidepressant effect in subjects with treatment resistant MDD following ketamine IV administration. The effect persisted for 7 days. Another study by

Salvadore et al. (2008) identified anterior cingulate cortex (ACC) as a biomarker for treatment resistant MDD. The response to repeated presentation of fearful faces was recorded. MEG recordings were used to assess the degree of activation of various brain regions. It was shown that patients with increased ACC activation responded rapidly to the ketamine treatment. Growing number of studies suggest that ketamine treatment results in rapid and sustained antidepressant effects. Ketamine might not prove to be the optimal treatment option, but it could be used for a short term as a supplement to regular antidepressant regiment.

In recent years, ketamine has been shown to be effective for treatment of pain: central post-stroke pain and neuropathic pain syndromes. Central post stroke pain (CPSP) occurs after ischemic or hemorrhagic stroke affecting spinothalamocrtical pathways (sometimes involving VPL thalamus) (Bowsher et al., 1998). CPSP is characterized by intermittent or constant pain associated with sensory abnormalities in the affected part of the body (Boivie et al, 1989). Central pain (CP) can occur as a result of spinal cord lesion or lesions due to neurodegeneration (Schott, 1995). Conventional analgesics and opioids were shown to be ineffective in treatment of CPSP. It has been proposed that increased activity of NMDA receptors leads to burst activity associated with nociception in the thalamus of patients with CP (Lenz et al, 1987). Several studies provide evidence for ketamine's effectiveness in pain reduction. Pain relief of more than 50% was documented in 2/3 of patients with CP following ketamine administration (Backonja et al, 1994). The relief lasted 2-3 hours. In another study IV ketamine reduced both spontaneous and evoked pain in patients with CP following spinal cord injury (Eide et al, 1995). The effect of ketamine was superior to fentanyl. Results of the study by Yamamoto et al. (1997)

indicate that almost 50 % of patients with CPSP reported pain reduction (lasting 1 hour) following ketamine IV administration.

The treatment of neuropathic pain with peripheral origin with topical (applied directly to the affected skin area) ketamine application was also shown to be effective. Topical 4% amitriptyline in combination with 2% ketamine produced analgesic effects in patients with postherpetic neuralgia (Lockhart, 2004). Topical 2% amitriptyline/ 1% ketamine used for up to 12 months produced reduction in pain symptoms in patients with neuropathic pain due to diabetic neuropathy, postherpetic neuralgia, and post-surgical/post-traumatic pain (Lynch et al., 2005).

Ketamine use is being investigated for potential protective effects against seizure activity. Over activation of NMDA receptors has been shown to play role in seizures (Kohl and Gannhardt, 2001). The study by Freitas et al. (2006) provided evidence that ketamine has a protective anticonvulsant properties. Rats were treated with Ketamine delivered IP in two dose formulations: 0.5 and 1.0mg/kg prior to administration of pilocarpine (muscarinic acetylcholine receptor activator) – convulsion producing agent. Ketamine dramatically reduced number of seizures and increased the survival rate in animals. Ketamine also affected the latency of first seizure two fold compared to pilocarpine (alone) condition. Higher dose of ketamine was associated with lower number of seizures. It was concluded that both doses of ketamine protected against pilocarpine induced seizures.

Ketamine continues to be extensively used in acute animal preparation. Research of sensory systems relies heavily on recordings of neural activity from anesthetized animals. The effects of various anesthetics on neural population and single unit

recordings need to be characterized. There are a limited number of reports on ketamine's modulatory activity of neural recordings. In the primate visual system ketamine anesthesia was associated with suppression of figure-ground modulatory activity (Lamme et al., 1998). In the auditory cortex ketamine significantly increased latency, duration, and peak latency of neural population recordings compared to awake condition (Rennaker et al, 2006). The increase in postresponse suppression was also observed. The duration of suppression increased almost twofold compared to awake condition. In another study, intracellular recordings in anesthetized rats indicated presence of inhibitory currents lasting 50-100ms (Wehr and Zador, 2005). In ketamine- anesthetized cats recordings of single units were carried out before, during and after the anesthesia (Populin, 2005). The recording electrodes were placed in the superior colliculus and both auditory and visual stimuli were presented. Ketamine was shown to facilitate auditory responses by increasing duration of initial burst and the later component of response. It was also concluded that ketamine changed inhibitory responses into excitatory. Visual responses were observed during recovery stage while animals were still under the influence of ketamine.

Rojas et al. (2006) recorded surface-evoked response potentials (ERPs) in the somatosensory cortex of rats following whisker stimulation during awake and anesthetized states. The effects of various anesthetic agents were examined, among them ketamine/xylazine. The analysis included comparisons along four measures: first ERP peak, gamma band (25-45Hz), fast oscillations (200-400Hz), and very fast oscillations (400-600Hz). The latency of first ERP peak was increased in anesthetized condition compared to both awake and sleep conditions. The amplitude of response decreased in

anesthetized compared to sleep condition. The latency of both FO and VFO decreased in recordings from anesthetized animals. The amplitude of both FOs and VFOs decreased significantly under anesthesia. The authors indicated that the overall shape of ERP was similar for anesthetized and awake conditions implicating involvement of the same neural circuitry in information processing during both conditions.

The evidence provided by the studies investigating ketamine's effect on sensory processing tends to be rather inconclusive. For example some reports document increase in the excitation while others report inhibitory effects. One of the aims of the present study was to obtain additional information on changes in neural activity following ketamine administration.

Methods

A total of 8 bonnet macaque monkeys (*macaca radiata*) were used. They are bred in-house in the monkey colony that exists for more than 30 years at Downstate. All procedures strictly adhered to institutional and federal guidelines.

Surgery:

To limit increase in the stress levels, minimal interactions with animals take place before surgeries. Standard aseptic techniques are used during surgeries. Animals' weights are recorded and doses of anesthetics and fluids are adjusted accordingly. Preanesthesia is induced by an IM administration of Ketamine at 10-15 mg/Kg (if required is supplemented by 1/3 of the initial dose). EKG leads, pulse oximeter, and blood pressure cuff are affixed to monitor vital signs. Blood pressure and heart rate are monitored throughout the experiment to ensure that the animal is in no pain or distress and that the optimal depth of anesthesia is achieved. At this stage atropine (0.04 mg/kg, IM) is supplied to reduce and/or prevent oral secretions. Animals are intubated and kept on 1-3% isofluorane inhalation anesthesia. Levels are adjusted throughout the procedure in order to keep stable level of relatively deep anesthesia. Animals are ventilated at 10-15 bpm. End-tidal CO2 levels are monitored and kept at 20-30mmHg. Body temperature is also monitored by the rectal temperature probe and maintained at 35.5°C with heating pads. Intravenous catheter is inserted and lactated ringer fluids are delivered to avoid dehydration and hypoglycemia. Infusion pump is used to deliver fentanyl at a flow rate of 2-10 mcg/kg/h. Usage of analgesic agents allows levels of gaseous anesthesia to be kept relatively low minimizing anesthetic effects on neural responses. Isofluorane levels are

kept at 0.25 – 1% for the duration of the surgery. Antibiotics (Cefazolin 0.5mg, IV) are administered systemically once during surgery. Brain edema is prevented by injection of steroids (Dexamethasone 0.1mg/kg, IV).

Animals are fitted in the stereotaxic frame (Kopf Instruments) with ear bars and mouthplate fixating both head position and orientation. Animal's head is shaved and scalp is disinfected. A local anesthetic (lidocane) is injected subcutaneously before skin incision. The scalp is incised and the temporal muscle is either retracted laterally or resected. More than 10 self-tapping titanium screws are inserted in the skull bone. The screws are needed to secure anchoring and adhesion of the dental cement to the skull and also for grounding purposes. Small craniotomies are drilled in the skull. The location of craniotomies is predetermined by the MRI-aided assessment of the location of the central sulcus relative to the ear bars and other fiduciary markers. The size of craniotomies varies in order to enable accommodation of one or more electrode arrays. The dura is removed. In some cases the pia also has to be removed (in order to place electrodes with blunt tips).

Brain regions:

The coordinates of primary somatosensory cortex (SI) and Ventroposterior Lateral nucleus of thalamus (VPL) are identified using rhesus macaque brain atlas. Within SI areas 3b, 1, and 2 are the main targets of the experiments. Area 3b is located in the central sulcus which makes it rather cumbersome to place electrodes in this region. Area 1 is adjacent and more caudal to area 3b which permits relatively unhindered access. Area 2 is yet more caudal to area 1. There is no distinct visible border between these areas. The correct placement of electrodes within each of these regions could be

only estimated based on topographical representations and physiological properties of neuronal populations recorded from these areas. Placement of area 2 recording electrodes in vicinity of intrerparietal sulcus (the most caudal region) serves as a valid indicator of proper area 2 by the topographical representations and neural response properties. Area 4 of the primary motor cortex as well as some premotor regions such as PMD and PMV are also localized. Mapping of motor cortex has to take place in order to ensure the correct placement of electrodes in the hand and arm representation. This is accomplished by electrical stimulation through electrodes or by physical manipulation of digits and limbs.

Electrodes:

Microelectrode arrays are used in all experiments. For cortical recordings these are typically comprised of 16 or 32 25 to 50 micron stainless steel microwires in 16 X 2 or 8 X 2 configurations. Two rows are separated by 500 μm. The rows span about half a centimeter. The impedance of electrodes is about 0.5 megohm. Electrodes with sharp tips (Microprobe, Inc.) are typically used for the acute preparation while blunt-tipped electrodes are placed in chronically implanted animals. Dull-tipped electrodes are used in the long term recordings because they induce less damage in response to normal brain movement within the skull (Nicolelis et al, 2003). The rectangular configuration of arrays allows spanning of a relatively large cortical areas therefore enabling simultaneous recording of neural signals representing many skin locations, i.e. multidigit representations.

The thalamic array consists of 4 stainless steel electrodes of 2 X 2 configuration developed in-house. The diameter of these electrodes is larger which makes them stiffer

than cortical electrodes. These electrodes need to penetrate deep in the brain (almost 3 cm) so the stiffness results in less angular deviation with the distance traveled.

Cortical arrays are lowered by microdrives (Kopf Instruments) orthogonally to the surface of the brain to ensure proper placement within cortical regions. Electrodes are placed on the cortical surface and appropriate position measurements are made. The brain is penetrated and electrodes are advanced into layers III/IV. The placement within these layers is assessed by the distance from the surface of the cortex and also by the analysis of characteristics of neural responses induced by the mechanical stimulation (such as presence of large units). To assess proper positioning of electrodes tactile stimulation on the skin of the contralateral limb is carried out for the duration of penetrations. The positioning is deemed satisfactory when Receptive Fields (RFs) of several locations on the skin are mapped onto the electrodes. Usually one electrode array spans representation of several digits and/or some arm locations.

Thalamic array is driven much deeper in the brain using the same methodology until the VPL is encountered. The end point is assessed by recording neural signals from the cells responding to the tactile stimulation to the periphery.

Both recording of neuronal responses and intracranial electrical stimulation are conducted through the same electrodes.

Procedure:

Mechanical stimulation:

The arm and hand of the animal are restrained by the cast designed to fit into the primate chair and punctate tactile stimulation of the skin of the forelimbs is applied with a hand-held vibromechanical actuator delivering stimuli of 1ms duration. The frequency

of stimulation ranges from 1 to 20 HZ with typical stimulation frequencies of 1, 2, 3, 5, 10, and 20 Hz. The tactile stimulation sessions are divided in one minute per location blocks for lower frequencies. For higher frequencies of stimulation the duration of blocks is decreased to 30s. This ensures that enough data is gathered for statistical analysis and that no prolonged stimulation is administered. The order in which skin locations are stimulated varies to account for possible interactions. Typically digits are stimulated first, then pads, then wrist, and arm locations. The skin locations usually encompass all 5 digits, 7 pads and other wrist and arm locations. Some experiments require longer sustained stimulation in order to assess patterns of neural representation and integration along temporal axis. In those cases constant pressure is applied for up to 5s followed by the rest period of 5 sec.

Electrical stimulation:

Intracranial electrical stimulation is administered bipolarly through closely spaced pairs of electrodes using constant current 32 channel stimulator developed in-house (E. Hawley). The pattern of stimulation such as pulse duration, number of pulses per train, amount of current applied could be manipulated. The stimulator is also capable of delivering stimulation concurrently or with a preset delay through several electrode pairs which enables investigation of stimulus-induced spatio-temporal characteristics such as summation as well as multidigit representation. Typically, 1ms biphasic microstimuli consisting of one 1 ms positive pulse followed immediately by another 1 ms negative pulse are administered. This is consistent with our 1ms mechanical touch stimuli, which activate cutaneous receptors during both onset and offset of the touch. Usually pulse widths range from 300 to 500 μs and current intensities are increased from 25 to 150μA.

Recordings:

Waveforms are recorded through a multiunit acquisition processor (MNAP; Plexon, Dallas, TX). Units are sorted on-line during each recording session to set each channel's recording threshold in order to capture spikes (digitized at 40kHz). Such sorted units may include spikes from multiple neurons. These multi-unit recordings undergo further sorting manipulations off line (Off-line Sorter, Plexon) using template-matching spike sorter. Principle component or other (peak, valley, etc) space representation algorithm also aids in defining clusters of waveforms that constitute a single unit. Sorted cells are termed single units if they form a distinct cluster based on some of the aforementioned parameters and display less than 0.1% of interspike intervals (ISIs) within a refractory period of 1 ms. Autocorrelograms are generated with NeuroExplorer software (Nex Technologies, Littleton, MA) to confirm that recordings meet this refractory period criterion.

Studies of the long-term reliability indicate that the microelectrode arrays retain their ability to record from the small ensembles of neurons over long periods of time (weeks to months), although the presence of a small number of individual neurons might fluctuate. Overall RF representations stay relatively stable although small statistically insignificant shifts do occur (in the course of a year) (Jain et al, 2001). Plasticity in the sensory cortex occurs over period of weeks as reported by the evidence of small changes in receptive field location (Merzenich, et al 1983) and over months with larger changes (Kaas 1991; Pons et al., 1991; Jain et al., 1997, 1998b).

For the chronically implanted electrodes the recordings from each session were compared. The sessions spanned several days and weeks so it is not possible to establish

with absolute certainty that the same neurons were recorded on the same channel. It is known that the shapes of the waveforms of a particular neuron can drift (Quirk and Wilson, 1999) and different neurons can have similar waveforms. The analysis of firing characteristics over time of a sorted neuron on a particular channel is required to ascertain the probability of recordings from the same neuron. The similarity could be assessed using shape of the waveforms, auto-correlograms, perievent histograms, firing rates, and RF localizations (Jain et al, 2001).

Data are analyzed using NEX and its Matlab and Excel extensions. Statistica and SPSS 16.0 are used for additional analysis and plotting. Poststimulus time histograms (PSTHs) are constructed from responses to stimulation of a specific skin location. Significant firing rate responses of single (SU) and multiunits (MU) are identified from PSTHs and perievent rasters using an in-built function of Neuroexplorer (Nex) analytical software (Nex Technologies, Littleton, MA). Significant responses are identified using 1ms bin size and setting confidence interval at 99%. The size of the projection field (PF - the number of channels, i.e. neural populations that encode the same receptive field) as well as response latencies are also identified using PSTHs.

Multineuron response peak amplitude in z-scores was found to be one of the appropriate criteria of response quantification. It allows mapping and discrimination of peripheral stimulus sites and there is nearly always enough background to estimate a reliable z-score. Overall pattern, spread, response intensity, latency, local response pattern, pattern of spread through cortex are investigated.

Pairwise correlation (Pierson's correlation coefficients) is used to assess neural responses. The procedure and rationale for using this method are explained in the Results section.

Acute experiments:

In acute experimental procedures electrodes are positioned in one or more regions and are advanced until satisfactory placement is achieved. These arrays are not permanently affixed to the skull which provides means for the repositioning and reutilization of the arrays.

Upon completion of experiments monkeys are euthanized by a high dose injection of pentobarbital (100mg/kg, IV). Animals are perfused transcardially with 0.9% saline followed by 3.5% paraformaldehyde in 0.1M phosphate buffer. The brains are fixed and subsequently subjected to histology. Recording sites are identified in Nissl-stained 40-80μm sections.

Chronic:

For long-term survival studies electrodes are positioned in the brain regions and fixed in place first with cyanoacrylate glue and then with dental acrylic. Once the electrodes are stably secured the connector is fixed to the bone with more dental cement with only female connectors exposed. The head fixation bolt is attached to the skull with titanium screws. When dental acrylic dries and becomes stiff the skin is sutured. To prevent infection, a topic antibiotic gel (gentamicin) is applied to the surgical wound and systemic antibiotics (Ampicilin, 100-500 mg/kg, IM) are given. Post-operative care includes systemic administration of analgesics (Buprenorphine 0.1 mg/kg, IM) and

antibiotics (Bicillin, IM) as well as topical antibiotic application. Animals are given 2 weeks to recover before experimental sessions commence.

Upon completion of experimental manipulations animals are euthanized and the brains are histologically processed according to above mentioned protocol.

Awake monkeys:

Four monkeys were used for the data collection from the awake animals. Initially monkeys need to get accustomed to the trainer so several weeks have to be spent on gentle handling of the animals. Animals begin to take food, approach the front of the cage, and show other signs of habituation. Monkeys are handled to the point when they allow gentle handling such as stroking or holding hands. Collars are put on the monkeys. The collars are fastened to the poles for guided walking outside the cage. Monkeys are trained to sit in the primate chair (Crist Instrument Co., Hagertown, MD) with collar fixed to the neck plate. One arm is immobilized in order to apply tactile stimulation to digits and pads. Fruits are used as reinforcements during all interaction with monkeys.

Following post surgical recovery period the integrity of implanted electrodes was assessed by recording spontaneous activity and stimulus-induced activity in the cortical areas: motor and somatosensory areas. Mapping of both RFs and PFs commenced. Various digit representations were found. RFs and PFs were stable for several weeks. Vibromechanical actuator was used to evoke cortical response to cutaneous stimulation. Monkeys were secured in the primate chair (Crist Instruments) with arm and hand fixated. Digits 1 through 5 were stimulated and the data were recorded using Plexon system.

Ketamine study design:

Two monkeys participated in the experiments. Each monkey was anaesthetized 2-3 times to produce large data sets. Each experimental session lasted 3-4 hours. Awake monkey was secured in the primate chair and headstages were connected to the recording hardware. The onset of the tactile stimulation was synchronized with the recording equipment. The stimulation was brief (1ms). The stimulation was administered at 3Hz. Tactile stimulation was administered to 5 digits in orderly fashion. Total session time of one digit stimulation was 30s to 1min. Each cycle of stimulation consisted of 5 session: stimulations to digit 1 through 5. Each cycle was repeated every 5-10 min. Such closely spaced time intervals insured almost continuous recordings from the animal. After first 30min of stimulation cycles, Ketamine was administered (10mg/kg IM). The stimulation sessions continued in the outlined fashion throughout the rest of the experiment. On average, 100 files were generated by each experiment. The experiment was terminated when monkey was fully awake. Behavior of monkey was recorded throughout the experiment. This behavioral measure was a guideline for establishing the depth of anesthesia.

Results I

Descriptive analysis

One of the goals of the present study was to assess neural responses to tactile stimulation across anesthetized and awake states. The parameters of tactile stimulation were held constant across these conditions, therefore differences in neural responses would indicate differential processing of information, i.e. signal detection and discrimination. Naturally, the perceptual aspects of the response could not be characterized using this paradigm. However, the aim was to identify channels/neural populations showing activation in response to tactile stimuli using correlation analysis that quantified activity (evoked by the same stimulus) on one channel at different times.

Initially, recorded neural activity is examined using Plexon software - Offline sorter. This software allows visualization of all the waveforms recorded. The amplitude and shape of the waveforms could be examined. The shape of the waveforms is a factor in sorting algorithms. Electrical artifactual noise could be excluded from further analysis. Single cells could be sorted out using this software.

The next step is to examine spatial and temporal distribution of the activity. Neuroexplorer software allows representation of signals in the form of rasters and histograms. The time stamp of the signal that has crossed a predetermined threshold is plotted in relation to the timing of a tactile stimulus. When tactile stimulation is administered at 3Hz – the activity for 3 cycles is grouped and plotted for each second of stimulation. Each cycle lasts 333ms. When the stimulation continues for 1 minute the total number of grouped intervals depicted by the histogram is 180 (Fig.1). Histograms yield a probability index of activity at one point in time. The time bins are specified by

the operator. Further examination of these responses reveals that “activation” – transient increase in firing rate within the examined time period (333ms after the tactile stimulation). There is also variability in the magnitude of response across the electrodes.

The magnitude of response of neural populations has been shown to be proportionate to the degree of their involvement in sensory information processing (see Introduction). The timing of the responses is crucial for determining the association between tactile stimulation and neural responses. The stimulus-response locking is assessed using histograms. The responses to the tactile stimulation occur with the latency of 17-20ms (consistent with conduction velocities and synaptic delays). Those responses tend to last for up to 35 ms (Rozenboym, et al, 2005, 2006). These responses indicate activation of neurons associated with transmission of information pertinent to the stimulus, its parameters and characteristics. Histograms of activity recorded from different electrodes show differences in both magnitude and temporal resolution of the activity (see Fig.1 ch. 13 and ch.18: differences in firing rate and the duration of the peaks). Therefore spatial distribution of neural activation could be assessed.

Neural responses within somatosensory cortex are usually characterized by the presence of increased activation (firing rate increase) following mechanical stimulation to the periphery. The neural groups that map center of the stimulated Receptive Field exhibit high firing rate and appropriate latency. This group responds most vigorously to stimulation to the center of receptive fields, but is also capable of responding to more flanking regions of the RF. In Fig.1, neural recordings indicate strong responses on channels 11-13. Those channels were identified during the recording session as the strongest responders to mechanical stimulation based on the shape of waveforms

recorded and the timing of firing. The time interval of 300 ms after the stimulation is plotted. Two peaks are evident on ch. 11, 12, and 13. The first peak has a latency of 18ms from the stimulus onset and the second peak occurs 200 ms after the first. The frequency of response is rather high and is around 50%. Activity recorded on channels 11, 12, and 13 represents responses to stimulation of the center of a RF.

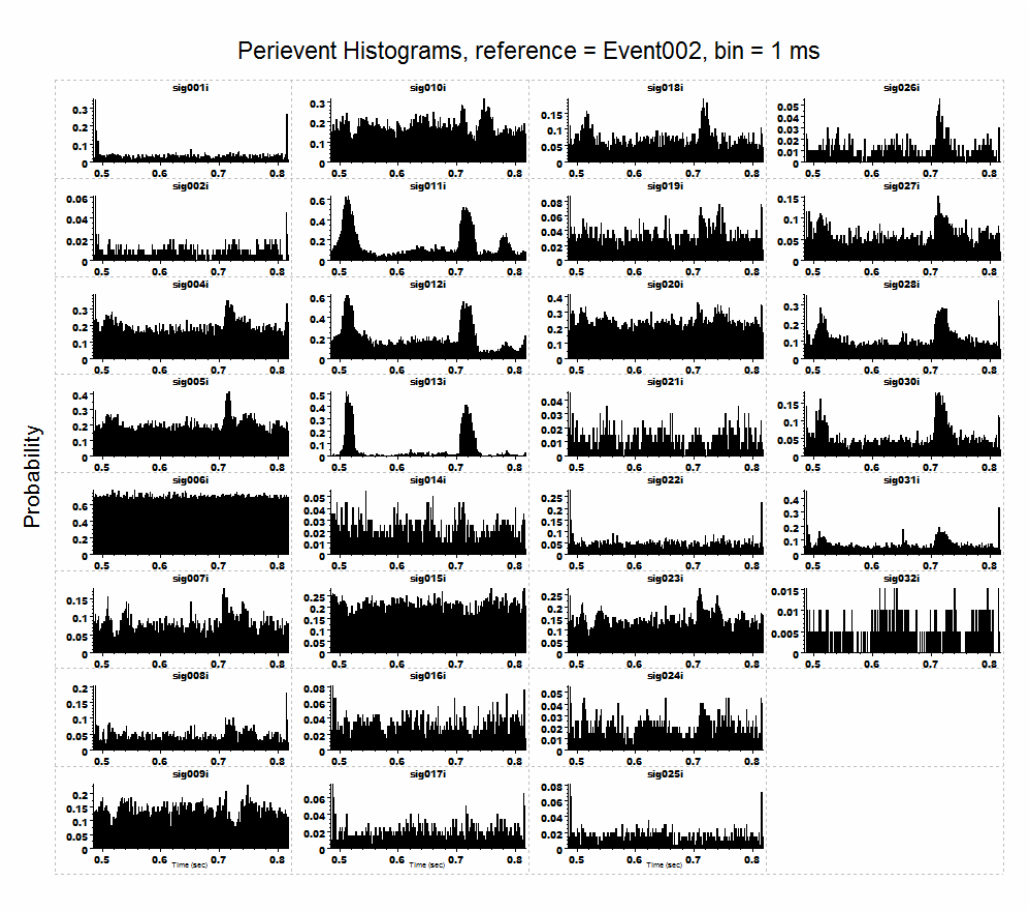

Fig.1. Histograms summarizing evoked responses to D1 stimulation.
Awake condition. Frequency distributions are plotted for 333ms.
Y-axis shows magnitude of responses in terms of probability.
Channels 3 and 29 were excluded from the analysis as no activity was recorded through these channels.

Stimulation of flanking regions of RFs results in lower response rate and typically more background activity. Channels 28 and 30 are seen as contributing to the sensory processing but the pattern of neural activity is not identical to ch 13, for example. The

overall response rate is lower (up to 65% decrease), the peaks of activity are not as well defined and signal to background ratio is decreased. These channels map the surround of a RF.

Within each recording session some channels were identified as “good channels”, “average” – contributing somewhat to the signal processing, “noisy” – no clear signal-response relationship was evident. The assignment of such grouping variables resulted from the qualitative analysis of recorded data. Records were made of each channel’s coding quality for each stimulation condition: for every digit. This preliminary data assessment serves as a control for further analysis using pairwise correlation.

Quantitative analysis

In order to establish the degree of “goodness” of recorded activity more quantitative analytical tools must be employed. Typically, several response parameters have to be included in a model. Estimation of “goodness” of a channel is reliant upon satisfaction of several conditions. First, channels that record relatively high firing rate have to be identified. That task could be accomplish either by the operator visually inspecting histograms or by the search/sorting algorithm developed by the programmer. The determination has to be made about the cut off point: what magnitude of firing rate has to be reached in order to satisfy the inclusion criterion? Second, peaks of firing activity have to be identified. The latency of response, duration, and magnitude of peak serve as guidelines. If neural responses occur with a predetermined latency, last a certain amount of time, and are significant enough these neural population encode the center of receptive field and are deemed “good” responses. So, in the discrimination algorithm these parameters should be quantitatively represented. For instance, the magnitude of

peak is usually assessed by drawing 99th percentile confidence interval on histograms (for further discussion see Fig.3). Channels on which this threshold is crossed will be included in further analysis. Signal to background ratio is also used to identify the magnitude of response. Another measure of the peak magnitude is a z-score: how many standards deviations above the mean is the peak?

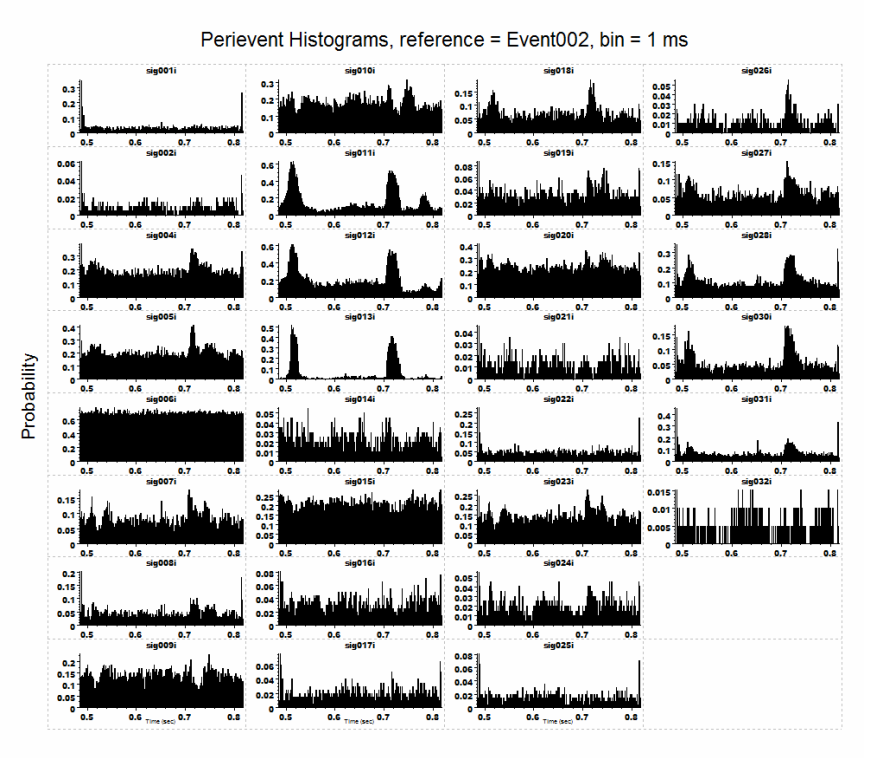

Variable	Mean Freq.	Peak Z-score
Sig001i	30.38378	14.726073
Sig002i	7.357369	8.970242
Sig004i	181.225241	4.650601
Sig005i	194.385388	5.729984
Sig006i	690.761538	
Sig007i	75.097499	4.272127
Sig008i	41.250522	8.607204
Sig009i	130.246984	3.777957
Sig010i	166.448934	3.932018
Sig011i	150.795285	3.763621
Sig012i	192.830798	3.680825
Sig013i	56.211532	4.630559
Sig014i	19.778702	3.628818
Sig015i	201.003942	
Sig016i	27.951846	4.267345
Sig017i	17.13128	6.224924
Sig018i	65.462116	5.090358
Sig019i	29.475653	4.388229
Sig020i	227.370414	4.45115
Sig021i	10.374198	4.883006
Sig022i	42.574233	11.738886
Sig023i	133.217637	4.414597
Sig024i	17.531472	3.969789
Sig025i	13.729651	8.086602
Sig026i	10.050967	5.975178
Sig027i	54.672333	4.696624
Sig028i	106.466366	4.576977
Sig030i	50.023954	
Sig031i	64.923396	10.581433
Sig032i	4.49446	
Sig032i	4.49446	
Sig032i	4.49446	

Fig.2a. Histograms depict activity on 30 channels following D1 stimulation in awake animal. 60s session. Table provides values of mean frequency and z-scores for each channel. Channels 11, 12, and 13 show time-locked responses to tactile stimulation. Channel 1, 22, and 31 produce high z-scores. Channel 6 – highest mean frequency.

In order to identify channels mapping the center of receptive field the following algorithm has to be followed: If activity significantly increases beyond 99th percentile confidence interval (as described by the predetermined magnitude of signal to noise ratio or a peak z-score) and the onset of such a peak has a certain latency and a specific

duration (a range could be provided) the neural activity recorded from such a channel will be associated with the stimulation of receptive field center. Typically, recordings from microelectrode arrays yield several channels that would fall into such a category. The next task is to determine an index or relative "goodness" of such channels. Another algorithm has to be worked out for the channels responding to the stimulation of a receptive field surround, etc. In order to compare activity or response to the same stimulation recorded from the same channel over time the outputs of the sorting algorithms have to be compared and an index of comparison has to be determined. Also, to compare responses recorded from the same channel to different stimuli or under different conditions an index of "goodness" has to be created that incorporates all the variables examined in the algorithm. All conditions outlined in the algorithm have to be met. Assessment of one of the variables alone cannot be used as the only inclusion criterion.

The following figures depict individual cases examined using only one variable for the analysis. The data for these figures corresponds to D1 stimulation session in awake animal. The full 60s file is depicted in Fig.2a. The histograms summarize activity recorded on 30 channels following stimulation. Table next to the histograms includes mean firing value and a z-score for each channel. Fig.2b and fig.2c show histograms for the same stimulation session, but they include only 30s of stimulation. Fig.2b corresponds to first 30s and fig.2c to the last 30s of session. Tables next to the histograms report mean firing rates and z-scores for each channel. Peak z-score measure yields high values on channels that are not necessarily responding to the stimulus and also provide

low discriminative power when several peaks are present. What magnitude of a z-score is sufficient?

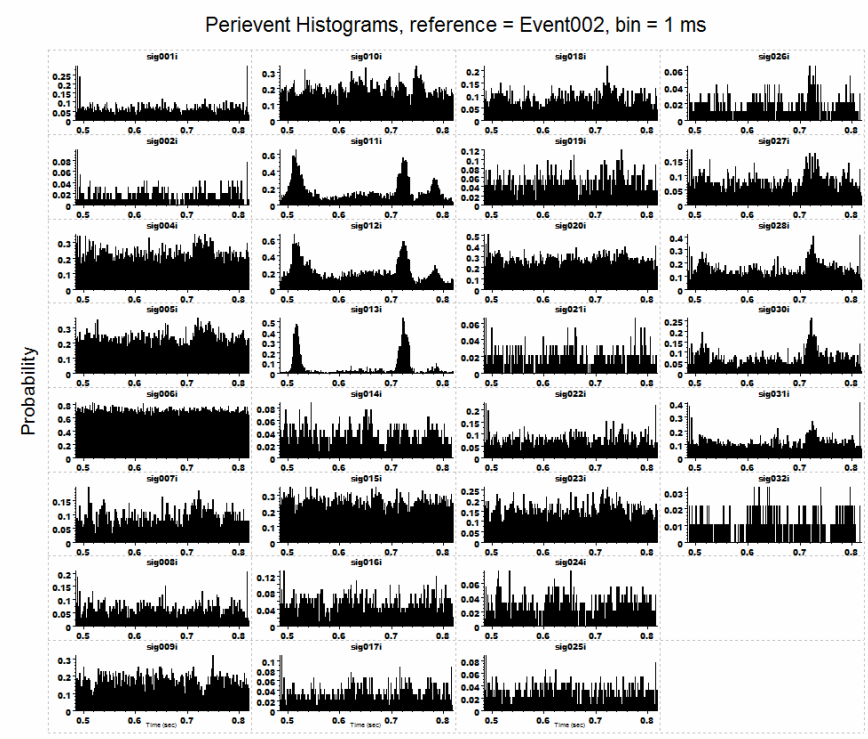

Variable	Mean Freq.	Peak Z-score
sig001i	57.8	
sig002i	14.9	7.022436
sig004i	215.8	
sig005i	220.6	3.386442
sig006i	694.43333	2.886362
sig007i	83.1	3.758285
sig008i	57.3	5.710251
sig009i	162.43333	3.85051
sig010i	179.6	3.498923
sig011i	154.03333	4.290264
sig012i	204.56667	4.167085
sig013i	57.266667	5.126537
sig014i	30.233333	3.535414
sig015i	243.2	
sig016i	46.8	3.780279
sig017i	29.833333	4.731928
sig018i	79.166667	4.709415
sig019i	44.166667	3.62092
sig020i	262.03333	4.929179
sig021i	15.233333	
sig022i	68.966667	5.906627
sig023i	146.56667	3.212228
sig024i	26.466667	
sig025i	25.733333	4.330134
sig026i	15.633333	
sig027i	70.6	3.766899
sig028i	145.33333	4.899878
sig030i	69	5.872155
sig031i	104.06667	7.145175
sig032i	9.666667	

Fig.2b. Histograms plot distributions for the first 30s of the stimulation session depicted in fig.2a. No high z-scores are observed.

Z-scores should provide a measure of selectivity based on this magnitude. In fig. 2a ch.1, ch. 22, and ch. 31 produce high peak z-score (above 10) that stand out compared to the rest of the distribution. On the other hand, the frequency distributions of these channels reveal no pronounced peaks of activity time-locked to the stimulus, which would indicate their involvement in signal processing. Ch. 11, 12, and 13 exhibit both early and late peaks, but did not produce high z-scores. Both, false positive and false negatives are created. In fig.2b where only first

30s were used none of the channels produced high z-scores, which indicates relative lack of stability of this measure. Further, in fig.2c which corresponds to the last 30s of stimulation ch1, 22, and 31 showed high z-scores and additional channels produced comparable statistics.

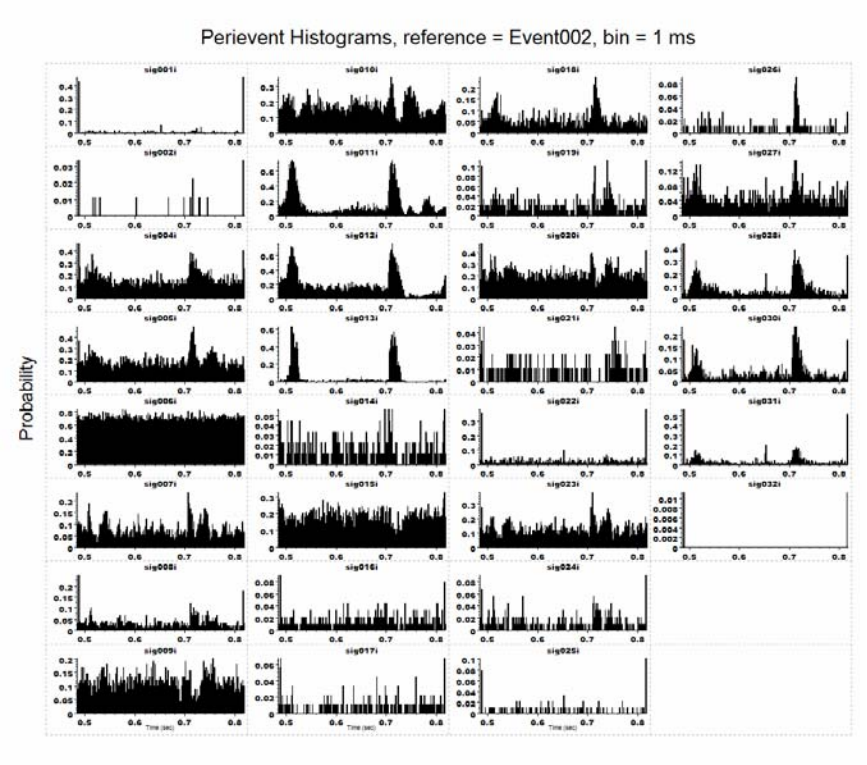

Variable	Mean Freq.	Peak Z-score
sig001i	7	16.225752
sig002i	0.689655	
sig004i	150.965517	5.059217
sig005i	171.931034	5.750747
sig006i	698.586207	2.969909
sig007i	69.344828	5.024698
sig008i	27.241379	9.120116
sig009i	104.931034	2.747941
sig010i	159.724138	3.978285
sig011i	149.137931	
sig012i	183.068966	4.108803
sig013i	55.310345	5.008026
sig014i	11.241379	
sig015i	171.206897	3.484331
sig016i	12.448276	6.458963
sig017i	6.310345	
sig018i	53.551724	5.78814
sig019i	17.241379	
sig020i	203.206897	4.681059
sig021i	6.448276	
sig022i	20.275862	13.899079
sig023i	124.551724	5.725026
sig024i	9.724138	6.591403
sig025i	3.517241	11.902318
sig026i	5.068966	10.367654
sig027i	42.137931	
sig028i	74.586207	5.246654
sig030i	35.241379	
sig031i	32.172414	11.661144
sig032i	0.034483	

Fig.2c. Histograms plot distributions for the last 30s of the stimulation session depicted in fig.2a. High z-scored are seen on channels 1, 22, 25, 26, and 31. Note stability of pattern of activity on channels 11, 12, 13.

Fig.3 illustrates changes in distributions for channels 1 and 31.The first 3 panels correspond file used in fig.2, the fourth panel shows activity recorded from the same electrodes one week later (same stimulation was applied). As can be seen from the figure, the recordings do not produce reliable results, as the data from second experiment would not produce high z-scores. The high z-score on channels 11 and 31 resulted from occurrence of an artifact in the beginning and the end of recorded period. The timing of

the signal indicates no time-locking to the tactile stimulus. The origin of the artifact is unknown.

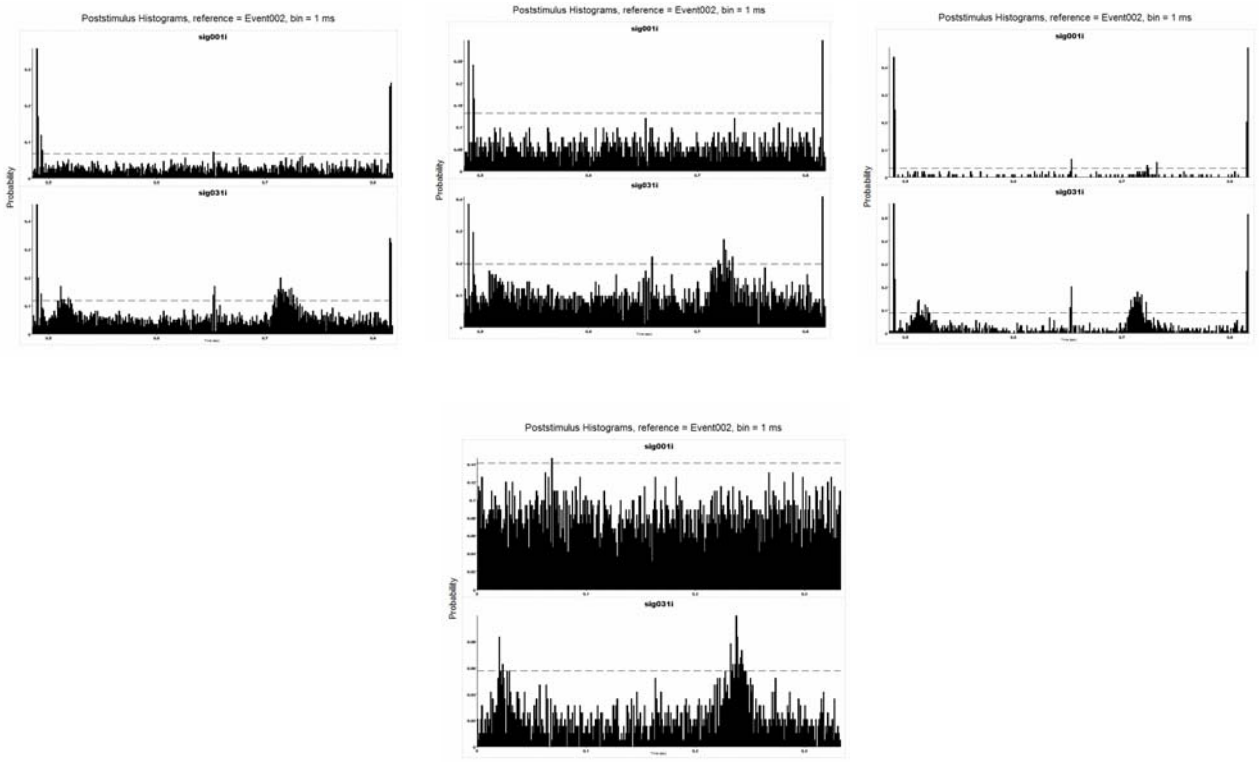

Fig.3. Histograms for channels 11 and 31. Panel 1: 60s session; panel 2: first 30s, panel 3: last 30s; panel 4: another stimulation session – 60s. 99% confidence interval is indicated by dashed lines. Fluctuations in signals are observed. In panel 1 and 3 peaks in the beginning and in the end of the time interval generate high z-scores.

As can be seen from the fig.3 these artifacts are more present in the first part of the recording session. Also, they disappear one week later (2nd experiment). Analysis using z-scores does not eliminate “noisy” channels, on the contrary it introduces an error. Analysis of correlation, on the other hand, eliminates channels showing instability of responses. Channels 11, 12, and 13 produced similar frequency distributions in fig.2a, 2b, and 2c. Further fig.4 indicates that the pattern of response on those channels remains relatively stable in time. Fig.4 depicts neural responses following just one stimulus application (single trial is used). Here, again small z-scores were generated by channels

11, 12, 13 while activity shows good correspondence with the stimulus. High frequency of response is observed on channels 11, 12, 13 forming primary and secondary peaks. Other channels show lack of stimuls-response pattern. Overall, this stimulation session did not produce channels with high z-scores. These results indicate compromised stability and sensitivity of z-score measure utilized for 2-peak distributions.

It can be seen from fig.5 that using high frequency of response measure – firing rate – as a guideline could create many false positives, as channels with no discriminative power would fall into this category (see ch.6i). High firing rates alone do not indicate presence of primary encoders. As can be seen from tables in Fig2a, 2b, and 2c the highest mean frequency is found on channel 6, which shows no discriminative temporal property. Channels 11, 12, and 13 exhibit much lower mean firing rates but provide good temporal resolution of signals. Mean firing rates do not provide good measure for assessment of "goodness" of a channel. Probabilities of firing (y-axis in histograms) for channels 11, 12, 13, and 6 are very similar – around 60%, but the patterns of responses show high degree of variation (channel 13 vs channel 6). Other channels such as channel 28 and 30 show lower probability of response, but the pattern of response points to their involvement in surround encoding (fig.2a, 2b, 2c). When used alone measure of probability of firing does not provide sufficient information for discriminatory analysis.

Fig. 3 also illustrates that crossing of 99th percentile confidence interval threshold does not translate into presence of a stimulus-response relationship (see ch. 1). Some episodes of frequency increases are encountered on channel 11 and 31 but they show no temporal correspondence to the stimulus. These peaks of activity could be due to an artifact. They are uncharacteristically short-lasting: about 1ms.

In fig.5 last panel depicts channel 4. This is another example of activity crossing 99th percentile confidence interval threshold. The threshold is broken, but the pattern of obtained peaks indicates at best, some weak encoding properties of this channel. This channel does not show stability, as can be seen from other panels of the same figure.

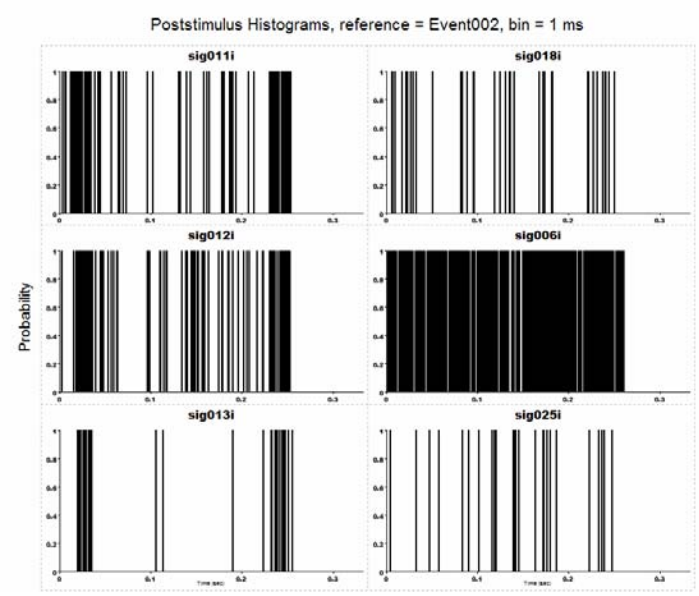

Fig.4 Histograms depict activity recorded from 6 channels. One trial was used to generate this figure. The stimulation of D1 in awake animal was conducted. Activity on channels 11, 12, and 13 is characterized by two peaks of activity: early and late increase in the frequency of firing rate. Activity on channel 6 is high throughout the poststimulus interval. Other channels also show spontaneous activity – no distinct patterns are observed. Table reports uniform z-scores for all channels.

Variable	Mean Freq.	Peak Z-score
sig001i	84.809053	3.295943
sig002i	3.217602	
sig004i	685.917076	2.695143
sig005i	109.587745	
sig006i	698.787484	3.140507
sig007i	46.82873	5.936552
sig008i	0.536267	6.401779
sig009i	93.2316	4.674751
sig010i	126.779835	3.957347
sig011i	193.198084	3.711727
sig012i	207.803474	3.720783
sig013i	66.7337	5.232894
sig014i	99.745667	3.495359
sig015i	188.639814	2.597479
sig016i	14.226849	3.679407
sig017i	47.270361	4.148979
sig018i	89.808955	5.473044
sig019i	39.526035	3.662355
sig020i	158.924311	3.535374
sig021i	6.65602	5.187055
sig022i	33.248556	3.817724
sig023i	86.133948	5.201419
sig024i	0.047318	
sig025i	56.213403	
sig026i	4.163956	
sig027i	104.919067	4.508339
sig028i	124.240453	
sig030i	66.323613	
sig031i	24.999507	5.14361
sig032i	0.031545	

These outlined examples stress the need for presence of a comprehensive algorithm that would include all of these variables in the estimation measure of "goodness" of a channel. This type of an algorithm has to be custom designed for each set of recordings and/or modified for different stimuli, conditions, or paradigms as neural

response characteristics vary. These modifications take time as well as knowledge of programming languages on the part of an operator. So far no commercially available software affords such discriminative acuity and precision.

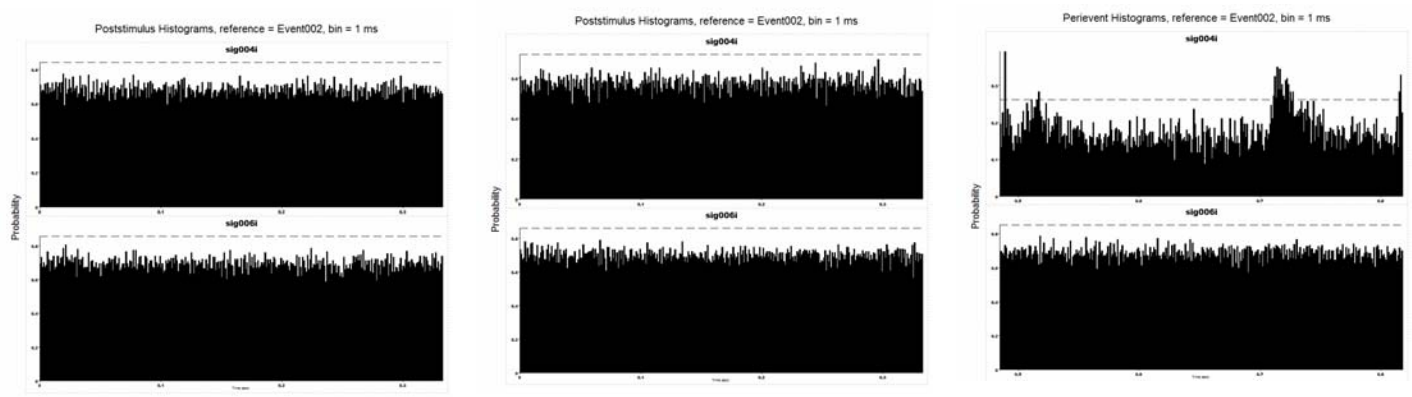

Fig.5. Poststimulus histograms for channels 6 and 4 exhibiting high firing rate. Each panel represents a separate stimulation session. High Firing rate: 60% - is uniform throughout the whole poststimulus interval. Activity on channel 4 in the third panel produced peaks crossing 99% confidence interval. Channel 6 shows stability across sessions.

When the goals of a study include: 1) identification of neural pools responding to the stimulation, 2) assessment of their relative strength or importance, and 3) comparison of these responses to stimuli over a period of time, is this proposed (and widely used) algorithm the most efficient way of analyzing the data? Are there other alternatives that would result in the similar quantitative analysis, including identification of “good” channels, estimation of relative “goodness” of channels, assessment of consistency of recordings over time, comparison of neural activity under various conditions? Is there one measure that results in one index of the activity? Is there a method that would be cost effective and user- simple? Is this method foolproof? What are the caveats? Is this method of analysis statistically sound? Data presented in this document aims at addressing these questions.

Neural codes rely heavily on two information categories: the strength of signal-firing rate and the timing of the activity. The analytical tool used to examine data from described experiments incorporates both of these categories. This method relies heavily on the premise that neuronal response shows stability. This premise constitutes the major condition that has to be accepted. This condition explicitly states that at time 1 neuron A (or a group of neurons) responds to stimulus X with the latency and magnitude approaching the response latency and magnitude of the same neuron to the same stimulation at time 2. This starting assumption pertains to neurons that are involved in primary encoding of the signal. Such neurons encode the center of the receptive field, i.e. respond to the stimulus. Every time the stimulus is encountered it activates the same pathways that transmit information decoding the parameters or characteristics of a stimulus. In nervous system that has to be valid. If all conditions are held constant at 2 different times the same stimulus evokes the same response. The similarity of response characteristics denotes stability of the system. Components of the system transmitting information about a stimulus have to be reliable. Those parts of the system that are not involved in the transmission of information do not show similarity of responses at two separate times. Alternatively, dissimilarity of response indicates variability in conditions. Interfering variables perturb the response parameters. Same stimuli could be perceived as dissimilar. Attention, emotion, state of arousal, habituation, multimodal integration contribute to such differential response. Nevertheless, a high degree of stability is evident within sensory systems (see histograms in Fig. 2: ch11, 12, 13). If the validity of stability within the system is accepted the analysis of data could rely heavily on this axiom. The statistical tool to assess this stability using both magnitude and temporal distribution of

the neural response is Pierson's correlation coefficient – r. Correlation coefficient yields a measure of similarity of two samples (pairwise comparison). The higher the coefficient the more similarity is detected.

To use correlation coefficient effectively following conditions have to be met. First, the degree of similarity of responses to the same stimulus at two different times is influenced by the purpose of the encoder. Neurons that transmit information associated (or in response to a stimulus) with the stimulus show more stability than neurons that are not involved in information processing. The degree of similarity is proportionate to relative involvement of neurons in the transmission and analysis of incoming information. Spontaneous activity is truly spontaneous – non correlated. An example is shown in fig. 5. Second, both magnitude and timing of neural responses are informative.

Two types of data sets are evaluated using r: the experiments comparing neural responses to tactile stimulation in awake and anesthetized animals and experiments comparing neural responses to tactile and electrical stimulation.

What's old? Correlation analysis has been used successfully to demonstrate coactivation and coincidental firing of neurons involved in the processing of same or similar stimuli. This coincidental firing has been implicated in information processing. Usually information theory is used to assess the importance of observed cross-correlations. Simple correlations between two channels cannot be used to ascertain their functional link, as high correlations due to chance cannot be ruled out (the more channels are recorded the more of the false positives become possible). The analysis of the data becomes more complex.

What's new? The use of correlations looking at the neural responses from the same channel under same and/or various conditions has been limited. Moreover, the use of correlation coefficient as a determinant of "goodness" of recordings has not been reported. Simple correlation can be used to show similarity of response on the same channel. This is inbuilt into the main assumption that the same channel shows same activity only to the same stimulus (which provides nervous system with the power to discriminate between stimuli). Therefore, the probability of exceedingly similar responses recorded from the same channel to 2 different stimuli becomes negligible.
How is it done? In order to assess similarity of responses accounting for both magnitude and timing postevent histograms need to be generated. Each histogram depicts cumulative activity for a specified time period (typically the duration of a session). The data is binned and plotted for determined time interval after stimulus presentation. When stimulus is presented 3 times per second for 1 minute the total number of stimulation is 180. Cumulative histograms spanning over 333ms (interval between the stimulation) are produced. When bin size is determined to be 1ms, 333 values of bins are generated. Each value corresponds to the cumulative response rate. Therefore the probability of activity is assessed using these values. If at time 17ms after the stimulation the activity was observed 90 times (90 = bin value), the probability of response occurring at that time is 50 %. This measure indicates firing rate. The histograms provide information on the magnitude and timing of each response. The same type of stimulation is conducted at another time. Responses recorded during the second session are plotted using the same method. Now two data samples are available. Each sample consists of 333 values. These sets are the two distributions of neural responses. Using correlation the similarity of

responses can be assessed. The values within bin are compared across two data sets. Pairwise correlation checks for similarity of the bin values respecting the order. High correlations are reported when the corresponding bins have similar values. Low correlations result from dissimilar bin values.

Neuroexplorer software generates histograms. The bin values are transferred in SPSS and analyzed using Pierson's correlation algorithm. The resulting correlation coefficient is assessed for meaningfulness.

Post event interval

Evoked responses are characterized by the increase in firing rate and decreased background activity. This decrease in the background activity is termed replacing inhibition. This phenomenon improves signal to noise ratio which aids signal detection. The peaks in firing rate point out to primary information processing when they occur with the short latency. Longer latency responses are widespread but more difficult to attribute to the primary response. They usually are associated with further information processing that could take place either locally and at other stations of somatosensory pathway. Postevent interval used in the analysis, as a rule includes longer time period after the stimulation. This ensures that arbitrary operator does not introduce bias in the analysis and also allows to investigate all responses associated with the stimulation. Typically time period between stimulations is used for correlational analysis. Choosing specific time intervals could yield higher or lower correlations. Correlating just the primary responses improves correlation coefficient.

Bin size

Bin size is chosen to be 1ms. Data binned in 1ms produces most sensitive correlations. Larger bins could result in higher correlations due to the averaging or smoothing effect. The manipulation of data prior to correlational analysis was kept at minimum. Each spike recorded lasts from 1 to 1.5ms. The timestamps of the preset threshold crossings are recorded and put into 1ms bins. This size of the bin is adequate for "raw" representation of discharges.

Artifact

Visual inspection of histograms has to take place in order to identify plots depicting artifactual data, such as electrical noise. Offline software could be used to exclude suspicious waveforms from the analysis. Correlations are sensitive to high frequency responses associated with a particular bin. For example high correlations could be produced if the background activity is low and there is one bin containing high values. It takes only 1 bin with large size value to produce a high correlation. Other than stimulation artifact – the occurrence of such signal is significant and should be examined. When artifact is accounted for any such event indicates "real" response and channel exhibiting such activity would be useful for further analysis.

Fig. 6a and 6b illustrate responses recorded from 30 electrodes in response to stimulation of D1. During recording session channels 11, 12, and 13 were identified as responding to the stimulation. This figure is based on the data from two successive stimulation cycles of D1. The interval between stimulation sessions was 5 min. The monkey was awake. Correlation coefficients were generated for all channels in order to estimate the "goodness" of channels. Correlations of channels 11, 12, 13 and 28 were the

highest (r=>0.8) (fig.7). This finding was in accord with the previous estimation of neural activity (see Descriptive analysis). Channels 7, 17, 18, 23, and 30 showed r=>0.5. Other channels showed r<0.5. The lowest correlation reported was 0.005. Visual inspection of histograms confirms presence of appropriate neural responses on channels 11, 12, 13, 28. These responses are characterized by two peaks of activity: primary peak with latency of 17ms on average and secondary peak occurring at 220ms after stimulation. The peaks are rather strong and well defined. The response rate is high from p=0.4 to p=0.6. Channel 6 shows high firing rate of p=0.8 but no presence of peaks which indicate rather spontaneous activity. The correlation for this channel was low, r = 0.117. Channel 1 showed high peaks, but their timing was not locked to the stimulus. The correlation for channel 1 was r =0.05. Channels that showed temporal stimulus-response locking yielded correlation of above 0.8, while channels recording spontaneous activity or "noise" showed correlations up to 100 times less. Channels with highly correlated activity (r > 0.7) were defined as strong contributors to the information processing; those showing lower correlations (0.5<r<0.7) as weak contributors; channels showing low correlations as non-contributing channels as their activity could not be linked to the stimulus. The strong contributors are assumed to map the center of the receptive field, while weaker contributorsrespond to the stimulation of the surround. The receptive fields in area 1 are known to span several digits, so the overlap in the activity of neural pools is expected. The meaningfulness of the correlation coefficient was established using r squared. When r squared was = > 0.5 the channels were selected as primary encoders. Therefore the most contributing channels should show r=>0.7. The significance of coefficients

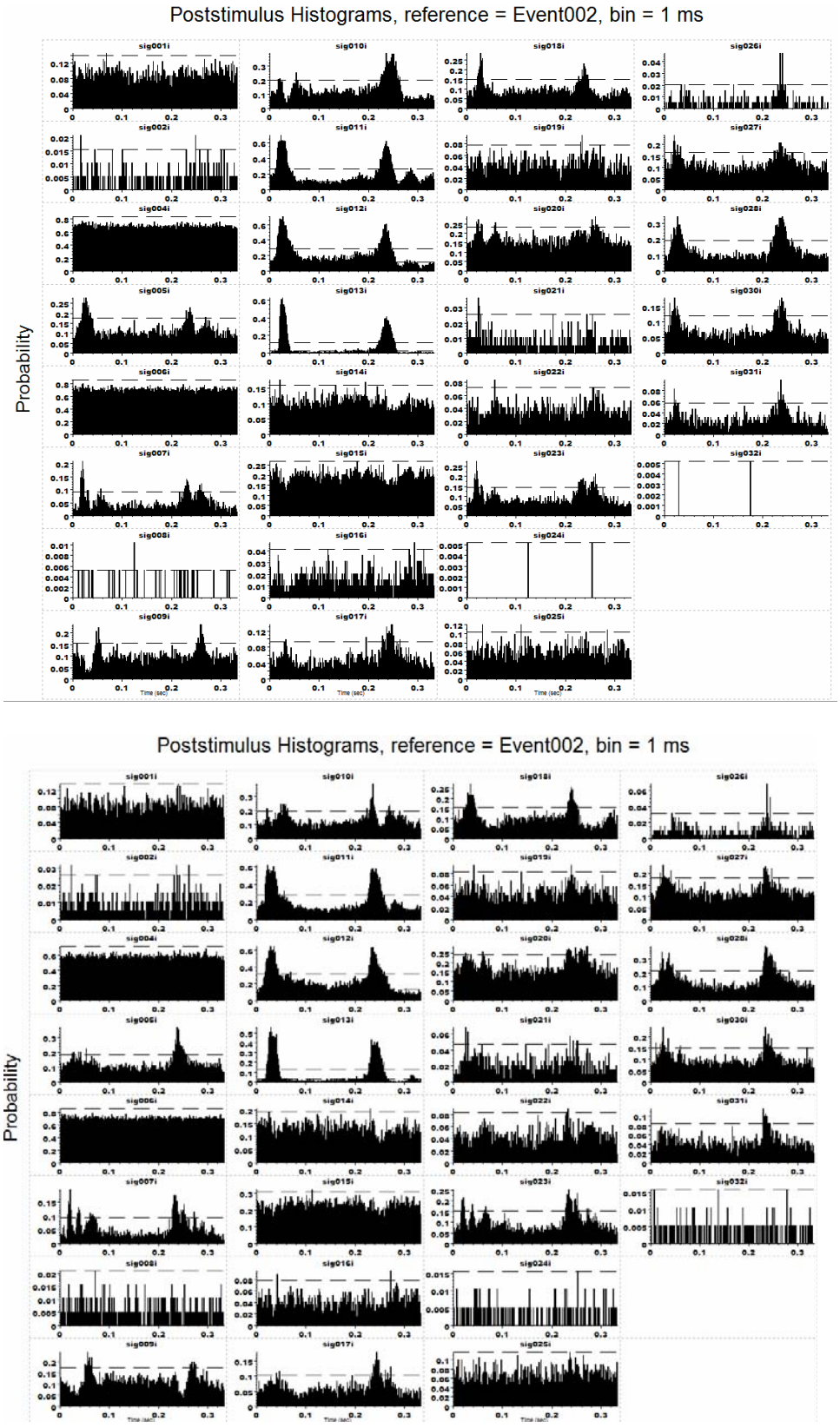

Fig.6. Poststimulus histograms depicting activity recorded from 30 channels following D1 stimulation in awake animal. These histograms were used to generate correlations for this condition. Fig.6a depicts first stimulation session. Fig.6b depicts second stimulation session. The responses on channels 11, 12, and 13 show stability.

becomes irrelevant as with such a range of r from 0.005 to 0.856 the significance is shown with coefficients starting at 0.1. The meaningfulness of r has to be considered when analyzing the results of correlational analysis. Some data might yield smaller coefficients that will be deemed meaningful. The meaningfulness criterion has to be established by the operator.

Based on the data channel 13 was chosen as an example of strong responder, representing D1. Channel 23 was chosen as an example of a weak responder: it responds somewhat to the stimulation of D1, but D1 does not constitute a center of the receptive field represented by ch.23. These results indicate high correlation for channels mapping the center of the receptive field and lower correlation for channels representing the surround of the receptive field. Spontaneous activity of the neural groups is associated with no meaningful correlation. Stimulation of D2 generates another pattern of activity as recorded from the same channels. Correlations for condition D2 are highest on channels 9 and 10 ($r>0.9$) (fig.7). Channels 11, 12 and 13 also show high correlation, although less than to D1 stimulation. Correlation on channels 7 and 23 is higher that in response to stimulation of D1. Channel 10 is chosen as an example of a strong responder, while channel 11 represents weak responsivity. Some channels show moderate and similar correlation in response to both conditions: channel 5 with $rD1=0.451$ and $rD2=0.495$. This channel contributes slightly to information processing regardless of the condition.

The lowest correlation observed in response to D2 stimulation was $r=0.007$. These results show that there is a deferential representation of evoked responses across channels and across conditions. D3 stimulation did not produce evoked responses with clear specificity to this condition. The highest correlation was $r=0.643$ on channel 7.

Digit / Channel	D1	D2	D3
1	-.005	.047	.019
2	.098	.312	.192
4	.032	.085	-.107
5	.451	.495	.204
6	.117	.106	-.064
7	.632	.843	.643
8	.033	.100	.043
9	.198	.949	.297
10	.313	.940	.537
11	.856	.685	.164
12	.854	.750	.247
13	.838	.855	.337
14	.137	.076	.078
15	.158	.033	-.089
16	.143	-.081	.005
17/1a	.562	.182	-.012
18/2a	.648	.355	.130
19/3a	.178	.273	.072
20/4a	.382	.625	.480
21/5a	.228	.028	.283
22/6a	.110	.229	.427
23/7a	.592	.842	.599
24/8a	-.063	-.059	-.032
25/9a	.054	.007	.070
26/10a	.231	.049	.014
27/11a	.457	.330	.002
28/12a	.797	.550	.205
30/14a	.578	.289	.141
31/15a	.472	.084	.012
32/16a	.005	-.063	-.034

Channel 23 correlation was r=0.599. Both channels were shown to be involved in responses to D1 and D2, although the center of receptive field was localized to D2. The multiunit activity on these channels points to a rather large receptive field representation. The lowest coefficient for condition D3 was reported to be r=0.002 (fig.7). Conditions D4 and D5 produced coefficients similar to condition D3.

Fig.7. Table of Correlation coefficients generated from two successive sessions of digit stimulation in awake animal. First two stimulation sessions were used for all conditions. Red highlight = r>.7; yellow highlight = r>.5; blue highlight = lowest r for the condition. The array of 32 electrodes was used for the recordings. Two rows of 16 channels. 30 channels are shown. Channels labeled with letter a form second row.

Recordings from awake animals are complicated by the behavioral responses to stimulation: repetitive stimulation could cause unpredicted movements on the part of an animal. These movements could interfere with the recordings. It could produce a movement artifact which is a neural activity that is not specific. Animals get tired of long sessions and that affects their disposition. They become moody and more difficult to handle. In order to establish feasibility of shorter stimulation sessions each 1 min session was broken down into two 30s intervals. Two successive stimulation sessions were used.

Fig.8a provides comparison of obtained coefficients for full 60s sessions and for 30s sessions in order to establish sufficiency of 30 trial session. A drastic change, e.g. a large decrease in the correlation coefficient would indicate insufficiency of such time interval.

Correlations of activity on channels encoding the center of the receptive field need to be evaluated. Both conditions D1 and D2 were assessed. The first 30 seconds of the session were used to generate histograms and correlations. As can be seen from the table channels 11, 12, and 13 show high correlation in response to D1 stimulation. These correlations are well above 0.7. Specifically channel 11 r = 0.780, channel 12 r= 0.797, channel 13 r= 0.769.Though high and meaningful these correlations decreased on average by 7.5% from correlations generated using 60s interval. Increasing the duration of the stimulation session to 5min did not improve the magnitude of the correlation coefficient. Other active channels show comparable decrease in the magnitude of correlation. D2 stimulation resulted in the following coefficients: channel 9 r=0.905 and channel 10 r=0.883. The decrease in coefficient strength with 30s trials averaged 5.5%. Other channels showed similar decreases in the correlation coefficient.

Number of stimulus presentation affects the magnitude of the coefficient. Therefore, longer stimulation sessions are more desirable. At 3Hz 1min of recordings provides more sensitivity to correlational analysis. The duration of session affects coefficients slightly. However, shorter sessions show usefulness as the correlation resulted from such sessions are meaningful (r>0.7).

Fig.8b illustrates results of paired samples t-test. The comparison was made between 2 correlation distributions shown in fig.8a. Paired samples t-test compares values on case to case basis; it does not rely entirely on the mean estimates like an

Condition / Channel	D1 60s	D1 30s
1	-.005	-.055
2	.098	.021
4	.032	-.059
5	.451	.253
6	.117	.128
7	.632	.459
8	.033	-.068
9	.198	.094
10	.313	.312
11	.856	.780
12	.854	.797
13	.838	.769
14	.137	.086
15	.158	.034
16	.143	.118
17/1a	.562	.267
18/2a	.648	.444
19/3a	.178	-.013
20/4a	.382	.253
21/5a	.228	.092
22/6a	.110	.026
23/7a	.592	.386
24/8a	-.063	-.018
25/9a	.054	-.081
26/10a	.231	.243
27/11a	.457	.266
28/12a	.797	632
30/14a	.578	.425
31/15a	.472	.173
32/16a	.005	-.018

T-Test

[DataSet0]

Paired Samples Statistics

		Mean	N	Std. Deviation	Std. Error Mean
Pair 1	D160s	.33620	30	.287204	.052436
	D130s	.22487	30	.261761	.047791

Paired Samples Correlations

		N	Correlation	Sig.
Pair 1	D160s & D130s	30	.955	.000

Paired Samples Test

		Paired Differences					t	df	Sig. (2-tailed)
		Mean	Std. Deviation	Std. Error Mean	95% Confidence Interval of the Difference Lower	Upper			
Pair 1	D160s - D130s	.111333	.086045	.015710	.079204	.143463	7.087	29	.000

Fig.8. Fig.8a summarizes correlation coefficients resulted from comparison of frequency distribution. Two conditions were used. 60s condition included two files of 60s length each. 30s condition resulted from splitting both full file into two 30s periods and correlating first 30s of each file. Red highlight r>.7; yellow highlight r>.5. Strong responders such as channels 11, 12, and 13 show slight decrease in correlation; weaker responders -channels 28 and 30 show more significant decrease. Fig.8b summarizes results of paired samples t-test comparing 2 correlation distributions. The decrease of time interval from 60 to 30s produced significant changes in coefficient distributions.

independent samples t-test. The results indicate significant difference between two distributions (p=.000 on a 2-tailed test). This difference is attributed to the change in the session duration. Statistical methods that are based on mean comparison produce results that are not necessarily useful when assessment of both temporal resolution and the magnitude of responses is required. The results of such tests indicate significance level, but meaningfulness of such results should be assessed by an operator. In this example, t-test shows differences in distributions, but the correlations show only slight decrease in

magnitude. Thirty second sessions could be used, as they generate meaningful correlations that still assist in establishing the "goodness" of recordings.

The duration of stimulus presentation might affect information processing. These changes in neural signals might be indicative of habituation. In order to investigate fluctuations in neural responses throughout one minute stimulation session the following analysis was implemented. D2 stimulation sessions were used. A total of 4 sessions was used. Each file was broken down into two 30s intervals. Correlations were generated for various combinations of these 30s interval files in order to assess the effects of continuous stimulation. In fig.9 correlations are summarized for all 30 channels. For condition D2 channels 9 and 10 were identified as strong responders (see fig.7). Correlations using the first 30s from two sessions were 0.925 for channel 9 and 0.880 for channel 10 (Fig.9a). Correlations between the first 30s of session1 and the last 30s of session 2 produced: r=0.879 for channel 9 and r=0.874 for channel 10. The decrease in activity was on average 2.5%. Other 2 sessions of D2 stimulation were correlated. Correlations between last 30s of both sessions yielded: channel 9 r=0.865 and channel 10 r= 0.841 (fig.9a). Correlations between last 30s of session1 and first 30s of session 2 show slight increase in the magnitude of the coefficients: channel 9 r=0.894 and channel 10 r=0.864.

The average increase in the coefficient magnitude was 3%. Overall, coefficients showed good discriminative power under these conditions: spontaneous activity showed exceedingly low coefficients (as can be seen on the "noisy" channels), and channels responding to the stimulation of RF surround showed lower but somewhat meaningful coefficients. The overall distribution of coefficients were stable across conditions

(regardless whether first or last intervals were used or whether first and last intervals were compared in the analysis). These results indicate that correlations could be obtained from split files without significant loss of information. The application for such analysis is needed when limited data sets are available to be included in the estimation of baseline

Condition / Channel	D2 First 30s & First 30s	D2 First 30s & Last 30s
1	-.066	-.004
2	.229	.105
4	.089	-.010
5	.440	.367
6	.127	.045
7	.772	.770
8	.082	.050
9	.925	.879
10	.880	.874
11	.603	.479
12	.675	.587
13	.822	.777
14	.018	-.003
15	.071	.029
16	.022	-.051
17/1a	.053	.063
18/2a	.265	.136
19/3a	.252	.106
20/4a	.511	.417
21/5a	.120	.105
22/6a	.263	.195
23/7a	.760	.745
24/8a	.024	-.080
25/9a	-.089	.025
26/10a	.050	.028
27/11a	.163	.175
28/12a	.404	.371
30/14a	.265	.123
31/15a	-.001	.143
32/16a	-.085	.032

Condition / Channel	D2 Last 30s & Last 30s	D2 Last 30s & First 30s
1	-.052	.115
2	.223	.323
4	-.010	.047
5	.279	.326
6	.056	.044
7	.773	.764
8	.063	-.102
9	.865	.894
10	.841	.864
11	.499	.411
12	.616	.610
13	.800	.689
14	.095	-.062
15	.031	.098
16	.048	.056
17/1a	.069	.285
18/2a	.180	.245
19/3a	.200	.341
20/4a	.497	.448
21/5a	.108	.128
22/6a	.225	.131
23/7a	.737	.743
24/8a	.064	.000
25/9a	-.017	.032
26/10a	-.035	.101
27/11a	.152	.129
28/12a	.372	.352
30/14a	.252	.202
31/15a	.097	.072
32/16a	-.033	.076

Fig.9. Fig9a lists correlation coefficients resulted from comparison of two sessions of D2 stimulation. Each session was spit into two 30s intervals. First column corresponds to the assessment of similarities between neural responses for the first 30s of stimulation. Second column provides comparison between first and last 30s intervals. Channels 9and a10 are strong responders for this condition. Fig.9b provides correlations between two last 30s sessions and between last and first 30s sessions.

level of neural responses. The correlations between several pairs of 30s intervals could be averaged in order to provide a more realistic index of activity. Correlation coefficients provided stable and sensitive measure of neural responses.

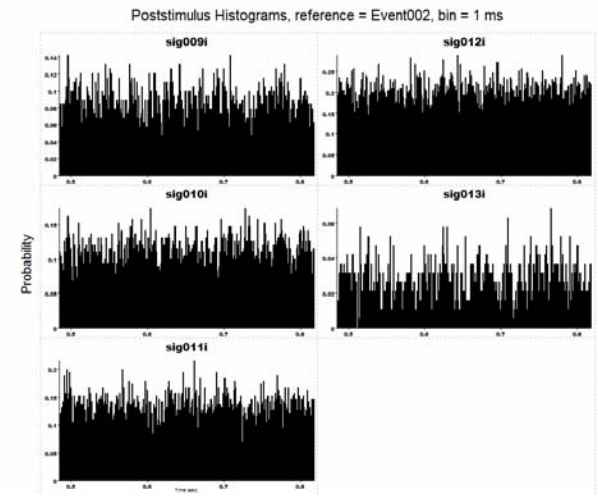

Channel \ Condition	Spontaneous activity
9	.069
10	.026
11	-.016
12	-.104
13	-.058

Fig.10. Poststimulus histograms depict the rate of activity on channels identified as strong responders for condition D1 and D2. The firing rate is low. Table of correlation coefficients reports values for these channels.

In order to assess activity in channels identified as strong responders in absence of any stimulation, spontaneous activity was recorded. Previous figures provide support for good discriminative capabilities of correlational analysis. As can be seen from fig.7 correlations yield a sensitive index of activity. For example, strong responders for D1 and D2 stimulation sessions show very low correlations during stimulation of D3. Correlations on these channels plummeted even further when no stimulation was presented (fig.10). All channels showed exceedingly low correlations, which supports previously presented evidence of their involvement in information processing.

Histograms indicate low firing rate (15%). The frequency distributions of recorded signals show very little fluctuation in activity for the duration of the whole interval.

Analysis of data using Pierson's r provides evidence for stability, sensitivity, and meaningfulness of such an index of neural activity.

Results II

Awake.

This section describes studies conducted on two monkeys, initially awake and later anesthetized, to assess the effects of ketamine anesthesia on cortical responses to tactile stimulation. Three to five cycles (each cycle consisted of five stimulation sessions – one for each digit) of stimulation were administered to the animals before the induction of anesthesia. Correlation coefficients were generated for all animals for all stimulation sessions. The best responding channels were identified for each digit. The correlations from these channels were compared for stability over several cycles of stimulation. These correlations also provide means for assessment of recordings over time as several experiments were conducted for each animal. Correlations within and between experiments were compared. The correlations were obtained by assessing similarity of frequency distribution. To establish reliability of coefficients multiple cycles of stimulation were used in each animal (three cycles of stimulation were used for animal 1 and five for animal 2). For animal 1 correlations for condition D1 are presented. For this animal 2 experiments separated by one week were analyzed (experiment 1 and experiment 2). For animal 2 correlations for conditions D2 and D5 are presented.

The results for animal 1 are summarized in fig.11 and fig.12. The first 3 correlations corresponding to awake state during experiment 1 produced following coefficients: channel 13 awake1 r=0.838, awake2 r=0.889, awake3 r=0.824; channel 12 awake1 r=0.854, awake2 r=0.766, awake3 r=0.729; channel 11 awake1 r=0.856, awake2 r=0.808, awake3 r=0.707 (fig.11). The mean r for channel 13 was 0.850; the range of coefficient magnitude constituted 7%. (For range estimation the difference between

highest and lowest coefficients was expressed in percentages of the highest coefficient. Range% = (r high – r low)/r high). Channel 12 average r=0.783, the range was 14%. Channel 11 mean r=0.790, the range was 17%. Experiment 2 yielded following results: channel 13 awake1 r=0.716, awake2 r=0.698, awake3 r=0.851; channel 12 awake1 r=0.727, awake2 r=0.687, awake3 r=0.864; channel 11 awake1 r=0.708, awake2 r=0.696, awake3 r=0.840. Channel 13 mean r=0.755, range = 18%. Channel 12 mean r=0.759, range = 20%. Channel 11 mean r=0.748, range = 17% (fig12). Despite such a high range of r (up to 20%), the magnitude of the correlation stayed meaningful (>0.7).

Averaging coefficients across several stimulation sessions for the awake condition

Channel / File#	7	9	10	11	12	13	17/1a	18/2a	23/7a	28/12a	30/14a
2&7	.632	.198	.313	.856	.854	.838	.562	.648	.592	.797	.578
2&13	.661	.537	.616	.808	.766	.889	.284	.535	.633	.758	.708
2&14	.304	.066	.191	.707	.729	.824	.249	.411	.302	.599	.447
2&19	.482	.302	.360	.697	.665	.762	.385	.406	.519	.738	.541
2&24	.496	.226	.072	.615	.492	.504	.405	.548	.514	.607	.590
2&31	.436	.393	.059	.673	.703	.643	.185	.517	.414	.630	.574
2&36	.394	.220	.428	.750	.622	.772	.099	.437	.307	.741	.658
2&41	.367	.219	.458	.792	.771	.855	.284	.612	.392	.773	.666
2&46	.604	.295	.570	.834	.759	.895	.476	.619	.617	.819	.752
2&49	.351	.139	.017	.280	.433	.467	-.109	-.111	.357	.475	.364
2&54	.308	.062	.011	.179	.383	.416	-.086	-.186	.305	461	.419
2&57	.367	.161	-.031	.549	.538	.620	-.055	-.010	.363	.528	.456
2&62	.243	.126	.023	.223	.403	.561	.115	.010	.182	.553	.392
2&67	.617	.479	.499	.883	.818	.844	.240	.568	.642	.800	.764
2&72	.400	.219	.462	.668	.580	.790	.395	.467	.382	.647	.648
2&77	.388	.165	.267	.579	.731	.705	.013	.142	.241	.447	.321
2&82	.370	.094	.163	.623	.531	.651	.098	.199	.236	.462	.395
2&83	.080	-.034	-.021	.387	.333	.361	.137	.191	.136	.230	.243
2&88	.100	-.105	-.073	.223	.307	.416	.122	.202	.101	.207	.173

Fig.11. Experiment 1, Animal 1.Correlation coefficients were generated for channels showing r>.0.5 in response to D1 stimulation. The correlations were generated for all stages of the experiment: awake, anesthetized, and recovery. First 3 lines correspond to awake condition. Red highlight (2&19)= Ketamine injection; light grey highlight = strong responders during awake condition. Darker grey (2&24) = decrease in correlation coefficients following Ketamine. Dark grey (2&49)= onset of drastic decrease in correlation magnitude (beginning of recovery stage).

Channel / File#	11	12	13
2&9	.708	.727	.716
2&11	.696	.687	.698
2&12	.840	.864	.851
2&14	.914	.858	.872
2&15	.866	.802	.830
2&21	.675	.667	.714
2&23	.714	.660	.711
2&29	.518	.365	.399
2&34	.304	.294	.269
2&36	.656	.739	.669
2&38	.520	.476	.576
2&40	.681	.708	.683
2&42	.322	.350	.254
2&47	.665	.696	.773
2&48	.774	.785	.727

Fig.12. Experiment 2, Animal 1: D1 stimulation. Correlation coefficients were generated for strong responders: channel11, 12, and 13. The correlations were generated for all stages of the experiment: awake, anesthetized, and recovery. First 3 lines correspond to awake condition. Red highlight = Ketamine injection; light grey highlight = strong responders during awake condition. Dark grey = onset of drastic decrease in correlation magnitude (beginning of recovery stage); yellow highlight = improvement of correlation magnitude following 1 hour recovery stage.

provides a more reliable index of similarity of neural responses. This averaging can be used only for conditions when internal state of the animal is assumed to be stable throughout a condition. In awake animal although such variables as attention and arousal interfere with the signal processing, the goal of the study was not to uncover the effects of those variables, therefore averaging of correlations could be used. Across two experiments channel 13 showed 12% decrease in mean r; channel 12 showed 3% decrease; and channel 11 showed 5% decrease. These results indicate that the fluctuation of responses within the experiment is comparable to the dissimilarity of responses across experiments. This points to reliability of the recording electrodes and stability of the system, as the period between two experiments was one week.

To support the data showing reliability of correlation coefficient throughout awake condition correlations from animal 2 are presented. D2 stimulation (fig.13a) produced following coefficients: channel 16 awake1 r=0.771, awake2 r=0.856, awake3 r=0.836, awake4 r=0.833, awake5 r=0.891; channel 23 awake1 r=0.712, awake2 r=0.933, awake3 r=0.819, awake4 r=0.869, awake5 r=0.876. Channel 16 mean r=0.838, range =

14%. Channel 23 mean r=0.842, range = 24%. The fluctuation in neural responses is observed, but the magnitude of coefficients indicates meaningfulness. Stimulation of D5 (fig.13b) in the same animal resulted in following coefficients: channel 13 awake1 r=0.679, awake2 r=0.837, awake3 r=0.832, awake4 r=0.770, awake5 r=0.734. Channel 13 mean r=0.770, range = 19%. These results are consistent with results obtained from animal 1.

Correlations show usefulness as indices of activity for pairs of sessions and for the condition overall. Correlations show stability across conditions and across experimental sessions. Similar ranges of r were obtained for both animals. The range of r was as high as 24%, but the magnitude of correlations was meaningful throughout all sessions (r>0.7).

Condition / Channel	Session 1 D2 Awake	Session 2 D2 Awake	Session 3 D2 Awake	Session 4 D2 Awake	Session 5 D2 Awake
16	.771	.858	.836	.833	.891
23	.712	.933	.819	.869	.876

Condition / Channel	Session 1 D5 Awake	Session 2 D5 Awake	Session 3 D5 Awake	Session 4 D5 Awake	Session 5 D5 Awake
13	.679	.837	.832	.770	.734

Fig.13. Fig.13a presents correlations obtained after stimulation of D2 in awake animal 2. The results for strong responders are summarized. 5 stimulation sessions were used. Fig. 13b reports correlations corresponding to D5 stimulation sessions in the same animal.

Anesthesia

The next stage of the experiment involved administration of the anesthetic agent. After the injection behavior of an animal was observed and recorded in order to correlate behavioral characteristics with neural responses. Behaviorally the induction phase of the anesthesia lasted from 5 to 15 minutes as was evident by the transition of an animal from fully awake to a catatonic and an overall non-responsive state: no reaction to otherwise aversive stimuli such as loud noise was observed. Any change in position and movement was recorded. Neural responses from animal 1, experiment 1 are presented for the induction stage (fig.11). Following injection of ketamine stimulation of D1 produced following coefficients: channel 13 r=0.762, channel 12 r=0.665, channel 11 r=0.697 (fig.11, file#2&19). These coefficients indicate slight decrease in the magnitude of coefficient: channel 13 decreased 11% from the mean coefficient for the awake state; channel 12 – 15%; channel 11 -12%. Five minutes after the injection D1 stimulation was repeated. Channel 13 r=0.504, channel 12 r=0.492, channel 11 r=0.615 (fig.11, file#2&24). The dissimilarity of distribution persisted and resulted in decrease in coefficients: channel 13 – 40%; channel 12 – 37%, channel 11 – 22%. It can be seen that the magnitude of the correlation has fallen to around 0.5. This decrease in the correlation coefficient was coincidental with the cessation of movement in monkey. Notes read: “Eyes blinking, open, no other movement”. The transitional state from awake to anesthetized condition corresponded to changes in the neural responses. Seven minutes later another stimulation session was conducted. At that point the animal was assessed to be anaesthetized based on the absence of blinking and unresponsiveness to tactile and auditory stimuli: “monkey has gone in deeper anesthesia”. During that session neural

responses recovered. Channel 13 r=0.643 (26% decrease from awake), channel 12 r=0.703 (9%), channel 11 r=0.673 (14%) (fig.11, file#2&31).

For the next 30 minutes monkey showed no significant movements. This stage was defined to be the maintenance stage of anesthesia. The recordings from this stage yielded high correlations comparable to those produced in the awake state. Channel 13 an.1 r=0.772, an.2 r=0.855, an.3 r=0.895; channel 12 an.1 r=0.622, an.2 r=0.771, an.3 r=0.759; channel 11 an.1 r=0.750, an.2 r=0.792, an.3 r=0.834 (fig.11, files#2&36, 2&41, 2&46). The coefficients never fell bellow 0.5 and showed acceptable stability. For the maintenance phase correlations were averaged. Channel 13 mean r=0.840, range = 14%; channel 12 mean r=0.717, range = 20%; channel 11 mean r=0.792, range = 10%. These correlations are very similar to the ones obtained during awake state. During deep anesthesia the distribution of neural responses shows high degree of similarity with the distributions obtained from awake animal.

For the next hour monkey was progressively showing more movement: from limb extension and blinking to fruit acceptance and consumption. This stage was termed recovery stage. Initially the onset of this stage was characterized by the plummeting of correlations, with the most severe decrease observed on channel 11 (fig.11, files#2&49 through 2&88). The correlations fell to the levels of “spontaneous” activity: channel 11 r=0.179(78%). Later during recovery stage the correlations recovered somewhat, but as a rule seldom passed 0.7 threshold. The averages for this period were as following: channel 13 mean r=0.598, 30% decrease; channel 12 r=0.535, 32% decrease; channel 11 r=0.532, 32% decrease. Behaviorally monkey was observed to recover from anesthesia, but the correlations never recovered fully to preanesthesia levels. As can be seen from the table

there is a good amount of fluctuations of coefficients during recovery phase, but the stability observed in awake condition is not obtained.

The results of sessions of D2 stimulation in anaesthetized monkey are summarized using channel 10 recordings (fig.14a). The maintenance stage showed stable coefficients – above 0.7. The average for this stage for channel 10 was r=0.774, range = 7%. These results support findings obtained from D1 stimulation sessions in the same animal.

Condition / Channel	Session 1 D2 Maintenance	Session 2 D2 Maintenance	Session 3 D2 Maintenance	Session 4 D2 Maintenance
10	.770	.788	.766	.721

Condition / Channel	Session 1 D2 Recovery	Session 2 D2 Recovery	Session 3 D2 Recovery	Session 4 D2 Recovery
9	.170	.181	.464	.537
10	.172	.312	.392	.327

Fig.14. Fig.14a summarizes coefficients for D2 stimulation sessions in anesthetized animal 1. Fig.14b presents coefficients for the recovery stage in the same animal.

The transition from deep anesthesia, i.e. recovery stage was characterized by plummeting coefficients (fig.14b): The lowest coefficient for channel 9 was r=0.170 and for channel 10 r=.0172. Such low coefficients indicate great degree of dissimilarity between distributions. The magnitude of the coefficients is exceedingly low and corresponds to “spontaneous” activity.

Strong responders for both D1 and D2 conditions show specific patterns of activity. For both conditions awake state resulted in stable coefficients, maintenance phase produced stable coefficients, but the recovery stage was characterized by decrease in the coefficients to the levels of "spontaneous" activity. It can be seen from the table that activity of strong responders was influenced by the stage of anesthesia and other channels: "surround" responders have shown decrease in the coefficients. This finding points to changes in neural activity encoding tactile stimuli during recovery period.

Experiment 2 in the same animal produced similar findings (fig.12). D 1 stimulation sessions are used to illustrate these results. Channels 11, 12, 13 show stability during awake, induction, and maintenance phases but coefficients decrease dramatically 40 min after the induction of anesthesia – during the recovery phase (fig.12, files#2&29 through 2&42). One hour after the onset of the recovery stage the coefficients increase across all 3 channels and therefore gain stability, reaching the baseline (awake values). The last 2 files show following coefficients: channel 13 r1=0.773, r2=0.727; channel 12 r1=0.696, r2=0.785, channel 11 r1=0.665, r2=0.774 (fig.12, files#2&47 and 2&48). This increase in stability indicates the end of the recovery phase.

To summarize, the results indicate that awake and anesthetized states are characterized by the comparable similarity indices (r) while recovery stage produces drastic fluctuations of coefficient magnitude as evidenced by decreasing values of the coefficients. In order to investigate the reasons for low coefficients produced during recovery stage – the frequency distributions (in the form of histograms) have to be examined. Following figures depict major changes observed within these distributions. Several variables were investigated: the firing rate, duration of the response (peaks of

activity), and relative contributions of first vs. second peaks to the decrease in the correlations.

In order to assess relative contributions of early and late peaks on the obtained correlations 333ms interval was broken down into first 150ms, that included first peak and background activity, and into last 183ms that included late peak and other activity. Only peaks were established to affect the magnitude of correlation coefficients: background (intervals between peaks) produced $r<0.01$. Fig.15 illustrates results for two time intervals: early and late. The data corresponds to the same experiment as fig.11, channel 13. As can be seen in awake animal (fig.15, files#2&7, 2&13, 2&14) both time intervals produced high coefficients ($r>0.7$). During the induction of anesthesia (fig.15, file#2&24) first 150ms contribute to the decrease in the magnitude of correlation. The last 183ms (late peak) period still shows high correlation. After the induction of anesthesia, during maintenance phase, first 150ms interval contributes to the decrease in coefficients (fig.15, file#2&31, through 2&46). The magnitude of correlations for this period remains relatively high ($r>0.5$), which explains only slight decrease in the coefficients for the whole 333ms period (fig.11). The recovery phase is associated with further plummeting of correlations, especially for the late 183ms period (fig.15, file#2&46, 2&54). The correlations for this late interval reach levels of “spontaneous” activity.

To summarize, in awake animal both peaks of activity contribute equally to the magnitude of correlations. Both show consistently high correlations. During induction, early peaks drive the decrease in correlations. Throughout the maintenance phase early peaks show stable decrease in the correlation magnitude. This decrease indicates changes

in neural signals – in primary response. During recovery phase both early and late peaks show decrease in the coefficients. Late peaks negatively affect correlations only during the recovery phase.

Interval / File#	0-150ms	151-333ms
2&7	.799	.901
2&13	.696	.780
2&14	.941	.695
2&19	.793	.740
2&24	.284	.864
2&31	.505	.835
2&36	.676	.939
2&41	.604	.934
2&46	.463	.859
2&49	.446	-.081
2&54	.537	.030

Fig.15. Data corresponds to animal 1, experiment 1, D1 stimulation, channel 13 recordings. Correlations were obtained by splitting 333ms file into two time intervals. Each interval contains a peak and background activity. Red highlight = Ketamine injection, grey highlight = r<0.5.

To investigate changes in neural responses associated with anesthesia, frequency distributions were further analyzed. The duration of responses (both early and late peaks) are summarized in fig.16. As can be seen, the duration of early peaks decreases from induction and continues through recovery phase. Early peaks become sharper. Average peak duration during awake stage was 25ms, while mean duration for anesthetized condition was 15ms (40% decrease). The firing rate (of the peak) during awake and anesthetized conditions varies slightly (fig.16). In awake animal average rate was 57%, while in anesthetized it constituted 53%. Late peaks also show decrease in duration during anesthetized condition. In awake animal average duration was 35ms; in anesthetized it was 24ms (30% decrease). The mean firing rate for both awake and anesthetized conditions was 47%. The major effect of anesthesia was observed on the

duration of the response. Overall the duration of responses decreases for early and late peaks. The firing rate was not affected.

Interval / File#	0-150ms		151-333ms	
	Peak Duration (ms)	Max Firing Rate (%)	Peak Duration (ms)	Max Firing Rate (%)
2	21	63	40	42
7	28	56	44	45
13	23	58	30	51
14	28	50	27	51
19	20	53	28	55
24	11	61	22	33
31	15	55	20	58
36	15	50	30	50
41	17	51	24	45
46	12	50	24	44
49	14	56	26	37
54	14	50	20	53

Fig.16. Same files were used as in fig.15. Red highlight = Ketamine injection. Peak duration and maximum firing rates are presented for early and late intervals.

Fig.17 illustrates patterns of frequency distributions corresponding to all stages of the experiment. Fig.17a shows that in awake animal there is a close correspondence of the timing and duration of evoked responses. Both early and late peaks show stability. Induction phase (fig.17b) is characterized by sharp early peaks (green trace). The onset of the peak occurs earlier. During induction, late peak becomes slightly shorter (this is not reflected by the magnitude of correlation coefficients). There is a greater degree of an overlap between late peaks than between early peaks. Fig.17c illustrates changes in the distributions characteristic of the maintenance phase. Late peaks show good correspondence for both anesthetized and awake conditions, while early peak for anesthetized condition (green) is shorter. The duration of this peak has increased since the induction phase. Also, the onset of the peak is more in phase with the onset for the awake

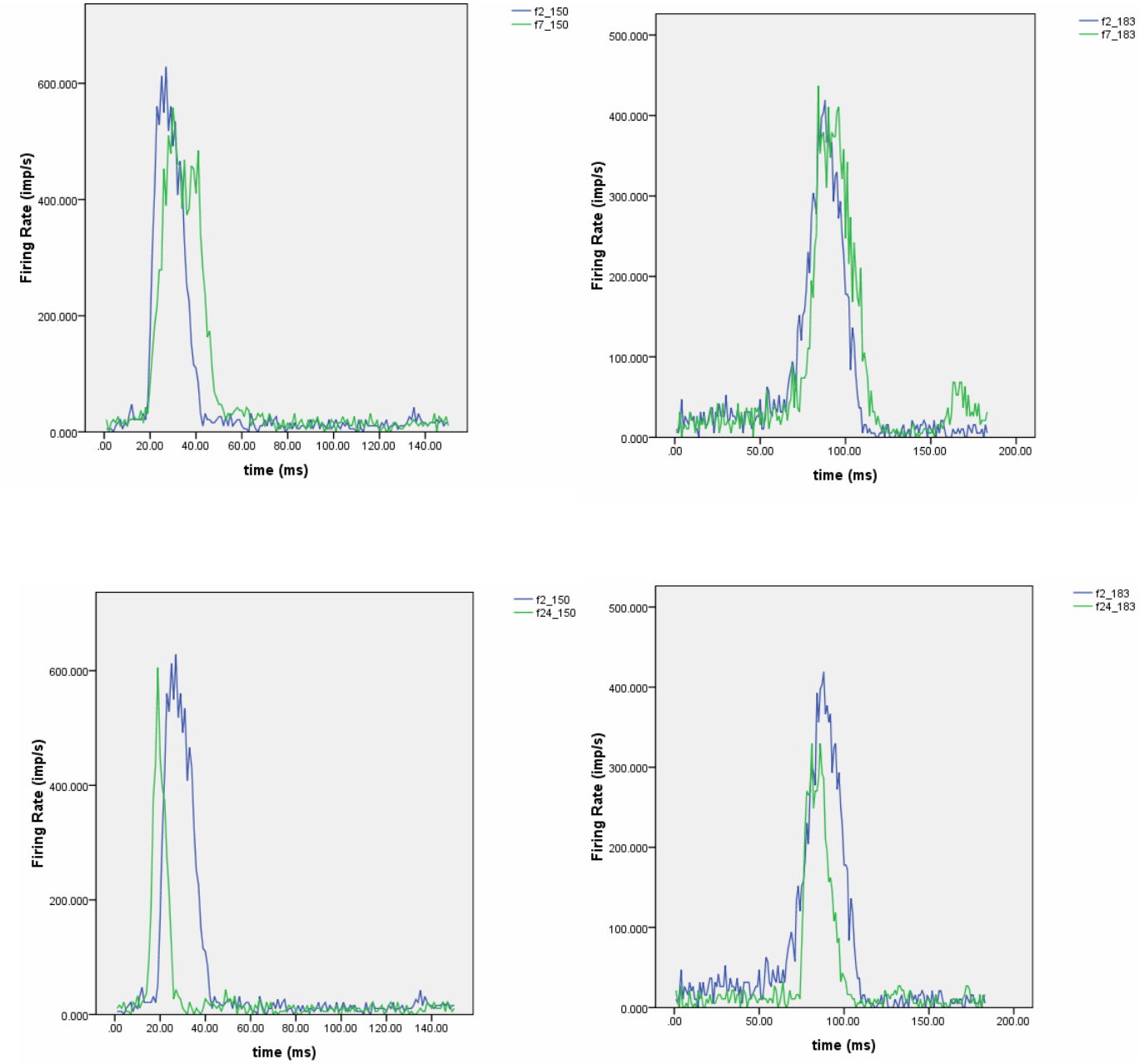

Fig17. Fig.17a - first panel: frequency distributions are plotted for two awake data files: file #2 = blue, file #7 = green for early and late intervals separately. Fig.17b – second panel: blue = awake, green = induction of anesthesia.

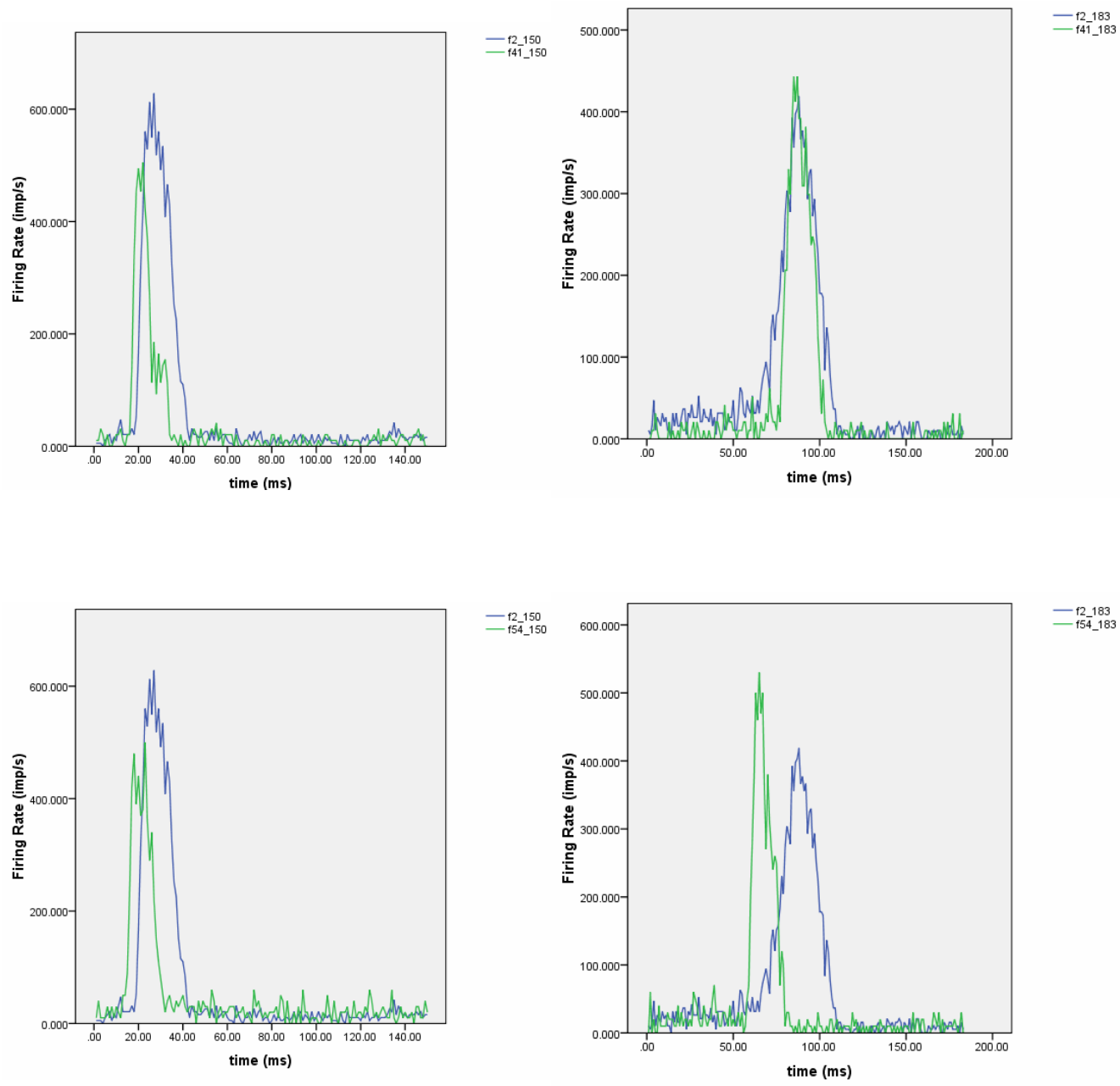

Fig17. Fig.17c - third panel: blue = awake, green = maintenance. Fig.17d – fourth panel: blue = awake, green = recovery.

(blue) condition. There is a greater degree of an overlap between these distributions than during the induction phase. Finally, during recovery (fig.17d) both late and early peaks show little correspondence between awake (blue) and anesthetized (green) states. The neural responses to stimulation are present, but their duration and timing has changed. Late peak has a much earlier onset; the duration of early peak decreases.

Throughout all phases of anesthesia the duration of neural responses decreases. The magnitude of responses changes slightly. The timing (latency) of response is markedly affected during induction and recovery phases. Maintenance phase is characterized by decreased response duration.

These findings indicate that the most dramatic changes in signal encoding occur during induction and recovery stages. Maintenance stage is associated with some changes in neural responses, but overall the pattern of activity is similar to awake condition. Ketamine anesthesia is suitable for investigation of patterns of neural responses evoked by tactile stimulation.

Results III

The results described in this section were obtained during acute preparations. Neural responses to tactile and microstimulation were investigated. Spatio-temporal characteristics of neural population recordings were described.

Tactile stimulation

Six monkeys were used in acute experiments. All were conducted under conditions of general anesthesia maintained by Isofluorine and Fentanyl. Experiments involving mechanical stimulation of several skin locations in anesthetized animals aimed at characterization of patterns of evoked responses. Somatotopic maps were produced in all animals. The following results illustrate how information about stimuli is represented in space and in time. As the majority of experiments involved SI, area 1 recordings more attention is given to the characterization of the patterns of neural responses collected from that area.

Fig.18 is composed of neural recordings from area 1 collected from a 32 channel microelectrode array. The postevent rasters plot neural population responses against time. Every dot on the raster represents a time point at which the preset threshold of activity was broken. The threshold was determined by initial assessment of activity on all channels, i.e. identification of neural responses: the amplitude of the response. The appropriate threshold values were chosen for each channel. In this example, sequential stimulation of all 5 digits and 7 pads was carried out. The duration of each stimulation session was 30s. The cumulative representation of the results of all stimulation experiments provides an opportunity to assess the degree of activation of SI units in response to stimulation of each skin location (receptive field encoding). Both spatial and

temporal domains are crucial in the description and analysis of the neural responses within the same or across all recording sites. The most typical patterns of neural responses encountered in all anesthetized animals are illustrated in Fig.18. In the

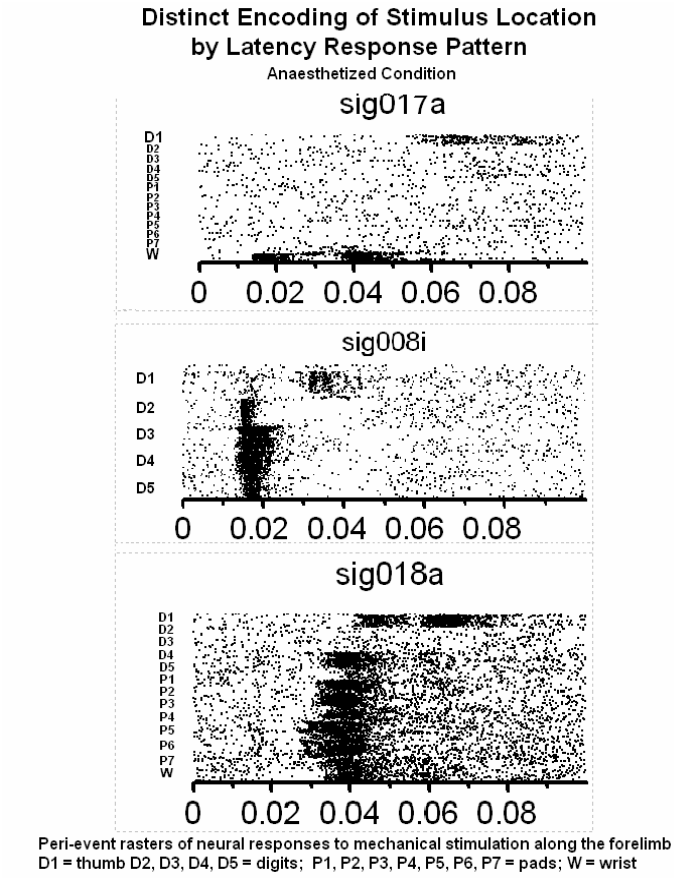

Peri-event rasters of neural responses to mechanical stimulation along the forelimb
D1 = thumb D2, D3, D4, D5 = digits; P1, P2, P3, P4, P5, P6, P7 = pads; W = wrist

Fig.18. Perievent rasters representing common encountered patterns of neural recordings from area 1. Hand locations were stimulated. Each raster line corresponds to the duration of the post stimulus interval. Each skin location was stimulated for 30s – yielding 30 lines for each condition. Responses are characterized by the 17ms latency onset, 10-15ms duration, early and late responses, generalized RFs.

illustrated example channel 17 recordings show primary response corresponding to the wrist stimulation at 17ms onset latency this primary response is followed by the second peak of activity at 36ms latency. The RF representation is primarily localized to the wrist. The high response rate indicates close to center RF encoding. The late response is also present and occurs at 60ms poststimulus. This response corresponds to D1 stimulation session. The firing rate shows decrease compared to the level of activation following wrist stimulation. This indicates that the channel is a primary encoder for the wrist and also is a surround encoder for D1. The duration of all responses spans 20-50ms. Signals recorded from channel 8 point to a large RF encompassing almost all digits. The early primary response is observed following stimulation of D2 through D5. The onset

latencies are comparable but the duration of the response varies with the longest associated with the D3 stimulation. D1 is also represented but both the magnitude of response and temporal signature are different from other digit representations. This is not surprising as D1 is the opposing thumb usually separated physically and functionally from other digits. The 35ms latency response to D1 stimulation is preceded by the suppression in the firing rate. Also replacing inhibition is observed following primary responses to other stimulation conditions. Channel 18 recordings show generalized activation pattern. Eleven out of 13 stimulation experiments elicit significant responses from these multineuron recordings. The onset of the responses is rather late. The earliest response occurs at 30ms poststimulus. Pattern of responses and timing for condition D1 is distinctly dissimilar to all other conditions. Firing rate is high and duration of responses is 20ms, on average.

Neural population recordings through multi-electrode arrays in the VPL and S1 cortical areas 3b, 1 and 2 revealed distinct response patterns that represent location, intensity, frequency and submodality of natural somatosensory stimulation in anesthetized monkeys. To highlight some of the features of these responses the relationship between firing rate and latency of response was investigated.

Fig.19 outlines both latency and response rate of the signals simultaneously recorded from 4 electrodes placed in the VPL (1-4) and 32 electrodes (5-36) arranged in two rows in the S1 (area 1) hand area. The data were averaged over 400 tactile stimuli on the D4. Firing rates are represented in Z-scores. As the amplitude of the responses increases the latency decreases. This inverse relationship is found to be valid for both VPL and SI recordings. Because the highest response magnitude is observed

corresponding to the primary peak in the activity this graph is most pertinent to the relationship between latency and primary peak amplitude. The relationship between later responses and their relative magnitudes cannot be appreciated fully from this graph.

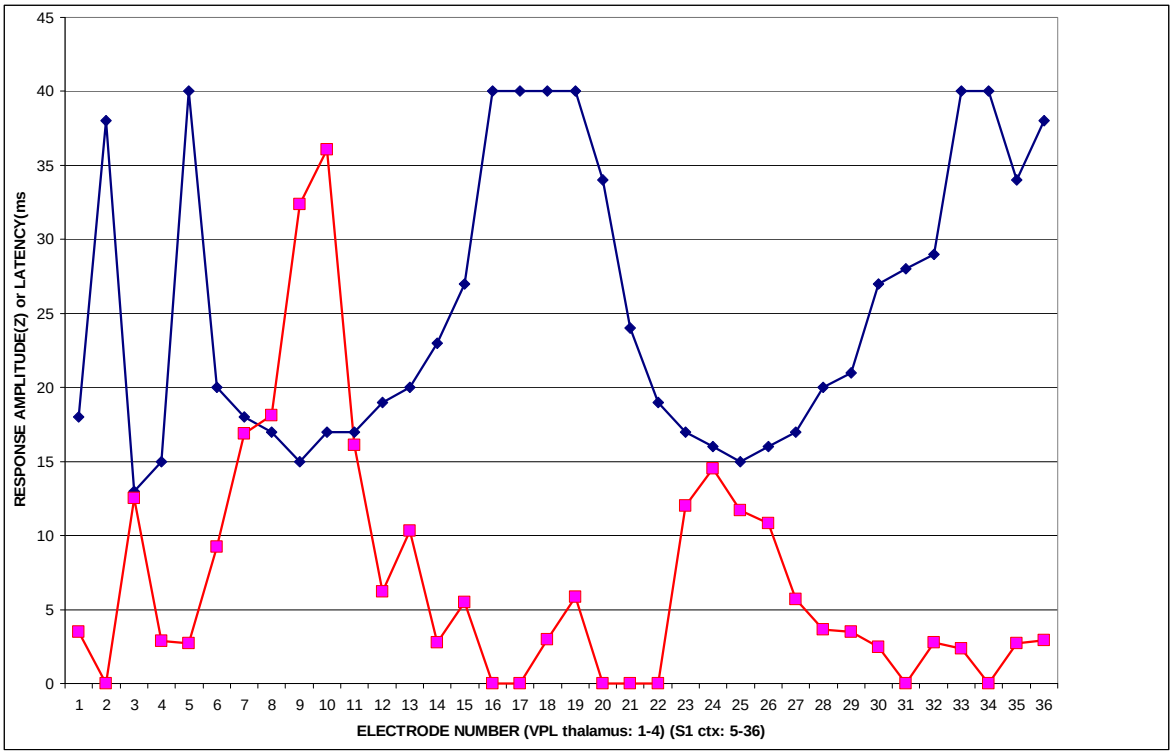

Fig.19. Data corresponds to VPL and area1 recordings in response to D4 tactile stimulation. The "Response Amplitudes" (red; in Z-scores) show peak combined neural responses recorded for each electrode. The "Response latencies" (blue; in ms) show an inverse relationship with amplitudes.

Fig.20a, b, c, d, e, f illustrate responses recorded simultaneously from the VPL and area 1 in the form of postevent rasters and histograms. These responses were observed following mechanical stimulation of the periphery: P6; P5, P4, D5 base, D4 base, D5 side. This is a typical example of both receptive field (RF) and projection field (PF) sizes in anesthetized animals. The RFs of the skin locations overlap – same channels are

responding several stimulation conditions. For example, channel 3 localized to the VPL exhibits elevation in the level of response to all stimulation and channels 26 and 28 show high firing rate in response to 4 out of 5 stimulation sites. Other channels exhibit lower activation across all stimulation experiments. The centers of receptive field shift depending on the location of the stimulation, but overall most of the channels mapping the same location tend to get somewhat activated following stimulation to all other sites. This particular RF encompasses rather large skin surface area – almost half of the palmar hand. The size of the PF usually spans up to four adjacent electrodes as can be seen in fig.20c – spanning channels 25 to 28. The use of multielectrode array presents a possibility of studying large neuronal pools representing rather focal skin location.

Large PF representation also aids in the assessment of the center of the RF. The earliest latency onset of the primary response in the VPL is documented to be 10ms, but usually responses appear at 11-12ms after the stimulus application. In area 1, latency onset is reported to start as early as 13 ms post stimulus, but more frequently in the range from 14 to 17ms. The duration of the VPL response ranges from 10 to 20ms. Area 1 primary response duration also varies from 10 to 20ms. Area 1 responses are characterized by the second peak in the firing rate occurring at about 30 ms postevent.

Fig.21 explores frequency of firing in response to the tactile stimulation. Interspike interval histogram depicts signals corresponding to P5 stimulation sessions. Both thalamic (ch.1, and ch.3) and cortical electrodes record multiunit responses. The distribution of responses is skewed in the direction of shorter interspike intervals. The majority of responses are characterized by the short interspike interval of less than 3ms.

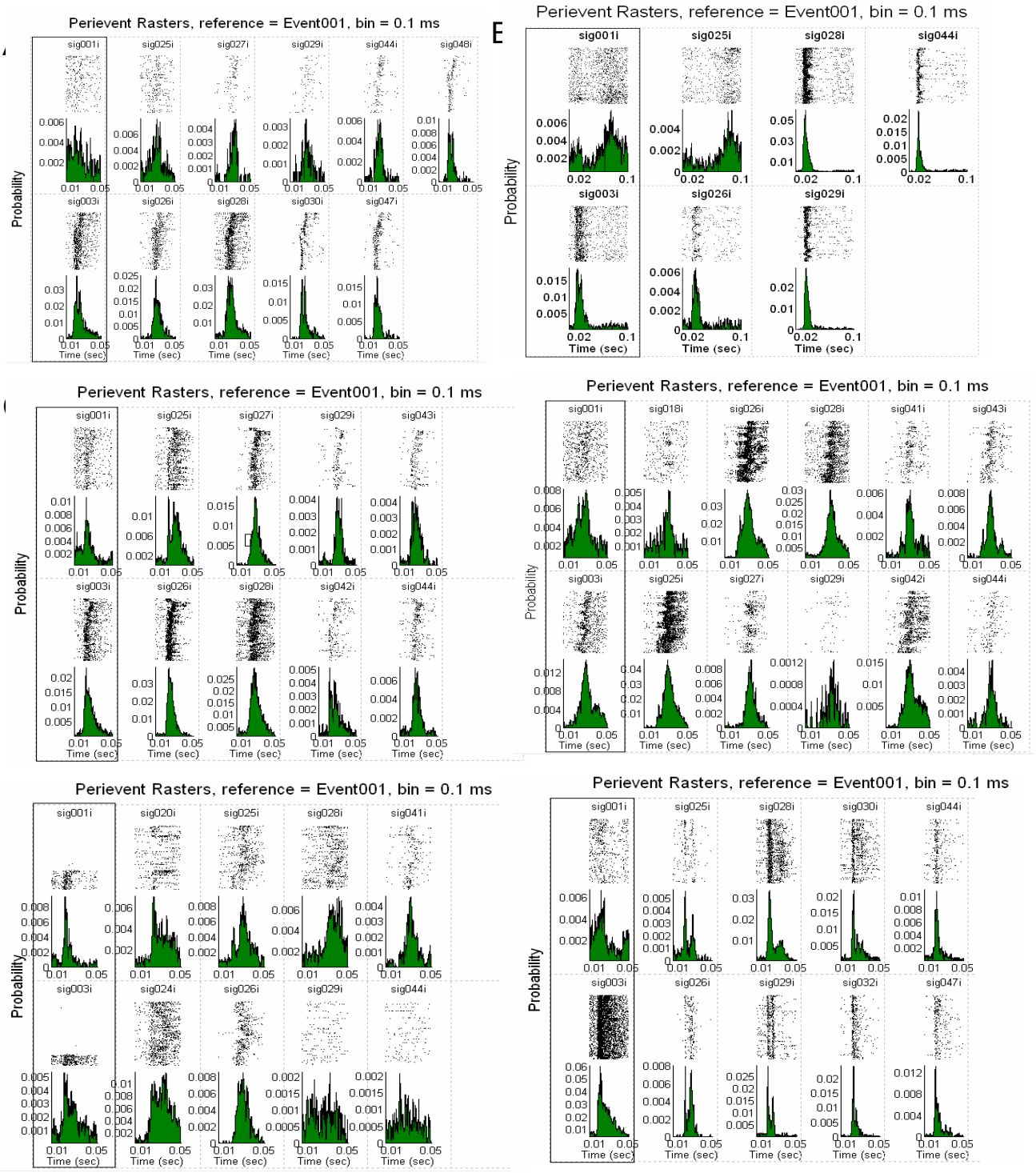

Fig. 20. An example of large RF in area 1 and VPL. Perievent rasters and histograms depict neural activity following mechanical skin stimulation at 5 Hz. A. P5 - strongest response on ch.3 and ch.28; B. P6 – strongest response on ch.3 and ch.28; C. P4 – strongest response on ch.3, ch.26 and ch.28; D. D5 base – strongest response on ch.3, ch.25, and ch.26; E. D4 base – strongest response on ch.3, ch.24, and ch.26; F. D5 distal side – strongest response on ch.3, and ch.28. The responses indicate large RF including all shown locations.

The frequency of firing ranges from 250 to more than 1000Hz. These high frequency oscillations (HFOs) are consistently found in most recordings in SI and thalamus. In the data oscillations appear as a series of peaks in the interspike interval histograms.

The results from other anesthetized animals confirm wide spread of the HFOs. Tactile stimulation to wrist area administered at 2 Hz induces oscillatory activity as recorded from the neural populations (area 1) responding to the stimulation of this skin location (Fig.22).

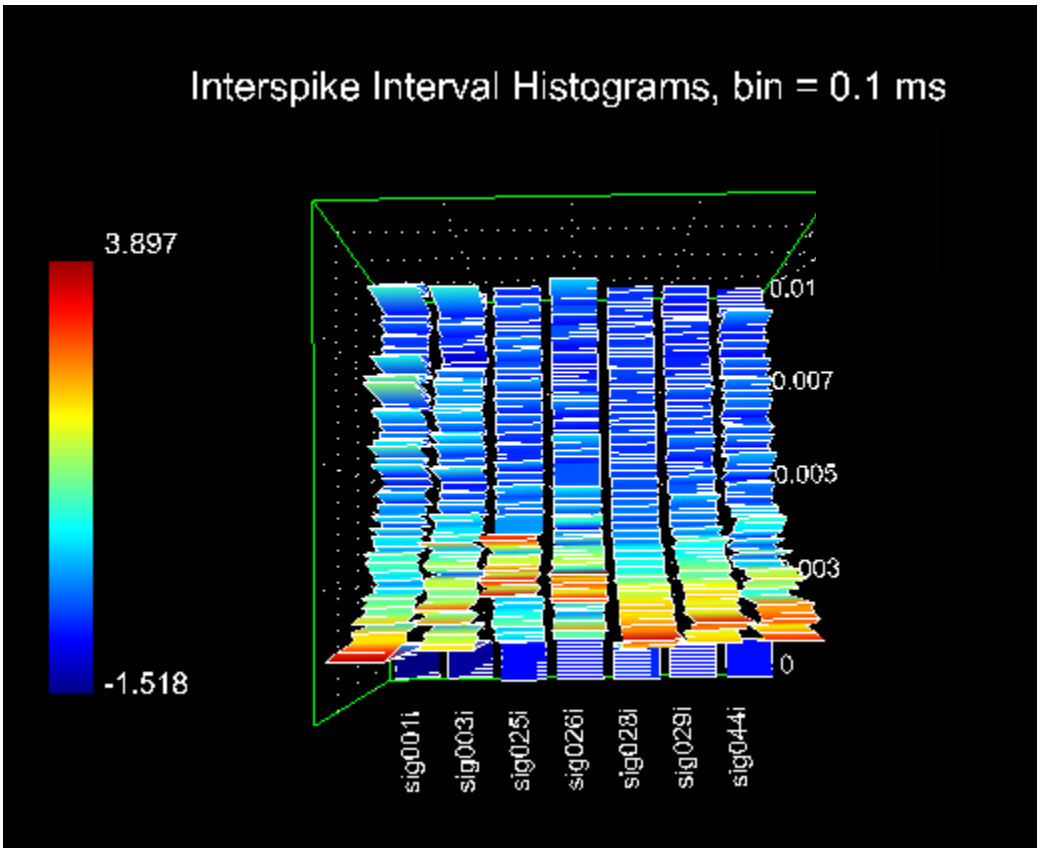

Fig.21. 3-D view of the interspike interval histogram for trials involving mechanical stimulation of P5. Thalamic electrodes are ch.1 and ch.3; the rest stand for cortical area 1 responses. The short interspike interval (< 3ms) provides supporting evidence for the presence of high frequency oscillations (230 to 1000Hz) in the VPL and area 1.

The adjacent electrodes show similar spatial and temporal patterns of activation as evidenced from the alignment of the peaks. This high level of synchronization is observed at all levels and all recording sites.

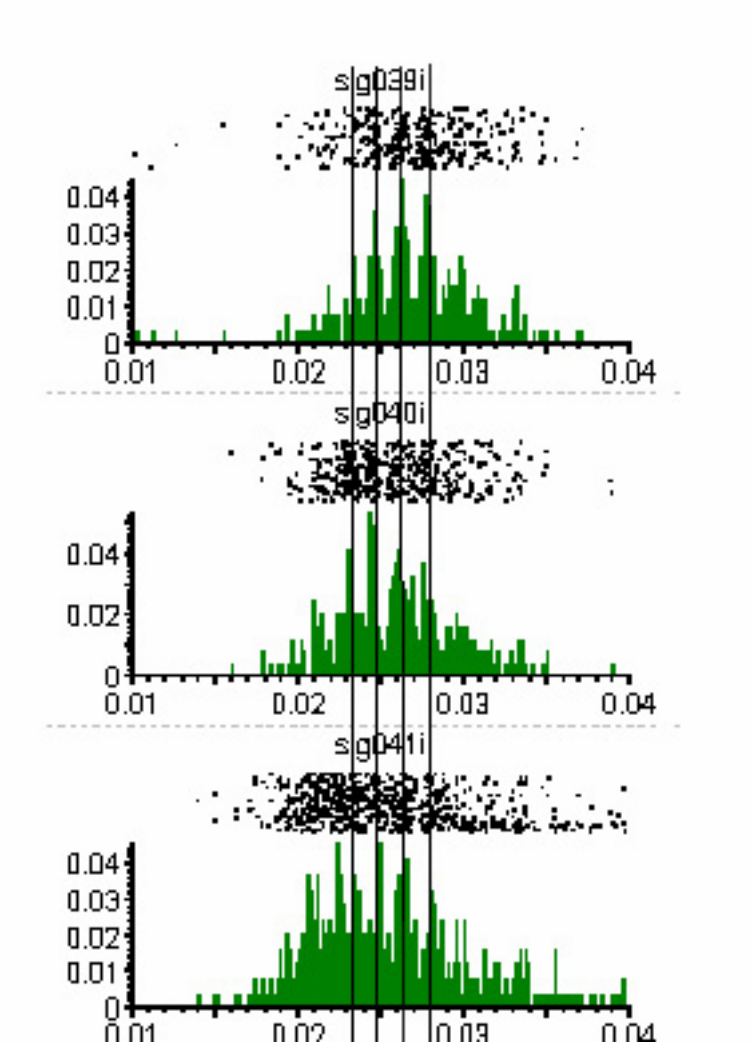

Fig.22. Perievent histograms and rasters of the data (area 1) acquired during 2 Hz stimulation of the wrist. The three channels encode RF of the wrist. The alignment of the peaks of activity signifies synchronization between neurons representing the same skin location. The interspike intervals are short suggesting presence of the HFOs.

Fig.23 outlines data from the experiment involving sustained stimulation applied to the skin in blocks of 5s. This figure includes recordings from 3 electrodes – channel 17, 18, 19 positioned in the areas encoding wrist, lower forearm, and elbow locations. Variability in neural responses corresponding to stimulation conditions was assessed. All 3 channels show marked increase in the firing rate ($p<0.001$) following stimulation of all skin locations. Each stimulus location is encoded by cells recorded thorough all 3 channels. All channels contribute to the information processing. For example ch17, 18, 19 for the wrist condition are all responding with high fidelity to the stimulation of the wrist, but the patterns of the

responses differ. On the other hand, pattern of responses as recorded from the same neural populations varies with the stimulation site.

Upon stimulus application to the wrist channel 17 recordings indicate activation at the time points associated with the onset and offset of the stimulation (within 5s intervals). When stimulation involves lower forearm the responses recorded on the same electrode change their temporal pattern. At this point cells are firing not only at the onset and offset of force application, but also at the times throughout the sustained stimulation (the whole 5s period). Therefore, these neurons are involved in the processing of the information about location and possibly force for the duration of the experimental trial. The same is true for the behavior of the neural populations obtained from all 3 channels. This consistent pattern is attributable to the interactions of slowly and rapidly adapting responses. The neurons associated with the slowly and rapidly adapting responses are thought to be segregated in area 1. Here it is evident that although some segregation might be present there are zones in area 1 where 2 classes of responses might be recorded from the same electrode. In this particular instance it is difficult to establish whether the activity recorded on the same electrodes induced by each of the 3 conditions corresponds to the same or different units. Further investigation of this phenomenon is required and might be carried out in the lab.

The following figure illustrates data collected from an electrode positioned in area 3b of the same animal. Fig.24 consists of recordings from a 32 electrode array. The hallmark features of the responses described in the previous section (area 1) appear to be present in area 3b recordings. The earliest primary response to the stimulation is observed

at a latency of 14ms. The projection fields (PFs- the number of electrodes that represent the same skin location) for area 3b are large although not as large as the PFs in area 1.

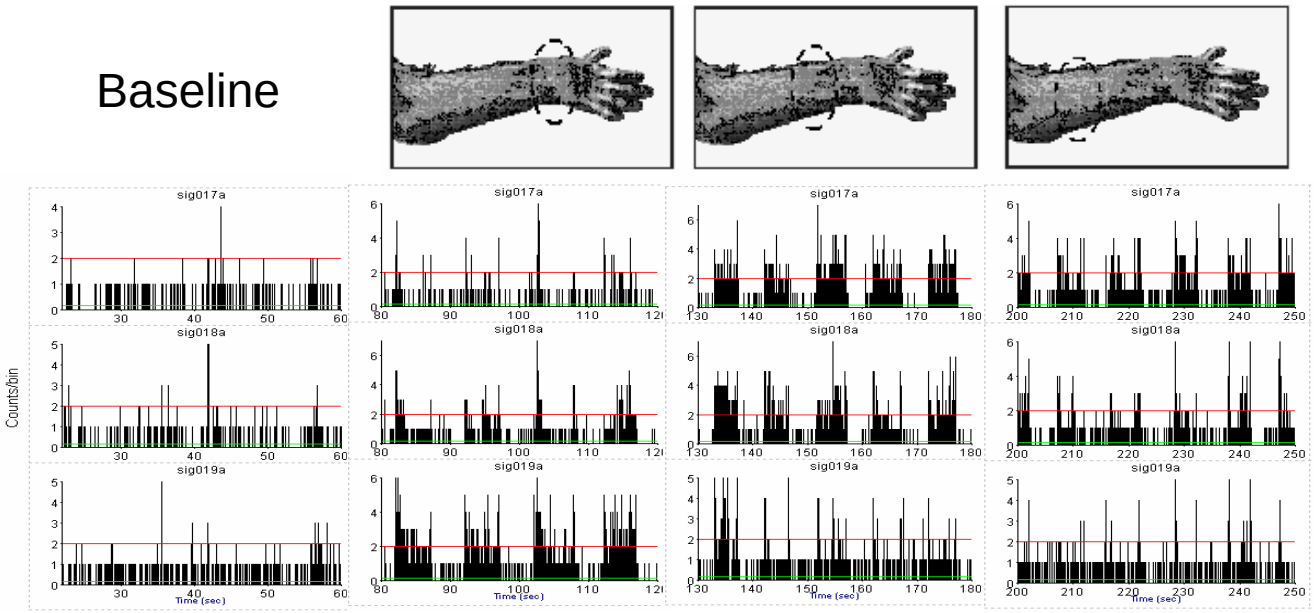

Fig. 23. Rate histograms of neural responses during baseline, wrist, lower forearm, and elbow stimulation. The stimulus is applied for 5s followed by the rest period lasting 5s. Slowly and rapidly adapting responses are observed on all channels. Neural clusters recorded from each electrode encode information pertinent to all stimulation sites. Same channel activity pattern varies according to the stimulus location.

Channels 11, 26, and 27 show neural representations of the same pad. Channel 11 is located in a different row (16 channels away), so, in this example, the sampling is acquired in both medio-lateral and rostro-caudal directions. The center of the RF (the size of the skin area represented by the same neural population) is localized to channel 11 as it shows the greatest magnitude of the response, i.e. activation as represented by dot density. Channel 26 shows less activation, although it is quite identifiable. A strong response to stimulation to the same pad is observed on channel 27. Here the

representation of a digit adjacent to the pad is also present. The level of activation associated with digit representation is high but relative to the pad it is low. The latency of responses evoked by both digit and pad manipulations are comparable, which points to similar contributions to information processing. The high firing rate observed in two areas is indicative of RF representation. The response to the pad is stronger, therefore the primary (center) RF is at the pad site and the secondary (surround) RF is at the digit. Hence, there is an overlap in the RF representations. In the instances when the rate and the latency of responses are analogous (as in Fig. 18) the RFs are thought not to overlap, but rather to have a large size. In the case of channel 18, the RF is larger as evidenced from firing rate and temporal patterns. On this channel, units transmitting information from several pad locations are recorded. The mid-latency response appears at the latency of about 30-32ms (ch. 3, 17, 18). The timing is earlier than the mid-latency response in area 1. In area 3b, the late response occurs at 55ms post stimulus which is also earlier than in the case of area 1. The duration of responses is comparable to the ones recorded in area 1.

The overall RFs in area 3b are smaller compared to the representations in area 1, although co-representation of pad and corresponding digit is prevalent. As in the case of area 1, the latencies of the responses following stimulation of the RF center indicate early activation while RF surround stimulations are associated with late activation (ch. 3, 17, 18).

Area 2 responses follow rather closely the characteristic features of area 1 responses. Fig.25 depicts simultaneously acquired neural recordings from electrodes

placed in the somatotopically corresponding sites in area 1 and area 2. Both responses are characterized by large RFs. The onset of activity in area 1 occurs at 13ms post stimulus.

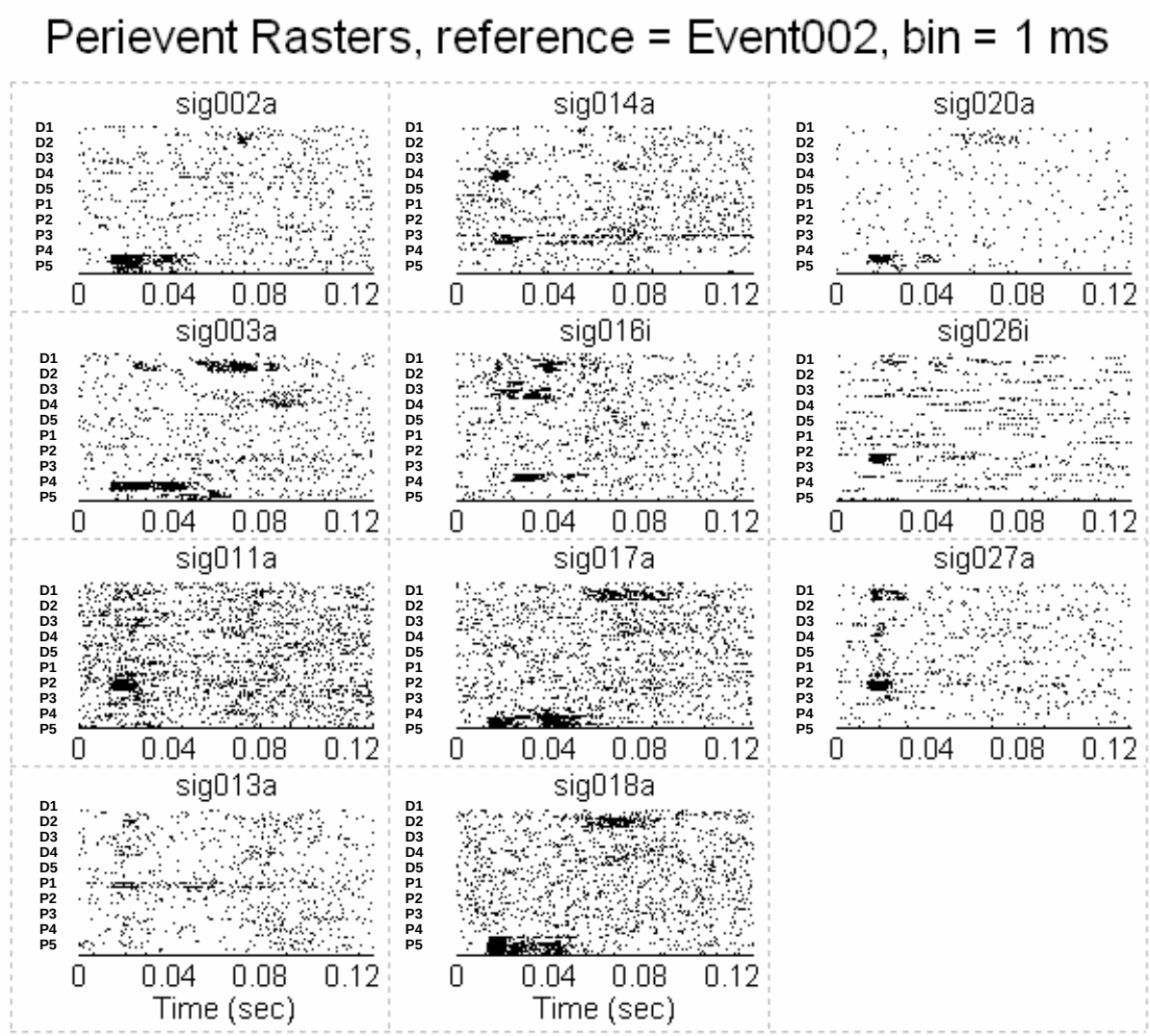

Fig. 24. Perievent rasters of the recordings from area 3b through a 32 channel electrode. The responses are characterized by emergence of early (14ms), mid (30) and late (55) bouts of activity. The RFs are relatively focal with several encompassing adjacent skin locations.

The area 2 response follows with the 3ms delay (i.e. the response onset occurred at 16ms). There is high degree of synchronization between these cortical locations that is evident in this example and other recordings. The overall patterns of response such as the representation of the size of the RF in these sites are strikingly similar. The durations of both responses are comparable.

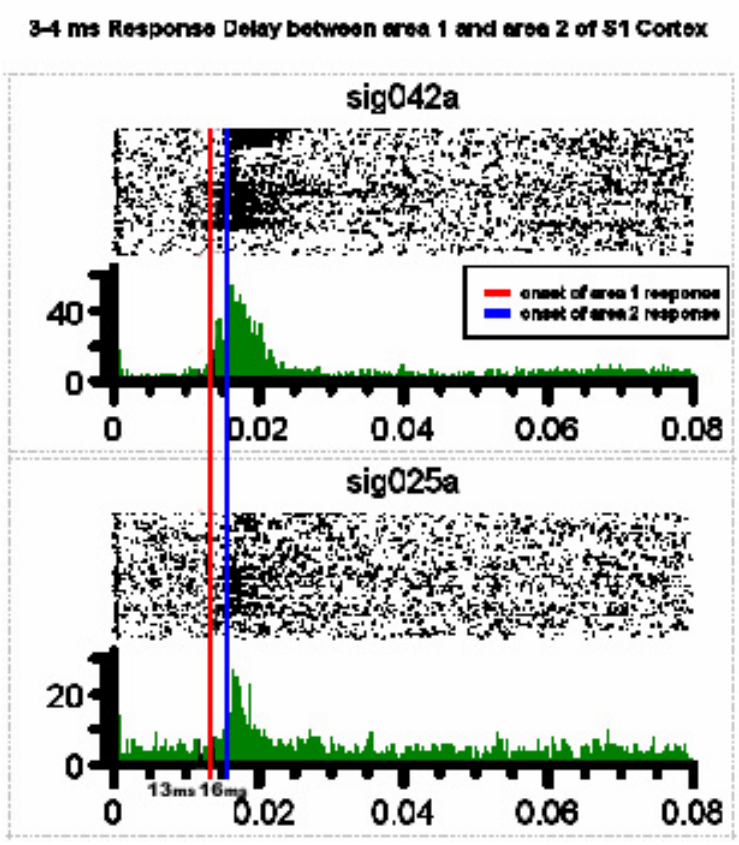

Fig.25. Poststimulus histograms and rasters of neural responses induced by tactile stimulation as recorded from somatotopically equivalent location in areas 1 and 2. Both spatial and temporal activation characteristics are similar. The latency onset for area1 supersedes area 2 response by 3ms.

Microstimulation

Fig.26 provides an example of typical recordings obtained through electrodes placed in the VPL and SI cortex. Tactile stimulation was conducted in order to map receptive fields. Prior to microstimulation through the VPL electrodes good somatotopical correspondence between VPL and cortical electrodes has to be established.

RFs represented by both VPL and cortical electrodes were identified. Thirty six histograms show averaged responses of multiunit populations recorded from each of the 4 VPL and 32 SI – area 1cortex electrodes to tapping stimuli (N=461) on the tip of the D3. Channels in both VPL and area 1 are selectively activated in response to the stimulation. The response is characterized by the large PF.

Collapsing multi-unit activity into 5ms bins provided a good statistical sample of the peak post-stimulus response for each electrode. Though the response intensity for each electrode can be qualitatively appreciated visually, a quantitative peak-detection algorithm (in NEX) was utilized to automatically find the maximal response bin and statistically compare it with surrounding "background" (averaged firing rate for the post stimulus time interval) activity. This yielded a single standardized "Z-score" for each histogram. This approach was found to be reliable for measuring and normalizing the response intensities recorded from the electrode arrays across the S1 cortex.

As noted in the Methods section, mapping of the RFs was conducted to establish a satisfactory placement for electrodes. Such topographical representations are established by applying tactile stimulation to various skin locations. One representative sample of such mapping session is presented in Fig.27. Twelve different hand locations were mechanically stimulated (450 trials) while neural populations were simultaneously recorded in 32 area 1 cortical and 4 VPL thalamic electrodes. Each hand stimulus location is color coded, and these colors indicate which stimulus produced the maximal responses in each of the 32 electrodes shown in the array at bottom. This defines the best mapping, consistent with the limited number of stimulus locations. Meanwhile, the RFs of each of the 4 VPL thalamic electrodes were mapped, as shown in the 4 color coded

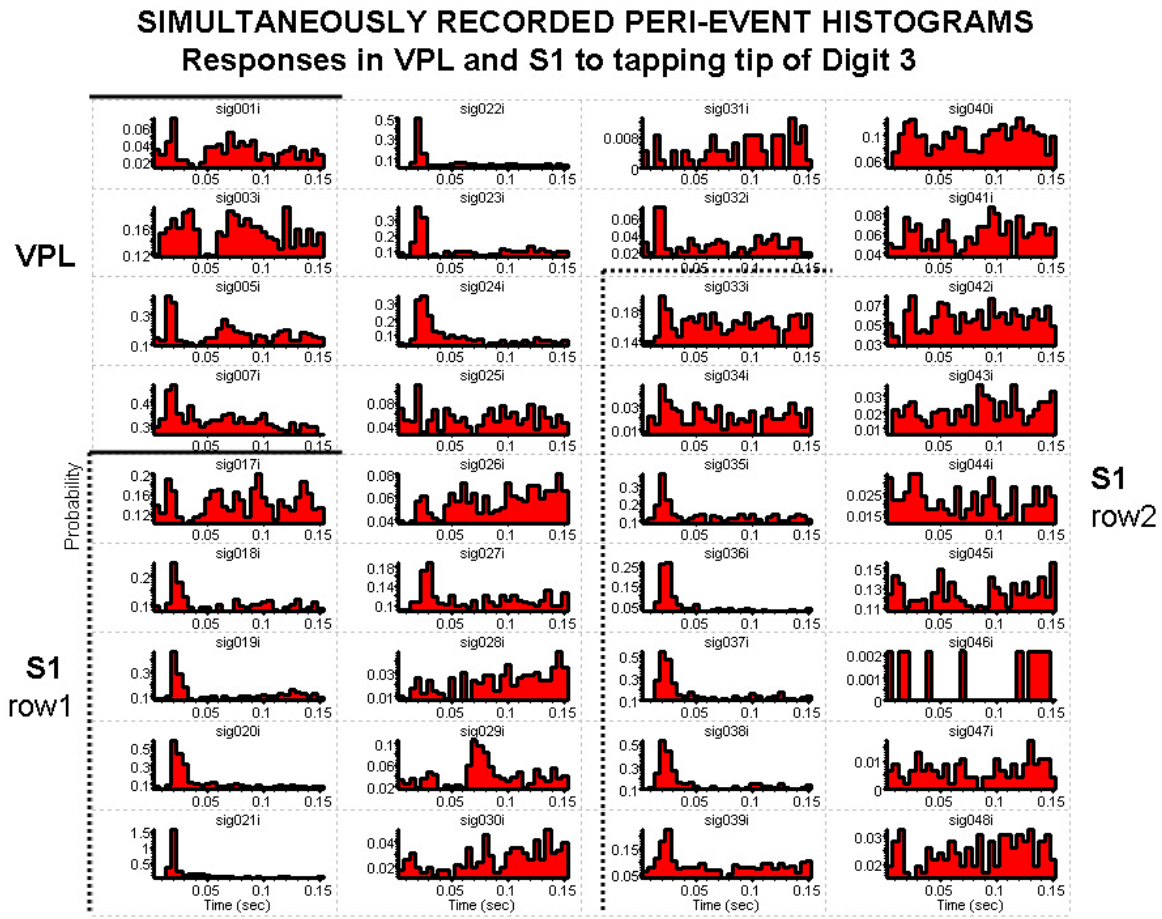

Fig.26. Perievent histograms of simultaneously recorded responses in VPL and area 1 to tactile stimulation of D3. Both cortical and thalamic electrodes show high level of selective activation in response to stimulation (Horizontal axis: 3-150ms, 5ms bins; Vertical axis: Spike response probability per trial per bin. Amplitudes normalized to fit box.)

"VPL stimulation sites" (top right) corresponding with 4 hand locations: VPL1=D3, VPL2=P4, VPL3=tipD2 (weak) and VPL4=dorsal D5 (weak). Electrical stimulation was administered through these 4 VPL electrodes. Six combinations of the VPL pairs were used. The predominant effects of these stimuli are indicated by arrows pointing to different locations on the S1 cortex array. These results show that VPL stimulation through electrodes 1 or 2 generally produced strong responses in somatotopically appropriate areas of the S1 cortex. In contrast, VPL stimulation through electrodes 3 or 4

generally did not produce strong responses in the S1 array. Bipolar stimulation should activate neurons around both electrodes as evidenced by the results of VPL stimulations through the electrode 1 and 2 pair. Therefore it is possible that

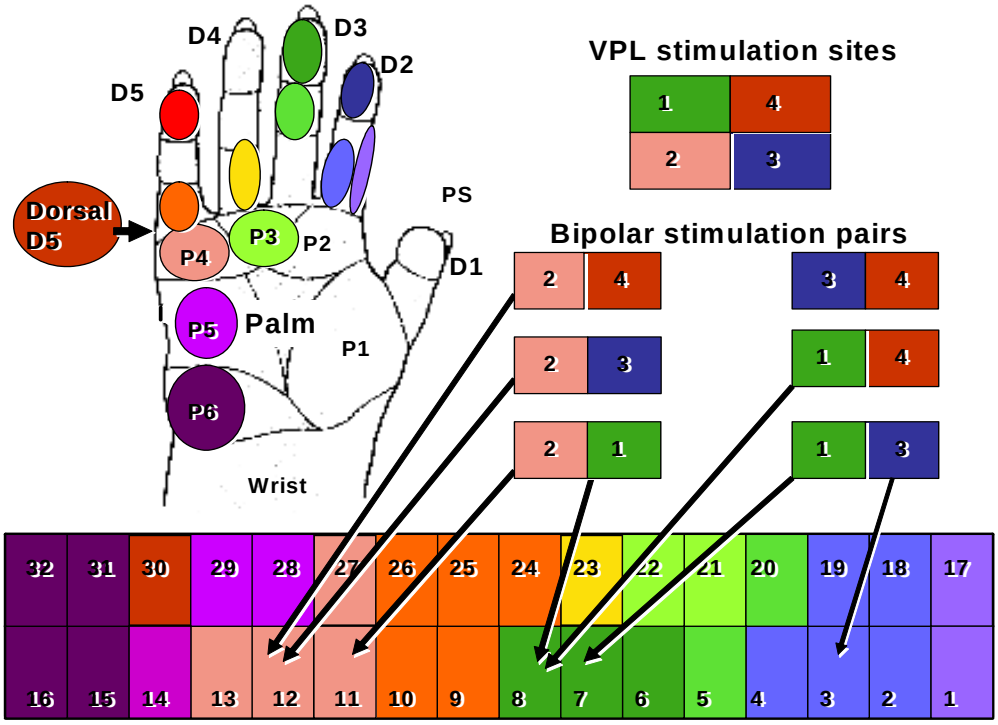

Fig.27. Color coded representation of the somatotopy of area 1 and VPL neural representations. The results of cutaneous stimulation indicate that the 32 electrode array spans most hand locations. Four VPL electrodes correspond to 4 hand locations. All locations represented on the VPL electrodes are represented by neurons recorded from area 1 array. Electrical stimulation of the VPL through electrodes 1 or 2 elicits strong responses in the corresponding cortical areas.

the VPL sites 3 and 4 had weak cortical projections, or that these projections did not happen to align with any of the 32 cortical electrodes. Overall, these results show that correct placement of both electrodes will be critical for determination of cortical responses.

To compare the sizes and locations of S1 cortical areas activated by natural vs. VPL stimuli, the locations and sizes of neuronal response patterns recorded from each of the 32 S1 cortical electrodes were measured. For consistency, an automatic peak detection algorithm was used to resolve peak amplitude of multineuron activity in each electrode. This peak response rate was then converted into a Z-score by standardizing across the entire post-stimulus histogram (5-50ms). For each stimulation condition, z-scores were generated for each electrode. The magnitude of neural responses was quantified by these z-scores. These z-scores were further standardized across all electrodes to allow for comparison of relative magnitude of the response between all channels during a particular stimulation condition. These z-scores were standardized across all 18 experimental conditions to permit comparison of relative response rates according to the condition. These z-scores were plotted in Fig.28. This color coded surface plot shows the response intensities recorded from each of the 32 area 1 cortical electrodes during 18 experimental manipulations: mechanical (labels at left) and VPL stimulations (underlined labels and demarcated with white lines). Twelve different hand/arm locations and 6 different combinations of 50μA bipolar microstimulation in the VPL were used. Each horizontal strip shows neural population responses recorded from each cortical electrode during a single stimulation experiment. The top strip, for example, shows the averaged neural responses to 450 mechanical stimuli on the tip of D1. Each square shows the standardized amplitude of the highest peak in the post-stimulus histogram recorded from that electrode (indicated at bottom). The significant response peaks (Z-scores > 2; $p<.022$) are shown in orange and red, and tend to appear in both electrode rows (Rostral: 1-16; Caudal 17-32). All of these horizontal strips were rank

ordered according to the positions of the strongest response. Appropriately, these progress down from D1-D5, and then across the palmar pads P4-P1. Interspersed among

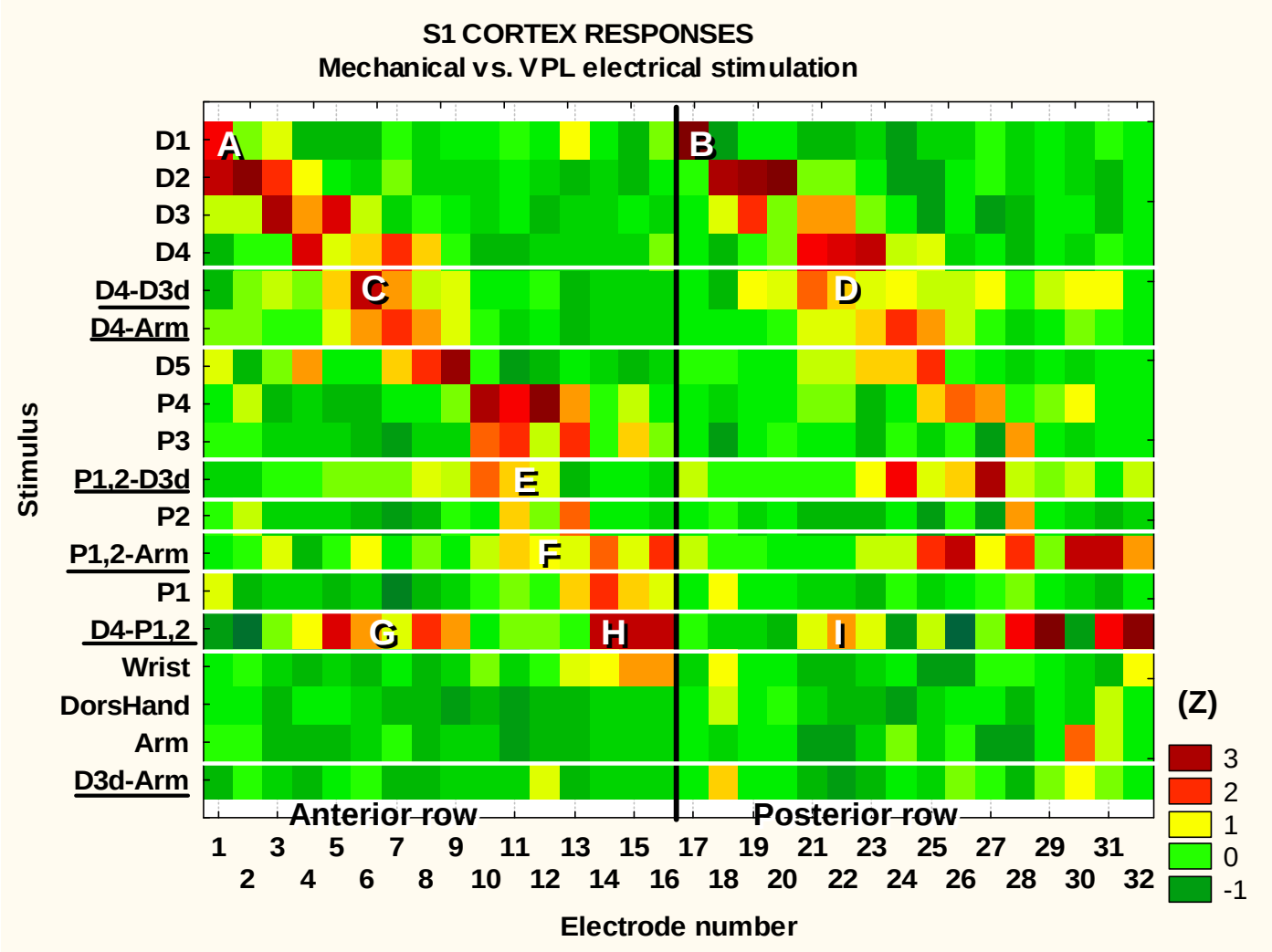

Fig.28. Color coded 2-D representation of the relative magnitude of the neural responses normalized across all electrodes and all conditions. Data includes 12 sites involving mechanical stimulation and 6 bipolar VPL stimulation sessions. Somatotopic correspondence between responses to natural and VPL stimulation is observed. Underlined labels correspond to microstimulation.

these horizontal strips produced by tactile stimulation are responses to microstimulation in the somatotopically equivalent area of the VPL. These are labeled to indicate the receptive fields previously recorded from the anodal and cathodal electrodes in the VPL. The results show that the bipolar VPL stimuli typically produced response peaks in the

correct somatotopic locations. Thus bipolar stimulation in VPL produced activation in two different somatotopic cortical zones. For example, stimulating across the D4-P1,2 areas of the VPL produced separate responses in the D4 zone – G label (ch.5-9, ch.22) and the P1 zone - H label (ch.14-16). Similar response was observed on the posterior row (I).

To quantitatively define the relationship between amplitude and projection field size, the responses in each S1 cortical electrode during natural touch stimulation on the hand (digit 3-tip) vs. microstimulation in the digit 3 tip representation in the VPL were compared (Figure 12). The microstimulation was applied at stimulation strengths of 25, 50 and 100μA. Typically neural responses maintained their "cortical response field" centers, but increased the overall sizes of these fields, often ranging over 4-6 electrodes, using ($p<.001$) significance criteria. Microstimulation of VPL at 50μA and 100μA activated the same general cortical areas as the natural stimuli, but their profiles tended to be smaller and narrower. Thus VPL microstimulation at these currents produced minimal non-specific neural activity in the cortex. Data recorded from the whole sample suggests that increasing stimulus currents produced nearly monotonic increases in the linear extent of the activated cortical areas (as measured on the electrode row with the strongest response). Increase in the stimulus intensity leads to the activation of a greater number of the electrodes: **25μA:**1.67±1.36; **50 μA**:2.56±1.33; **100 μA**:3.56±1.4 and **130μA**:4.29±1.4. But these enlarged response areas retained their bell-shaped profiles, suggesting that the stimuli were merely activating increased numbers of nearby thalamocortical axons. Activation profiles indicate that 50microA stimulation intensity produced optimal selective activation of channels involved in encoding of tactile stimuli.

Stimulation at 25microA failed to produce evoked responses in the cortex, while stimulation at 100microA produced slight shifts in topographical representations (as evidenced from peaks in red).

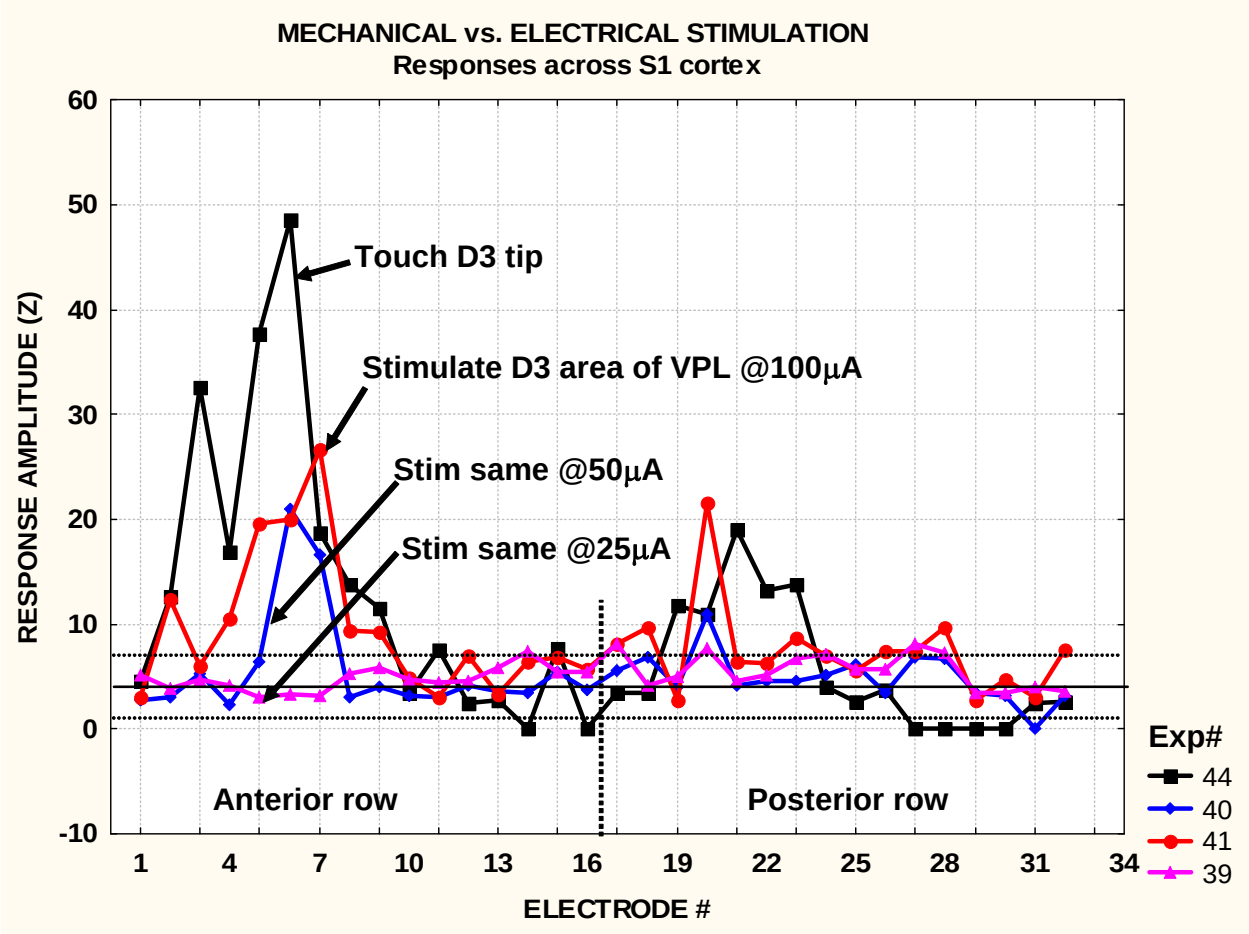

Fig.29. Comparing S1 cortical responses to mechanical touch vs. electrical stimulation in the VPL thalamus. Responses across the 32 S1 cortical electrodes to the D3 tapping stimuli were compared with responses to 3 intensities of electrical stimulation in the D3 area of the VPL. Here the maximal responses to the touch stimuli and 50µA VPL stimuli were both in electrode 6, while the 100µA stimuli were maximal in the adjacent electrode 7. The 25uA stimuli were ineffective. General similarity of responses to natural and electrical stimuli can also be seen in the posterior row of electrodes.

Using data from another similar experiment Factor Analysis was employed to determine whether correlations between the S1 cortical responses to different mechanical or VPL electrical stimuli could be used to define a somatotopic map based purely on functional

interactions between recorded neurons (Fig.30). Principal components analysis (PCA) was used to define an optimal 2D space in which to embed the results of different stimulation experiments. The data included 19 experimental conditions: 10 mechanical stimulation experiments and 9 electrical stimulation experiments (3 VPL stimulus sites, each using 25, 50 and 100uA stimuli). Each of these experiments yielded 32 data points, corresponding to the maximum Z-scores (peak responses) recorded from each electrode. These 19 vectors were used to generate a 19x19 correlation matrix. PCA yielded 19 eigenvectors, the first 2 of which comprise the factor space in the plot. “Cluster” PCA rotation produced factor loadings for each condition. Those were plotted in the 2-D factor space. Again, the results show a good correspondence between mechanical and VPL electrical stimuli. Moreover, this factor analysis defined spatial mapping of all of the functional variables (i.e. all experiments). Dotted lines outline color coded clusters of mechanical and electrical stimulation experiments corresponding to each digit. Though the 50uA and 100uA experiments tended to cluster together, the 25uA experiments yielded little response, and thus have been omitted from this plot (they would be behind the legend at right).

In order to validate the usefulness of correlation analysis, data from tactile and microstimulation sessions were compared using previously described methods (Results I). Results obtained from data analysis employing z-scores served as a control. The first step was to identify primary encoders for each condition of tactile stimulation. This would result in a somatotopic map. Fig.31 summarizes correlation coefficients that resulted from tactile stimulations of various skin locations.

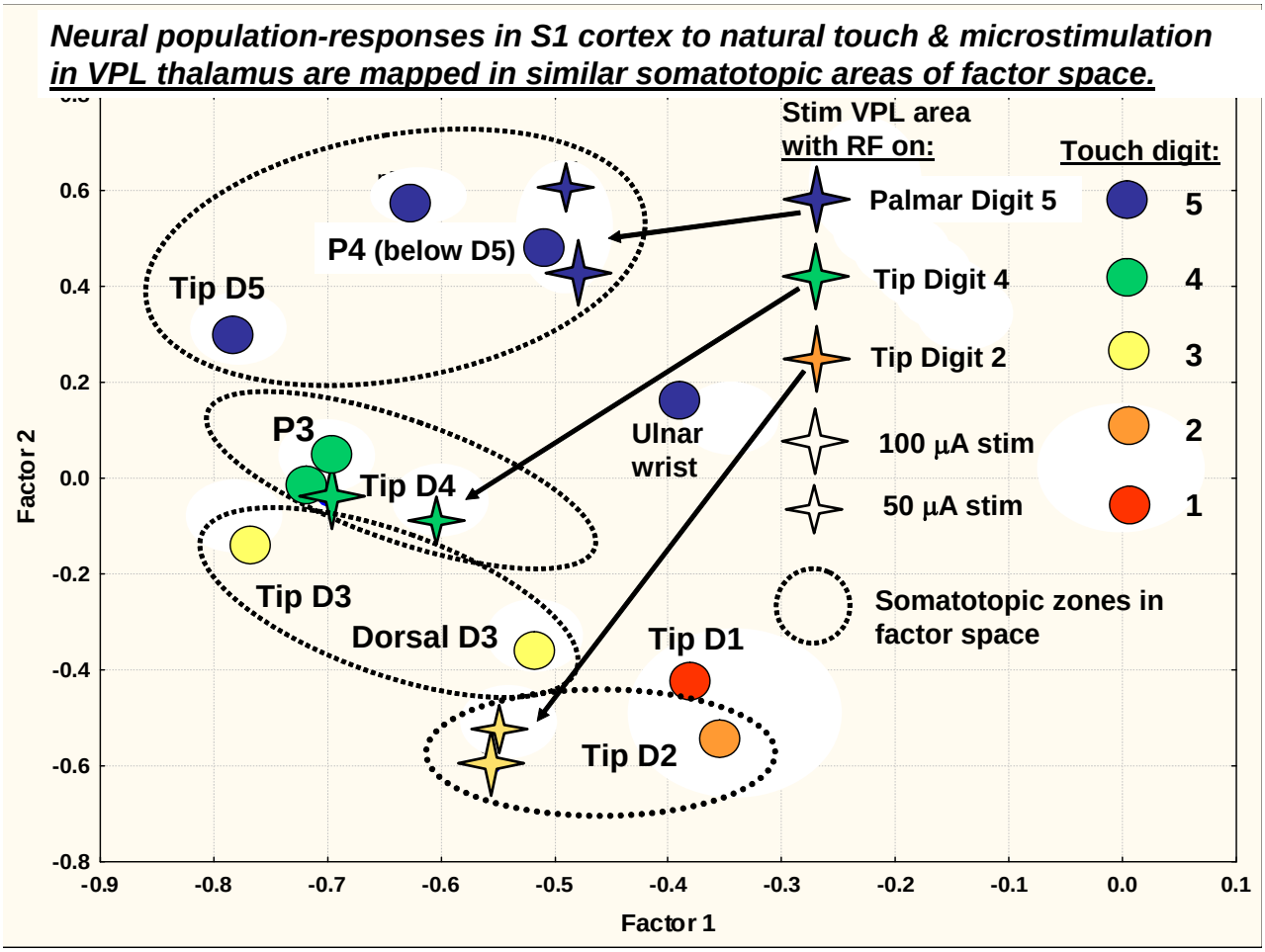

Fig. 30. 2-D mapping of the neural responses to mechanical and electrical stimulation in factor space. 19 experimental sessions were used for the analysis. These included 10 vibromechanical and 9 electrical VPL stimulation experiments (25, 50, 100microA). The neural responses were recorded from the same electrode array consisting of the 32 channels. PCA yielded two "latent" factors, together explaining 50% of the total variance. Factor loadings for each condition were mapped. The emergence of clusters representing distinct skin locations, i.e. individual digits is observed. Further, pads and wrist locations are also mapped in somatotopically correct fashion. (The results for the 25microA VPL stimulation were omitted as the stimulation did not yield significant neural response).

Channels 1, 3, 5, and 7 correspond to recordings from an electrode placed in the VPL. Other channels correspond to 32 array electrode positioned in somatosensory area 1. Again, somatotopic correspondence between thalamic and cortical encoders has to be present. In the table, correlations larger than 0.7 are highlighted. Each condition produced a unique spatial pattern of activation. Correlations indicate that the size of the receptive

fields represented by neural population tend to be large. This holds true for both thalamic and cortical responses. For example, channel 5 (VPL electrode) responds to stimulation at 6 out of 9 skin locations. In the cortex, channel 20 contributes to the representation of digits 2 through 5. Some channels show more specificity. Channel 1 in the VPL was activated exclusively following stimulation of D4. In the cortex, channels 44 and 48 respond selectively to stimulation of Pd1w (pad 1 wrist) and Pd3 (pad 3). Sessions corresponding to stimulations of digits 2 through 5 produce similar maps of responses: most activity is observed on channels 19 through 25 and on channels 35 to 39. The results of pad stimulations are characterized by the presence of strong signals on channels 29 through 32. Again, these results point to the presence of rather large receptive fields. Stimulation of D1 evoked responses on both “digit” and “pad” channels: channels 19 belongs to the “digit” cluster and channels 29, 32, and 33 belong to the “pad” cluster. These results are comparable to the map presented in fig.27. Correlations provide reasonable visualization of signal distributions. Good somatotopic correspondence is observed between thalamic and cortical recordings. The presence of large RFs could lead to compromised specificity of responses following microstimulation of VPL.

Evoked responses were further quantified by assessment of the degree of representation for each condition. Some stimulation conditions produced responses on many channels and some resulted in activity confined to only a few channels. Fig.32 illustrates the extent of the representation for each condition. Only cortical responses were included, as this measure could be used to compare responses evoked by tactile and microstimulation sessions. Stimulation of D4 resulted in responses recorded from 8 channels which constituted activation of 25% (8/32) of all channels in the array.

Condition / Channel	D1	D2	D3	D4	D5	Pd1w	Pd3	Pd5	Pd5w
1	.555	.461	.655	.948	.659	.284	.434	.159	.138
3	.857	-.021	.008	.199	.051	.699	.945	.776	.890
5	.717	.510	.894	.871	.737	.733	.702	.610	.502
7	.797	.247	.441	.470	.293	.476	.708	.371	.402
17	.167	-.011	.042	.120	-.080	.147	.151	.094	.203
18	.171	.469	-.150	.122	.045	.170	.272	.154	.048
19	.731	.712	.932	.376	.371	.323	.150	.071	.006
20	.108	.772	.813	.876	.752	.072	.271	.235	.357
21	.014	.519	.976	.820	.444	.076	.112	-.012	.149
22	.132	.625	.936	.902	.622	-.049	.113	.077	-.022
23	.697	.712	.493	.949	.589	.698	.328	.725	.209
24	-.031	.272	.574	.941	.849	.022	.490	.234	.386
25	.198	.043	.097	.405	.747	.102	.230	.261	.100
26	.177	-.069	.084	-.077	.071	.277	.644	.525	.215
27	.411	.253	.407	-.083	.015	.309	.704	.470	.399
28	.234	-.019	-.130	-.063	.063	.116	.685	.634	.244
29	.962	.583	.641	.287	.348	.948	.984	.751	.875
30	.688	.226	-.105	-.018	-.004	.855	.894	.644	.728
31	.104	.027	.103	.103	.001	.549	.739	.075	.734
32	.771	.288	-.108	.647	.099	.802	.742	.200	.643
33	.945	.249	.183	-.012	-.028	.245	-.019	.349	.186
34	-.036	-.070	.071	.047	-.055	-.192	-.045	-.086	-.035
35	.078	.816	.655	.265	-.062	-.029	.061	.279	.146
36	-.110	.850	.352	.134	.039	.057	.169	.121	-.011
37	.278	.765	.901	.857	.647	.204	.522	.603	.313
38	.322	.744	.913	.820	.715	.288	.571	.612	.278
39	.292	.412	.612	.833	.563	.301	.056	-.042	.015
40	.139	.014	.013	.433	.444	.196	.045	.026	.049
41	-.021	.042	.082	.460	.427	-.042	.229	.060	.202
42	-.050	-.139	.076	.003	.143	-.037	.215	.123	.163
43	.167	-.137	-.028	-.013	-.104	.084	.006	.078	.152
44	.255	.003	.009	-.221	.104	.666	.711	.435	.506
45	.052	-.051	-.050	-.039	-.098	.118	.164	.187	.151
46	-.036	-.029	-.036	-.040	-.020	.064	-.044	-.047	.046
47	.028	.064	.058	-.044	-.026	-.103	.027	-.070	-.123
48	.177	.101	.226	.100	.038	.763	.051	.081	.000

Fig.31. Correlation coefficients are presented for all tactile stimulation sessions. Channels 1, 3, 5, and 7 correspond to the VPL electrode. Other channels – cortical array. Highlighted coefficients crossed 0.7 threshold. Each condition is color coded. Correlations yield a somatotopic distribution index.

Stimulation of D1 and D5 resulted in activation of 12.5% (4/32) of channels. The digits show variable degrees of representation on the electrode. Stimulation of pads resulted in

lower levels of representation. The highest resolution was obtained after stimulation of Pd3 – 15.5%. The lowest was associated with Pd5 (pad 5). Other pads were stimulated, such as pad 1, 2, and 4 but showed no representation on the array.

D1	D2	D3	D4	D5	Pd1w	Pd3	Pd5	Pd5w
4ch=12.5%	7ch=22%	6ch=19%	8ch=25%	4ch=12.5%	3ch=9%	5ch=15.5%	1ch=3%	3=9%

Fig.32. Table reports number of channels and percentages of channel activation (out of 32) representing each condition.

After establishing good somatotopic correspondence between thalamic and cortical recordings, electrical stimulation through the VPL electrodes was in order. This microstimulation was carried out through pairs of electrodes (1, 3, 5, 7). Six combinations were used. The intensity of stimulation was varied. Three levels of stimulus intensity were used: 25, 50, and 100μA. In order to assess the relative effects of stimulus intensity on evoked responses the number of activated channels was compared across four conditions (tactile, 25, 50, and 100μA stimuli).

Fig.33 is an example of such a comparison for stimulation through electrodes 1 and 3. In order to establish the optimal stimulation intensity, the number of correctly activated channels should approximate the number corresponding to tactile stimulation and the number of incorrect should be minimal. As can be seen from the table, stimulation through electrodes 1 and 3 resulted in a generalized activation. Stimulation at 25μA resulted in activation of 17 channels, 50μA of 19 channels, and 100μA of 25

Stimulation / Condition		1->3		
		25μA	50μA	100μA
D1	Correct	3ch=9%	3ch=9%	3ch=9%
	Incorrect	14ch=44%	16ch=50%	22ch=68%
	Missing	1ch=3%	1ch=3%	1ch=3%
D2	Correct	5ch=15.5%	5ch=15.5%	7ch=22%
	Incorrect	12ch=37%	14ch=44%	18ch=56%
	Missing	2ch=6%	2ch=6%	0ch=0%
D3	Correct	3ch=9%	6ch=19%	6ch=19%
	Incorrect	14=44%	13ch=40%	19ch=60%
	Missing	3ch=50%	0ch=0%	0ch=0%
D4	Correct	6ch=19%	7ch=22%	8ch=25%
	Incorrect	10ch=31%	12ch=37%	17ch=53%
	Missing	2ch=6%	1ch=3%	0ch=0%
D5	Correct	2ch=6%	4ch=12.5%	4ch=12.5%
	Incorrect	15ch=47%	15ch=47%	21ch=65%
	Missing	2ch=6%	0ch=0%	0ch=0%
Pd1w	Correct	4ch=12.5%	4ch=12.5%	4ch=12.5%
	Incorrect	13ch=40%	15ch=47%	21ch=65%
	Missing	0ch=0%	0ch=0%	0ch=0%
Pd3	Correct	2ch=6%	5ch=15.5%	6ch=19%
	Incorrect	15ch=47%	14ch=44%	19ch=59%
	Missing	4ch=12.5%	1ch=3%	0ch=0%
Pd5	Correct	1ch=3%	1ch=3%	1ch=3%
	Incorrect	16ch=50%	18ch=56%	24ch=75%
	Missing	0ch=0%	0ch=0%	0ch=0%
Pd5w	Correct	2ch=6%	3ch=9%	3ch=9%
	Incorrect	15ch=47%	16ch=50%	22ch=68%
	Missing	1ch=3%	0ch=0%	0ch=0%

Fig.33. The table compares the degree of correspondence between channel activation following tactile stimulation and microstimulation. Three microstimulation conditions are presented: 25, 50, 100microA. In this example electrical stimulation led to generalized activation for all conditions. Grey highlight - # incorrectly activated channels; red highlight – number of missing channels as compared to tactile stimulation condition. Optimally, number of hits should be high and numbers of incorrect and misses should be low. 50microA stimulation provided the most suitable proportion.

channels. Other stimulation pairs were analyzed and produced more specific activation patterns. For example, 50μA stimulation through electrodes 1 and 7 produced activation on channels encoding for D4: 6 channels = correct, 2 channels were incorrect, and 2 were missing. This proportion of correct vs. incorrect activations following 1->7 stimulation was optimal for the D4 condition. For all analyzed stimulation sessions, 50μA was shown

to produce optimal activation patterns. These results are comparable to the results presented using z-scores as a measure of channel activation (fig.29). The proportion of correctly activated channels could be assessed using correlations.

Fig.34 reports correlations obtained from microstimulation sessions through various pairs of thalamic electrodes. Stimulation was administered at 50microA, as it was shown to be the optimal intensity for each stimulation pair. The pattern of cortical activation following microstimulation can be observed. This figure can be compared to fig.28. In the cortex, a 32 electrode array was used to record evoked responses. As can be seen from the figure, stimulation through electrode pair 1->3 (channel 1 – anode, channel 3 – cathode) produced a generalized pattern of activation. All channels activated during tactile stimulation (fig.31) sessions were showing high correlations. On the other hand, stimulation through electrode pairs 1->5 and 1->7 produced responses on the channels involved in the representation of digits 2 through 5 (compare to fig. 31). Channel 1 selectively represents D4. Channel 3 was shown to contribute to encoding of information on D1 and pads, but was not associated with encoding of D2 through D5. Channel 5 was implicated in representation of D2 through D5. Channel 7 showed specificity for D1 and some pad locations.

Stimulation through electrode pairs 3->5 and 3->7 yielded high coefficients on the channels associated mostly with pad and D1 representations. Stimulation through 5->7 produced only minimal activation of cortical channels – only one channel showed high correlation. Stimulation through 1->7 produced patterns of response closely associated with D4 stimulation, while stimulation through 3->7 fits D1 stimulation. Overall, microstimulation sessions resulted in specific responses in the cortex. Activation patterns

were confined to locations associated with the representation of tactile information. Relatively large receptive fields in the thalamus and cortex led to large representations following microstimulation. There was a good correspondence between the activation patterns following tactile and microstimulation sessions.

The results obtained using correlation coefficients are comparable to results obtained using z-score measures (fig.28).

Fig.35 provides a visual illustration of the selectivity of responses following microstimulation. Similarities of correlation magnitudes between D4 and 1->7 stimulation sessions can be observed in fig.35A. The distributions of correlations (peaks and valleys) show good correspondence on most of the channels. These represent best matching of microstimulation to tactile stimulation. Two peaks on 1->7 correspond to activation of channels 45 and 48, which do not show activation during D4 condition. Stimulation of D4 induced responses on 8 channels, and 6 of the same channels were activated after 1->7 stimulation. This constitutes 75% hit rate. After 1->7 stimulation 2 channels were activated incorrectly and 2 channels were missing.

The distribution results for D3 and 1->5 stimulation exhibited close correspondence both in activated channels and the degree of activation (fig.35B). A total of 6 channels were implicated in D3 encoding. Four of the same channels were activated following 1->5 stimulation (66% hit rate). Two channels were activated incorrectly (false positives) and 2 were missing.

Stimulation of D1 produced patterns of response similar to condition 3->5 (fig.35C). Tactile stimulation of D1 results in activation of 4 channels. Stimulation through electrodes 3->5 induced activity of 3 of the same channels (75% hit rate). Two

channels were activated incorrectly and 1 channel was missing. Stimulation through 3->5 results in activation patterns similar to pad stimulation (fig.35D).

Stimulation / Channel	1->3	1->5	1->7	3->5	3->7	5->7
17	.473	-.161	.196	.005	.147	.016
18	.634	.399	.662	.618	.495	.130
19	.929	.854	.695	.885	.947	.190
20	.701	.862	.355	.660	.416	.411
21	.853	.943	.917	.306	.690	.362
22	.845	.966	.931	.982	.969	.754
23	.673	.971	.926	.653	.847	.459
24	.909	.805	.899	.600	.691	-.082
25	.893	.566	.599	.150	.530	.006
26	.928	.165	.508	.213	.516	-.032
27	.734	.132	.308	.196	.566	.106
28	.886	.044	.027	.536	.787	-.088
29	.939	.223	.462	.995	.961	.099
30	.974	.019	.479	.937	.971	.095
31	.786	.003	.309	.025	.713	.184
32	.944	.267	.410	.864	.937	.037
33	.496	.226	.137	.182	.151	.238
34	.000	.000	.000	.000	.000	.000
35	.652	.669	.385	.670	.334	.045
36	.895	.364	.077	.436	-.147	.212
37	.923	.686	.875	.581	.684	.065
38	.913	.675	.845	.483	.696	-.017
39	.767	.681	.739	.469	.625	-.001
40	.681	.357	.634	.102	.458	-.021
41	.677	.448	.442	.109	.607	-.111
42	.634	-.022	.006	-.114	.511	-.103
43	.696	.065	.154	-.149	.050	-.102
44	.883	.412	.398	.324	.651	.001
45	.199	.346	.968	.041	.984	.698
46	-.023	-.044	-.113	.034	-.050	.104
47	.407	.222	-.039	.219	.470	-.040
48	.961	.028	.990	.496	.757	-.102

Fig.34. Correlation coefficients are summarized for all microstimulation sessions at 50microA. Cortical array consisted of 32 electrodes. Red highlight: r>0.7. This figure could be compared to fig.31 – responses to tactile stimulation. Same electrodes were activated following tactile stimulation.

Finally, Pd1w (pad1 wrist) stimulation leads to activation of 4 channels, while 3->5 stimulation results in activation of 3 of those channels (75% hit rate). Two channels

were activated incorrectly and 1 was missing. Most of the “incorrectly” activated channels were identified as encoders for other tactile stimulation conditions, which points to coactivation of RF representations.

Data analysis using both z-scores and correlations led to similar findings. The topographical maps produced by both methods show high degree of similarity. Activation of cortical regions following microstimulation is characterized by high precision and selectivity.

Neural responses to both tactile and electrical stimulation are characterized by the presence of high frequency oscillations (HFOs). Fig.36 provides an illustration of this wide spread phenomenon. Poststimulus rasters and histograms are composed of data from a 32 electrode array positioned in area 1. Mechanical stimulation of D4 (Fig.36a) produced large SFs as recorded on 6 channels. Each channel corresponds to unsorted cluster recordings. The emergence of HFOs is evident in the firing histograms as interpeak intervals that are less than 2ms. Some peaks exhibit temporal alignment across channels as indicated by the vertical lines. Three to four peaks in firing histograms were typical for cortical recordings induced by mechanical stimulation. Electrical stimulation of 50μA through a pair of electrodes placed in the VPL at a location corresponding somatotopically to the D4 representation produces neural responses selectively on the same 6 channels (Fig.36b). The patterns of responses are similar to the evoked responses following tactile stimulation. The HFOs are more pronounced following microstimulation partially due to the decrease in the background activity. Three to four peaks of activity are apparent. The temporal alignment or synchronization is quite pronounced. The duration of responses following both types of stimulation are comparable: both induced

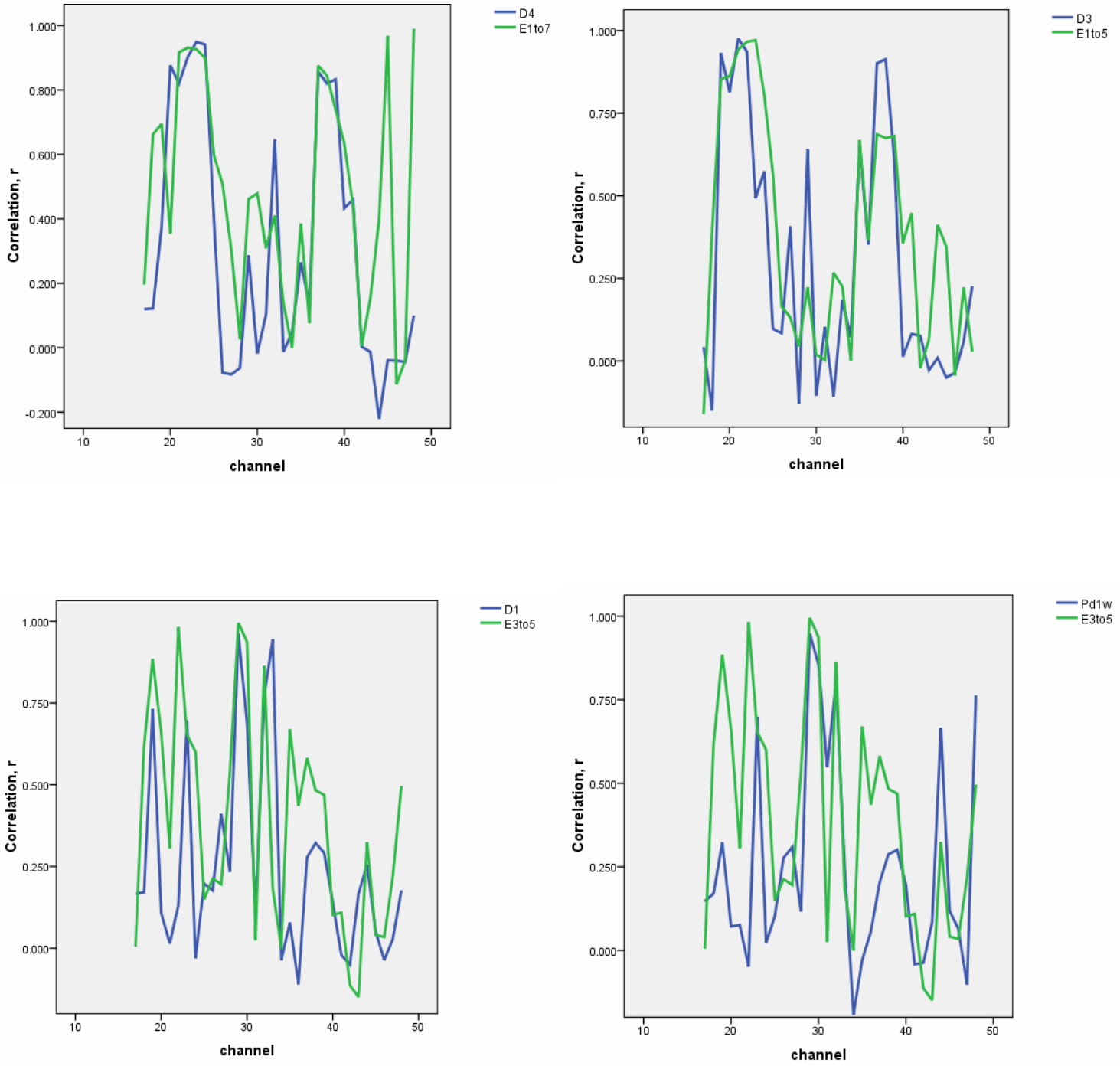

Fig.35. A (upper left) compares tactile stimulation of D4 to microstimulation through electrodes 1 and 7. B (upper left) plots condition D3 and 1->5. C (lower left) plots condition D1 and 3->5. D (lower right) plots Pd3 and3->5.

increases in activity lasting about 10ms. The oscillatory signature is commonly found in neural representations of all skin locations. Synchronization was encountered between single neurons recorded from the same electrode, between neural populations (different channels) representing the same skin location, and between cortical and thalamic areas.

Mechanical and electrical stimulation of other arm regions was investigated. Fig.37a illustrates responses recorded from area 1. The tactile stimulation of the arm region was delivered at 5 Hz. The duration of these responses was 15-20ms with an onset latency of 15ms. Electrical stimulation of 50 μA of the VPL region corresponding to the arm location elicits responses in area 1 similar on both duration and magnitude dimensions to the ones following tactile stimulation (Fig.37b). The 25μA stimulation failed to elicit significant responses. At 50μA, the topography of responses resembles the topography of responses to tactile stimulation and the magnitude of the responses were comparable to those recorded under 'normal' conditions. HFOs are apparent on both mechanical and electrical stimulation records. Overall, the responses in areas with larger RFs such as lower arm follow the trend discussed for more focal RF representations (single pad or digit).

Highly distinctive temporal patterns of neural responses are also encountered in the single unit recordings. These patterns remain present under various stimulation modes. For example Fig.38 demonstrates responses to tactile stimulation of D3 and electrical stimulation of the VPL. These VPL stimulation experiments involved two intensity levels: 50 and 75μA. The template matching discrimination enabled relatively clean separation of up to 8 single neurons from each microelectrode, though the templates' exclusivity eliminated many multi-spike waveforms. The poststimulus

raster/histograms illustrate response patterns of three such neurons (C, D & F in electrode 18) over three successive experiments. Each of the 3 neurons (18C, D & F) exhibits a distinctive temporal pattern (in dot rasters and histograms) that is surprisingly well conserved through the three different stimulus conditions. Each neuron's response

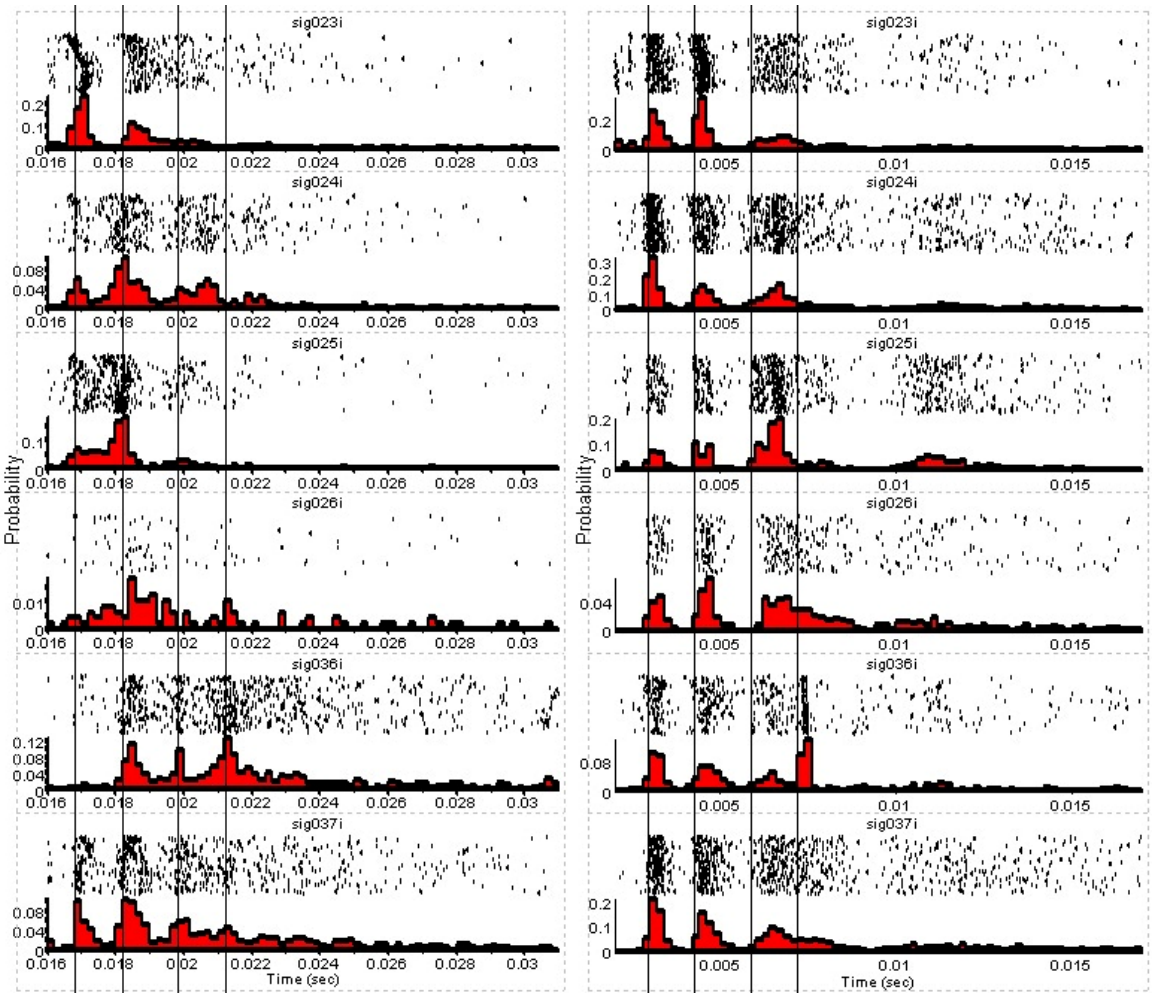

Fig.36. Poststimulus rasters and histograms of neural responses recorded through electrodes positioned in area 1. A. Cutaneous stimulation of D4 is associated with the occurrence (3-4 peaks) of HFOs of higher than 500Hz frequency. B. Electrical stimulation of VPL produces cortical responses of similar spatial and temporal characteristics. The oscillatory tendency is more pronounced with higher degree of synchronization and decrease in the noise.

patterns were compared (at right) by directly aligning their major features, thus compensating for their normal latency differences. These superimposed profiles reveal that each neuron exhibits a distinct response pattern that is well conserved across different stimulus conditions. Highly significant cross correlations ($p<0.001$) were found for all but one of the same-neuron comparisons. The outlier was neuron 18F, in which VPL stimulation triggered a tightly coherent series of 6 neural response peaks in the first 25ms post-stimulus. Though this has a relatively low (significant at $p=0.006$) correlation with the "Touch D3" experiment, the autocorrelation histogram shown in the inset at

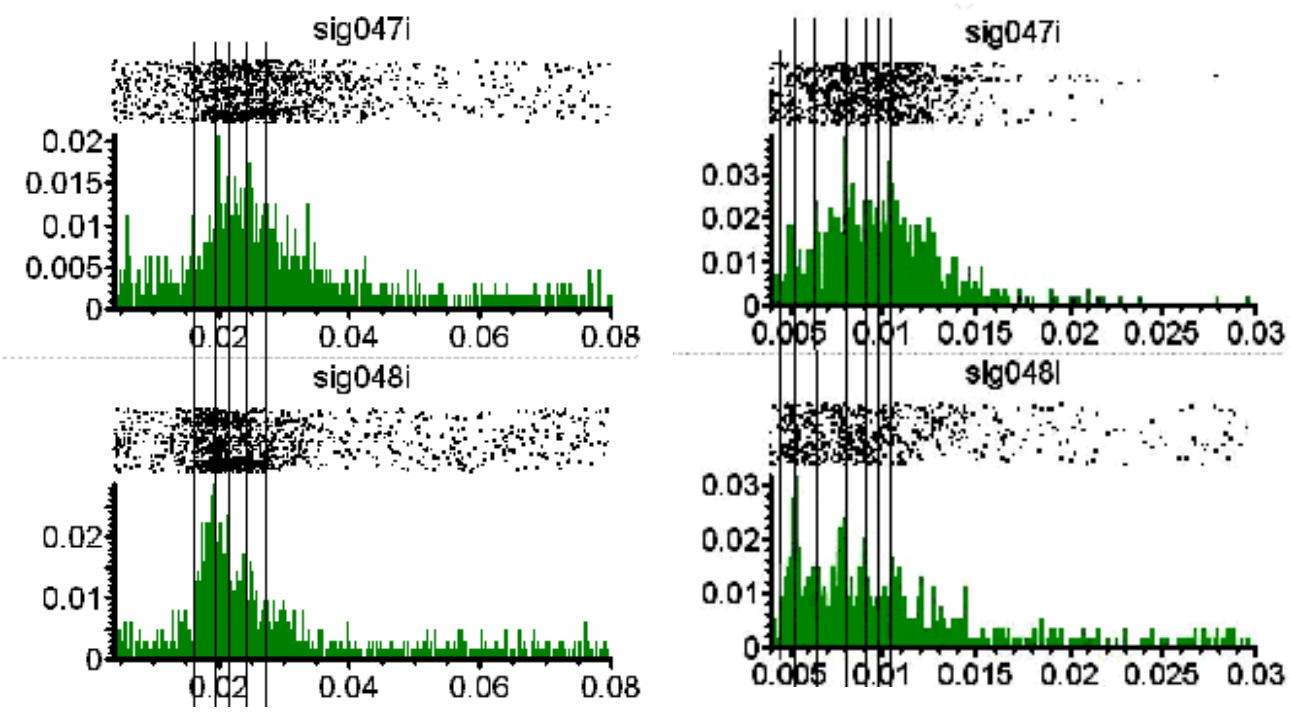

Fig.37. Perievent rasters and histograms of responses recorded in area 1. A. Mechanical stimulation of the wrist at 5Hz induces responses starting at 15ms poststimulus and lasting 15-20ms. B. Electrical stimulation of the VPL causes responses in the area 1 of 3ms latency and of 15ms duration. The mapping of the responses is consistent between the conditions. The strengths of the responses are comparable. High degree of synchronization is observed between units recorded from the same electrode and also between neurons recorded from adjacent electrodes.

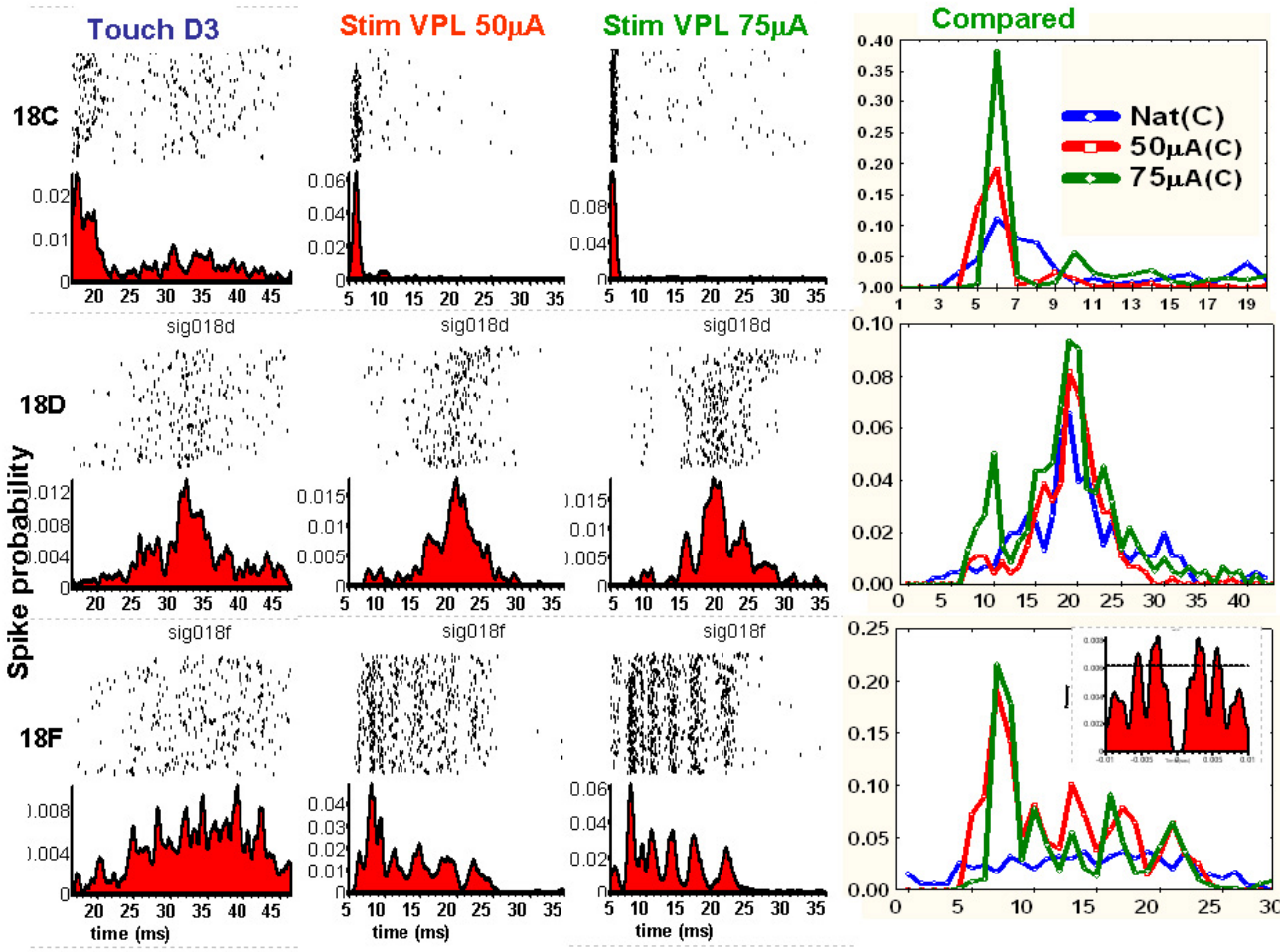

Fig.38. Comparison of patterns of neural firing as recorded from 3 discriminated neurons in response to 3 experimental conditions. Column 1 18c depicts one of the most prevalent response pattern characterized by early onset of activity with the presence of a sharp peak. This trend is persistent across all conditions. Channel 18d recordings indicate late onset at about 30ms postevent and longer duration of the response. In response to both 50 and 75microA VPL stimulation this pattern of activity stays stable. Responses of neuron 18f are dominated by high frequency oscillation having more latent character following mechanical stimulation and exhibiting more pronounced appearance following electrical stimulation. "Compared" figures show good correspondence of responses across all conditions.

right indicates that it also exhibits oscillations in the same frequency as the VPL stimuli. The difference, therefore, may be mainly due to the relatively high noise level in the natural touch stimuli relative to the 75µA VPL stimuli. HFOs on channel 18f are the most apparent under 75microA stimulation protocol. Six characteristic vertical bands on dot

raster are phase coherent with the stimulus. Though responses to natural touch show less coherence with the stimulus they exhibit similar frequency oscillations (~360Hz) as indicated in the autocorrelogram (inset at lower right).

In Fig.39 the activity of 8 discriminated cells from channel 18 is plotted against the latency of response. The responses are recorded following VPL stimulation. There is a high degree of synchronization exhibited by the neurons. Later responses show coactivation and HFOs. The response duration is 15ms. Later responses are characterized by 3-4 peaks of activity which is comparable to the oscillatory responses to tactile stimulation. This type of synchronization is regularly observed in SI recordings from anesthetized animals.

Electrical stimulation of the VPL was shown to produce naturalistic patterns of responses in area 1. Electrical stimulation of area 1 was also investigated. Microstimulation was administered through pairs of electrodes positioned in area 1. Area 2 responses required characterization in order to establish feasibility and goodness of the area 1 stimulation protocol.

Fig. 40 shows the result of electrical stimulation of area 1. The stimulation selectively activates neural populations encoding for D1. Stimulation at 150μA produces response in area 2 with the latency of 3ms. Two peaks of activity are separated by less than 1ms. The next figure (Fig.41) depicts the patterns of responses following tactile and area 1 stimulation. The stimulating electrode in area 1 had a receptive field on the monkey's thumb. The same "thumb" receptive field was observed on electrode 31 (Sig031) in S1 area 2 (fig.41A). An apparent connection between these two areas is indicated by the strong peak in the foreground of the figure. Moreover, Sig. 20 (lower

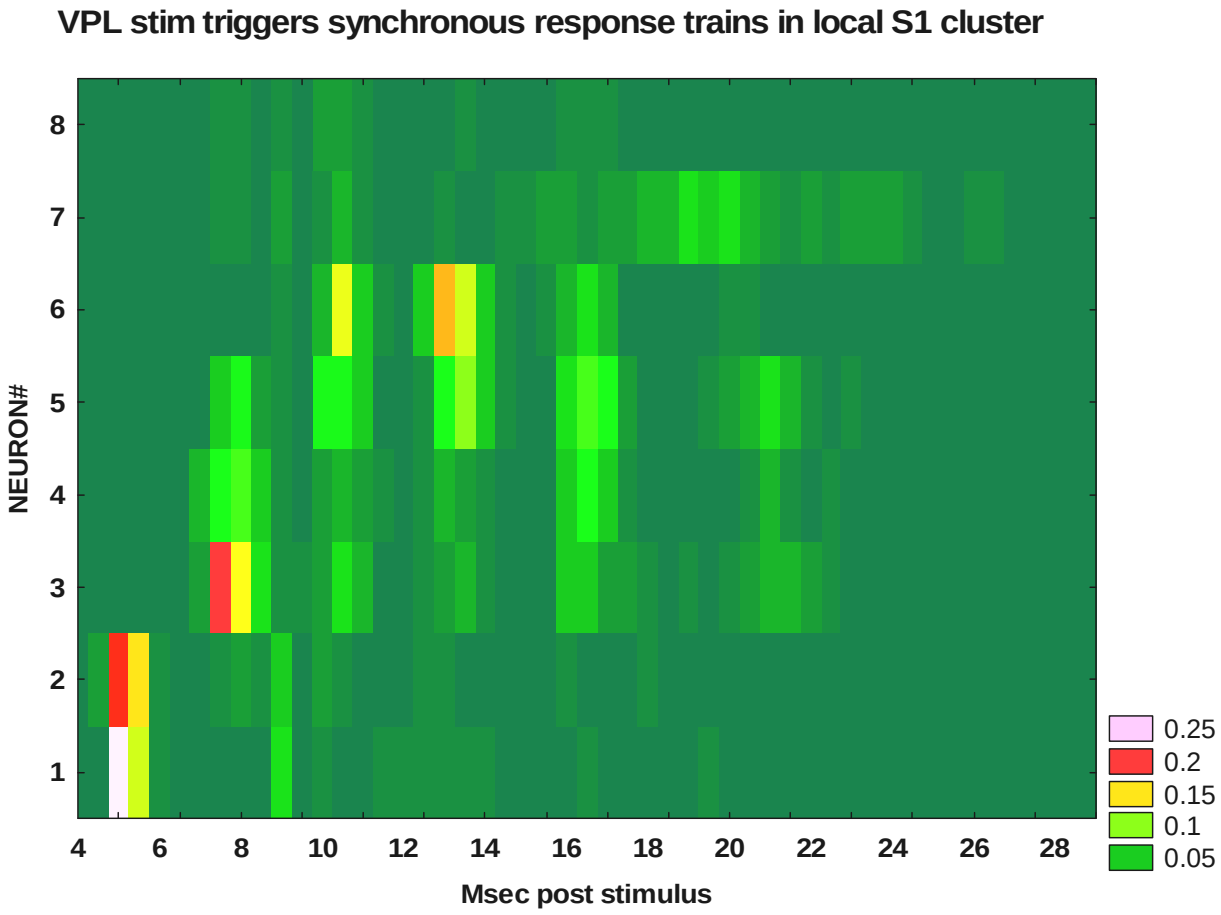

Fig.39. Color spectrum plot of the neural responses recorded from 8 cells discriminated from channel 18. These responses are to the electrical stimulation of VPL. X-axis represents latency of response. The good spatial and temporal resolution of the responses aids in identification of trends in the neural activity. Neuron 1 and 2 respond with short latency and high firing rate. Neurons 3 to 6 follow n.1 and 2 at later time points and exhibit pronounced HFOs lasting 15ms. The synchronization between these neurons is observed.

peak in background) had a receptive field on the hand proximal to the thumb. The remaining 30 channels did not exhibit clear tactile receptive fields near the thumb area. Microstimulation of the area 1 produces activation patterns in the area 2 comparable to evoked responses following tactile stimulation.

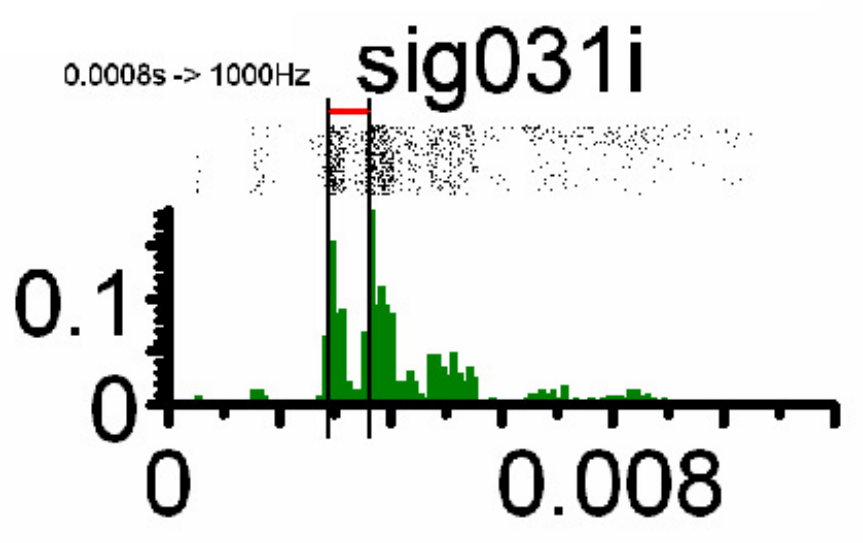

Fig.40. Perievent histogram and raster of the data recorded from neural cluster responding to electrical stimulation of area 1 (D1 representation). The onset of activation is observed at 3ms.The response is characterized by the HFOs.

As has been shown in experiments on VPL stimulation that spatiotemporally patterned stimulation through multiple electrodes can improve the ability to produce naturalistic neural responses in the cortex (Xu and Chapin, unpublished results). These results were obtained using acutely prepared rats. The following results provide additional evidence for optimization of the stimulation patterns using area 1 stimulation in monkeys. Fig.41B illustrates that bipolar stimulation at 50μA through one electrode pair fails to induce appropriate responses in area 2. Fig.41C shows that increasing the intensity of the stimulus results in rather non-specific activation of neurons in area 2. Finally, Fig.41D indicates emergence of appropriate response as supported by highly selective activation of the channels. The stimulation in this experiment was conducted through two electrode pairs separated in time by 1ms. The intensity of stimulation was 50μA as in fig.41C. High current stimulation through a single

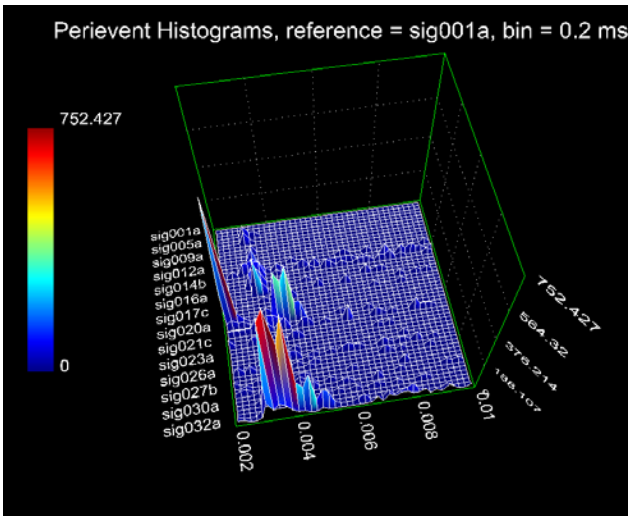

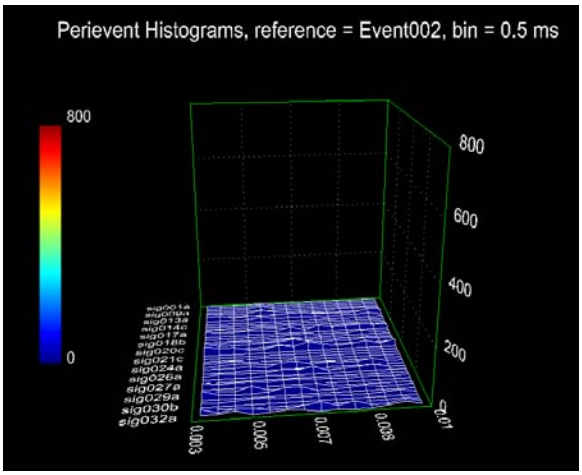

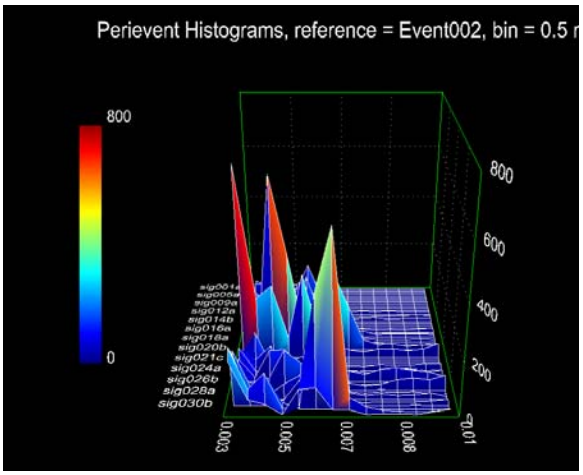

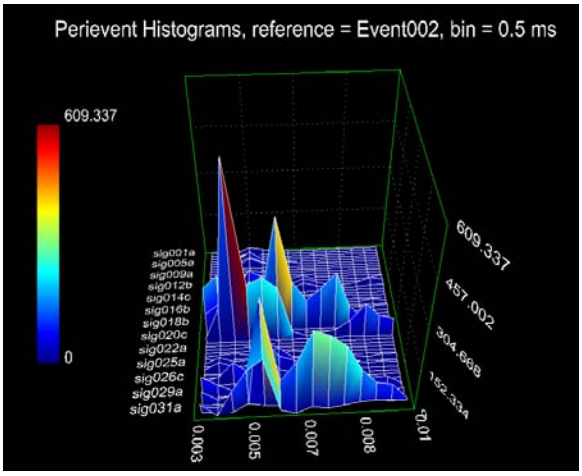

Fig.41. 3-D reconstruction of neural responses in area 2 as recorded through 32-electrode array. A. Tactile stimulation of D1 results in selective activation of channels 20 and 31.A. Bipolar electrical stimulation at 50μA through single electrode in area 1 produces subthreshold activity in area 2. B. Stimulation at 100μA

through the same electrodes produces generalized responses in area 2. C. Spatiotemporal patterning of the stimulation increases selectivity of responses: sequential 50μA stimulation through two bipolar electrodes results in activation of the somatotopically correct zones in area 2 (channel 31 and 20).

bipolar electrode may produce more nonspecific and artifactual neural activity than spatiotemporally patterned low current stimulation through multiple electrodes.

Discussion

The present study examined properties of neural responses following tactile and microstimulation recorded from the somatosensory thalamus and cortex. One of the methods used for the quantification of evoked responses was analysis of correlation. The technique was developed to identify neural populations involved in the detection of stimuli applied either to the periphery or intracranially through thalamic and cortical electrodes. The magnitude of the correlation coefficient was utilized to assess the relative involvement of neural populations in representation of receptive fields. The neural representations of the signal localized to the cortical sensory areas were compared for two conditions: tactile and electrical stimulation. Following multi-site tactile stimulation neural responses in the cortex were characterized by the presence of discrete stimulation fields associated with receptive field representation. Electrical stimulation through the electrodes placed in VPL resulted in similar pattern of activation as recorded from the cortical arrays acutely implanted in monkeys. The effects of ketamine anesthesia on sensory evoked potentials following tactile stimulation were investigated in chronically implanted animals. Neural responses to stimulation as recorded from the cortex showed stability for the duration of the maintenance phase of the anesthesia. The responses were characterized by similar duration as well as magnitude of firing rates for awake and maintenance conditions. Shorter duration of neural responses was observed during the recovery phase. The recovery stage lasted close to an hour which was twice as long as the maintenance phase.

Analysis of correlation to define receptive and projection fields

One of the goals of the study was to develop a methodology for simple analysis of evoked responses recorded from the somatosensory regions in the thalamus and cortex. The responses to stimuli delivered to the periphery need to be characterized in a way that allows comparison of these responses to various stimulation conditions. If the comparison is done with the method that is computationally simple and fast it could be carried out in real-time which would allow for optimization of experimental manipulations. Neural responses possess characteristic spatio-temporal representation. The method of analysis, optimally, should include both of these parameters.

Recordings from the cortical arrays indicate that neural populations respond differentially to stimuli applied to various skin locations (Woolsey et al, 1958). Receptive field refers to a localized skin area whose sensory endings are associated with a group (groups) of primary afferent neurons. Projection field consists of all channels (all groups of neurons) that record evoked responses to stimulation of a particular receptive field. This ability to selectively encode information from a discrete skin location constitutes a basis for comparison of neural responses to tactile stimulation (Kaas, 1997). The temporal domain of the response includes such parameters as the onset and duration of the response as well as fluctuations of firing rate throughout the recorded poststimulus interval. Firing rate is indicative of the fidelity of responses. In monkey experiments, the probability of firing by cortical cells recorded on one channel following stimulation was as high as 65% (action potentials occurred within a single 1 ms bin in 65% of trials). Typically, responses were characterized by early and late peaks. The latency of responses recorded in area 1 was 15 to 17ms (early peak). The early peak corresponds to “initial

encoding", representing the most direct activation of cortex, while the later peak is presumed to be associated with further processing of sensory information. The peaks were separated on average by 200ms. This delay could accommodate synaptic transmission to and from various association cortices as well as subcortical structures.

Firing frequency distributions of evoked responses for interstimulus interval were generated. These frequency distributions were compared across two sessions for the same channel, for the same condition. Analysis of correlation was used to assess similarities between distributions. Pierson r was shown to yield a reliable index of involvement of neural population in the stimulus encoding. Highly correlated activity was observed on channels associated with encoding of receptive field of stimulated skin location. Channels that did not contribute to the encoding of a stimulus showed low correlations. The "best channels" showed up to a 100 fold increase in the coefficient magnitude compared to the "noisy" channels. The magnitude of correlation coefficient served and as an index of degree of the participation in the information processing. The correlations provide a universal measure of comparison across conditions as the magnitude of correlation is predetermined to be in the range of 0 to 1. Changes in neural firing induced by different experimental manipulations can be assessed using correlation analysis.

As a standard, the analysis of correlation is included in most statistical software packages allowing for relatively easy access. There are certain conditions that need to be met in order to use this analysis with maximal efficiency. Analysis of correlation could potentially produce false high coefficients (false positives). Analysis of correlation discussed in the Results I section was applied to compare neural signals recorded from the same channel under various conditions. The data is typically segregated into bins; the

value of these bins denotes the firing rate of the neural population at a particular point in time. The values of the bins are compared with respect to the order. High bin values at corresponding time points produce high correlations. If data obtained under both conditions includes only one bin of high value at corresponding time points correlation between the conditions will be high. It takes only one bin of high value to dramatically improve correlation. Biologically, any such instance should be of great importance and deserves investigation, but such results could be produced also if the high value is obtained as a result of artifactual recordings such as of electric noise. Prior to the analysis the data in the form of poststimulus histograms needs to be inspected for such occurrences. Ideally it should be filtered automatically by the threshold settings in the recording software.

Correlation coefficients were shown to be useful for generation of somatotopic maps. In awake monkeys, the neural representations of each digit showed a high degree of stability. Recordings from several sessions within and across experiments were correlated yielding the index of stability. Unique spatial patterns of activation were uncovered for each digit. Some channels showed a high degree of conditional specificity: those channels corresponded to neural populations encoding small receptive fields. Other channels were activated upon stimulation of several digits and did not show high correlations associated with a specific condition. These neural populations represent larger receptive fields, corresponding to the flanking regions of the RF (not RF center). Analysis of correlation was shown to be a highly reliable index of the extent of neural encoding properties of multiunit populations.

Cortical arrays used for both microstimulation and ketamine experiments had the following characteristics: the spacing between adjacent electrodes in the same row was 300μm and the two rows were separated by 500μm. The figures in the results sections summarize correlation coefficients for all electrodes for a particular stimulation condition. Typically, analysis of correlation localized projection fields (number of channels responding to stimulation of a single peripheral skin location) in area1 of SI to 3 adjacent electrodes (fig. 7, fig. 31). In some instances projection fields included 5 adjacent electrodes. Electrodes from both rows were observed to yield high correlations. Typically, the rostral row of electrodes showed better spatial resolution of projection fields than the caudal row, i.e. less number of channels fell into the projection field corresponding to a skin location. The total number of channels from both electrode rows responding to stimulation of a single skin location was up to 8. Therefore, the electrodes mapping the same digit spanned up to 1.5mm in mediolateral direction and 0.5mm in the rostro-caudal direction. As can be seen from the ill. 2, these distances are consistent with the mapping results obtained using single unit recordings (Nelson et al., 1980).

It can be seen from fig.7 how representations of digit 1 (ch11, 12, 13) maps to electrodes adjacent to electrodes mapping digit 2 (ch 9, ch 10). Slight overlap in the digit representations (in RFs) is observed. The same tendencies were observed between the electrode maps for D2 and D3. The representation of digits in area 1 follows a medio-lateral scheme with D5 being the most medial and D1 the most lateral (the electrode was positioned in the cortex with low numbered channels being more medial). This is highly consistent with the findings reported by others (see ill.2).

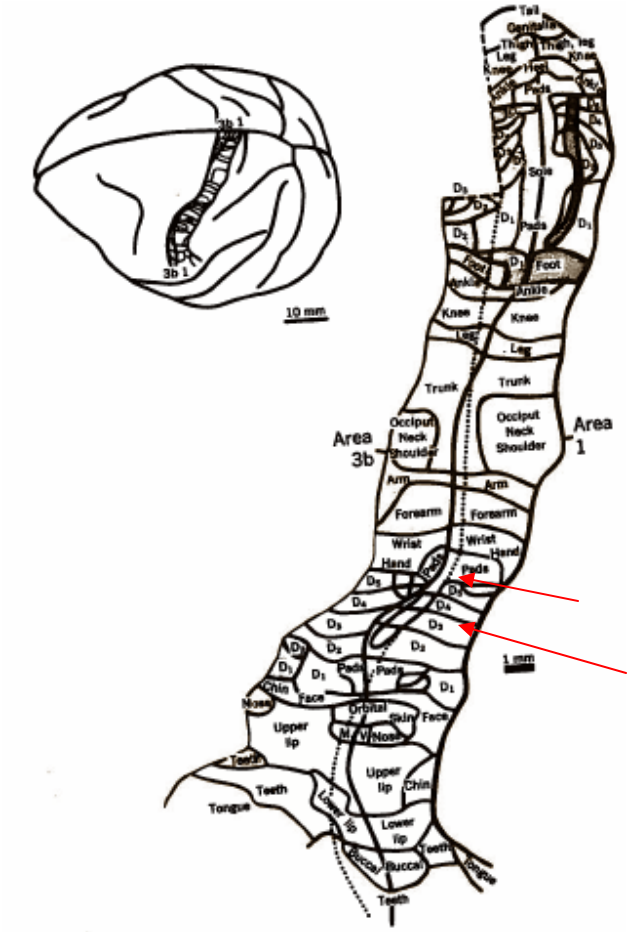

Illustration 2. Representation of the body surface in areas 3b and 1of the cynomolgus monkey. Digit representations show are labeled D1 through D5. Pad representations are identified. From Nelson et al., (1980).

Results described in fig. 31 provide further evidence for similarity of the mapping results obtained using correlational analysis and more conventional methods (such as detection of firing rate increases time-locked to the onset of the stimulus). This array was positioned in the area 1 with the lower numbered channels being more lateral: so that channels representing digits are localized to more lateral regions (ch.1-ch.7) than most of the channels mapping pads (ch. 11-ch.16). Another set of pad representations is found on channels 3 though 7. To conclude, pads were mapped to more lateral (overlapping with D1) and medial regions, while digit representations are found more centrally in the area 1. The same pattern of neural representation is shown in ill.2. Also, while digits were mapped on both rows of the electrode, pads were mapped to both rows only on the more medially located electrodes. Laterally located pad representations mapped only to the first row which was more rostral (see consistency with the ill.2).

The sizes of RFs estimated using high correlation coefficients (as determined by recordings in area 1) varied from an area spanning 2 to 4 digits and/or pads. A single channel could show high correlation in response to stimulation of several digits (see fig. 7 and 31). As can be seen from ill.3, neurons in area 1 map RFs spanning several digit and

pad locations (Woolsey et al., 1942; Woolsey et al., 1958). A good consistency of results obtained by correlational analysis with results produced by other analytical methods, validates apllicability of the analysis of correlation.

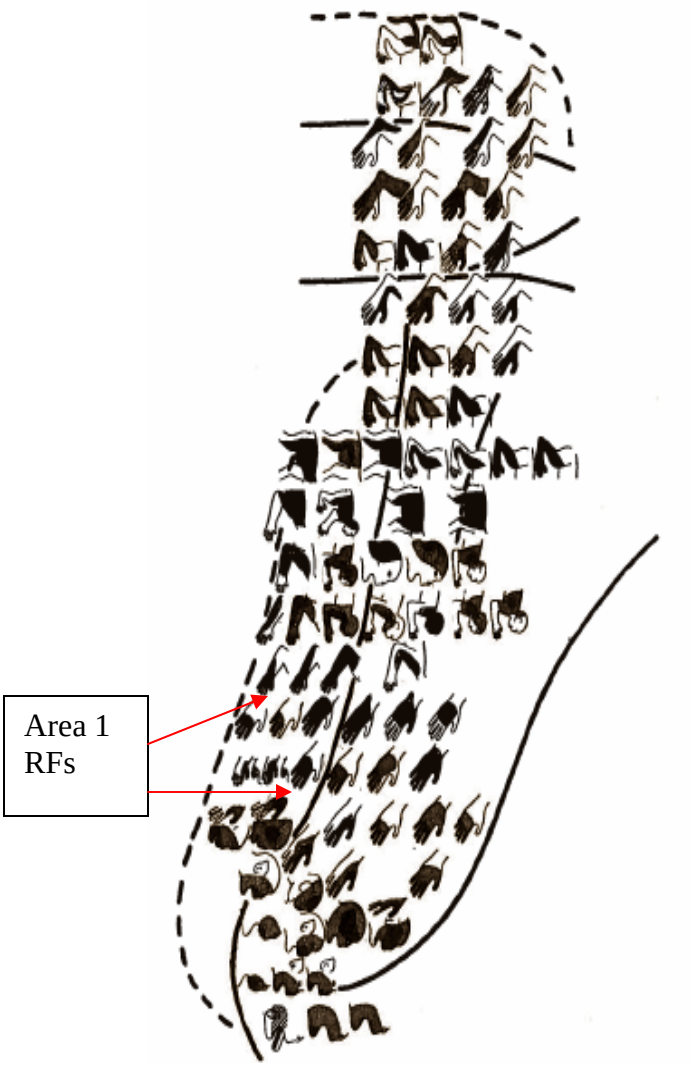

Illustration 3. Map of projections of skin locations (RFs) on the SI. From Woolsey et al., (1942) and Woolsey (1958).

The analysis of correlation was shown to be suitable for the identification of neural populations involved in sensory processing. This method is particularly sensitive to increases in firing rates (detection of peaks). Neural representation of sensory information is also associated with decreases in firing rate, such phenomena as surround and replacing inhibitions. The presence of inhibition improves signal detection and discriminative capabilities of the sensory system. Both types of neural responses (increased and decreased firing rate) carry information about stimulus. Both contribute to the encoding scheme of the system. The analysis of correlation is not an appropriate tool for localization of channels showing inhibition. Inhibition as well as

spontaneous activity produce low correlations which makes is impractical to differentiate between the two types of activity.

Analysis of correlation could be employed to assess stability of recordings over extended periods of time, even decades. This particular application might prove to be useful in clinical settings. The integrity of electrodes chronically implanted in patients (for the BMI or other projects) has to be periodically evaluated to monitor for potential damage and dislocation. Utilization of analysis of correlation would be an easy and economical way to ensure proper functioning of the implanted devices.

The relative ease of application of correlational methods described in this thesis to data analysis makes it possible to use this method in real-time in order to assess neural activity in response to various stimuli and behavioral states. The index of similarity of the activity of neural populations could be incorporated into "biofeedback" training sessions for users of motor neuroprosthesis. For example, for the motor neuroprosthesis, neural commands in the form of specific neural activation patterns have to be generated by the motor cortex. The temporal and spatial patterns of neural activation for the same condition (ex. planned movement in the specific direction) have to show stability over time (Chapin and Nicolelis, 2001). The neural commands originating in the motor cortex need to be under (semi)conscious control of the patient (Zacksenhouse et al., 2007). The pattern of activation of the motor cortex determines the trajectory of movement of a robotic arm or an exoskeleton. Correlation coefficients were shown to reliably detect dissimilarity between neural population activation patterns in both temporal and spatial domains.

Comparison of cortical responses to tactile and thalamic stimulation

One of the major aims of the study was to aid in the development of a somatosensory neuroprosthesis - a brain stimulation device that can be used to artificially produce tactile sensations in patients who have lost normal somatosensation due to spinal cord injury or amputation. It will be used to provide both tactile and proprioceptive feedback in a closed loop brain-machine interface. Central to the development of sensory neuroprostheses is an understanding the parametric characteristics of electrical microstimulation of brain regions to produce cortical responses and percepts similar to those evoked by the natural tactile stimulation of the skin.

Microstimulation of VPL was shown to produce selective activation of the neural population involved in the encoding of specific tactile stimuli. Somatotopic correspondence between evoked responses following both tactile and electrical stimulation was established using two methods of analysis. The measure of the magnitude of the firing rate – z-score produced results similar to the analysis of correlation. Rather large RFs were established in both the VPL and area 1. The size of the RFs could be influenced by the anesthesia. Typically, receptive fields spanned several digits. The size of the RFs defined the extent of spatial activation of the neural populations following tactile stimulation. It was shown that the extent of the activation was similar following microstimulation of VPL. Preparations with smaller RFs would be helpful in order to further improve discriminatory power of the signals.

The parameters of stimulation affected the degree of activation of the cortical populations. Location of the stimulating electrodes in the VPL affected the amount of

activation. The intensity of stimulation was proportional to the spread of activation. Stimulation at 50μA produced the most naturalistic responses in the cortex.

Inspection of neural responses following microstimulation revealed similarity to patterns of responses produced by tactile stimulation. Specifically, the duration of response did not change significantly. Presence of oscillatory activity characteristic to sensory evoked potentials (Shadlen and Movshon, 1999) was noted. The high frequency oscillations (up to 800Hz) were observed in multiunit recordings following both tactile and microstimulation. The number of peaks following electrical stimulation tended to be larger, and increased with the intensity of the stimulus. Single unit recordings were also analyzed for the presence of HFOs. Highly synchronized activity of the single units was observed across several channels. The timing of the HFOs often was similar between neighboring neurons or neural population, with near zero time lag. This finding lends support to the hypothesis of a time-locking function of the HFOs that serves to enhance detectability of the signal (Valencia et al., 2006).

Effects of ketamine anesthesia on sensory cortical activity

Similar analysis was carried out on the data from anesthetized monkeys in order to assess the influence of ketamine anesthesia on the encoding properties of neural populations. Following ketamine injection, monkeys showed behavioral signs of the induction phase (Carter, 1995). They became catatonic and unresponsive to stimulation. This induction phase was brief, lasting only 5-7min. The neural recordings from one animal indicated lack of synchronization of responses compared to awake condition. The responses were characterized by drastic decrease in duration, while firing rates were comparable to rates seen when the animal was awake. The induction phase is relatively

short and the current experimental paradigm had limitations in investigative powers of such phenomenon because in the future, continuous recordings should be implemented in order to better define firing by cortical neurons throughout induction.

Following induction, the maintenance phase was characterized by stability of neural responses. This stage lasted on average 30 min. High correlations were obtained between responses during anesthetized and awake stages. The findings point to similarity between frequency distributions for the two conditions. The firing probabilities during responses did not show significant changes. The duration of responses was slightly decreased by the anesthesia. Decrease in the response duration produce minor fluctuations in the magnitude of correlation coefficient. These findings indicate relative stability of recordings across anesthetized and awake conditions. Ketamine anesthesia was concluded to exert minimal effects on the population recordings. High degree of synchronization between responses provides evidence for usefulness of ketamine preparation for acute experiments. Other studies examining effects of ketamine anesthesia on other sensory systems showed increase in the duration, latency and firing rate of the response (Rennaker et al, 2007, Populin, 2005). Present findings to do not support such occurrences: the duration and latency of responses decreased. The effect of ketamine might be system dependent.

The recovery stage was characterized by fluctuations in temporal properties of the response. The duration and onset of responses decreased which contributed to exceedingly low correlation coefficients because major peaks shifted out of temporal alignment. The temporal characteristics of the early and late peaks were analyzed. The late peaks contributed profoundly to the desynchronization of responses. These findings

suggest changes in the information processing during the recovery stage. The design of the study precludes investigation of the underlying reasons for such changes in the encoding properties. These changes could be due to alterations in the sensitivity of the peripheral receptors or sensitization of neurons within the somatosensory pathway (possible disinhibition). Further studies could examine the properties of responses at synapses along the somatosensory pathways in order to establish whether this change in the encoding properties is a purely cortical phenomenon.

The influence of ketamine on neural responses to tactile stimulation was shown to be the most profound during the recovery phase of the anesthesia. Maintenance phase, on the other hand, was characterized by responses closely resembling awake condition. In order to be able to generalize results obtained under anesthesia to awake state experimental manipulations involving neural recordings has to be made during the maintenance phase in order to prevent confounding influences of ketamine observed during recovery. Furthermore, changes in neural responses during recovery phase could be used as a guideline for estimation of depth of anesthesia.

Results obtained in the course of the ketamine study have certain clinical application. Oftentimes, procedures during neurosurgery require measurements of neural responses in “awake” patients. Ketamine was shown to affect neural responses the most during recovery stage (lasting up to 1 hour): the responses were the most variable during this period. If ketamine is used as the anesthetic during such procedures, this thesis demonstrates that patients have to be fully recovered from the anesthetic state in order obtain neural recordings the most comparable to the awake state. Other anesthetics

currently used during neurosurgical procedures should be evaluated for potential signal perturbations resulting from the transition from anesthetized to awake state.

The central hypothesis was that one can mimic the neural responses to natural touch stimulation by optimizing the spatiotemporal patterns of microstimulation in the somatosensory thalamus or cortex. Simultaneous neural recordings from multielectrode arrays implanted in the somatosensory (S1) cortex provided a suitable criterion for optimizing of spatio-temporal patterns of microstimulation in the VPL (ventroposterior lateral) thalamus. Using neural recordings through microelectrodes positioned in the sensory thalamus (VPL) and cortex of monkeys, responses evoked by tactile stimulation were compared with the neural activation produced by electrical stimulation in VPL thalamus and SI area 1. The results indicated that microstimulation in somatotopically defined subregions of the somatosensory (VPL) thalamus produces relatively natural patterns of neural population response in somatotopically equivalent subregions of the S1 cortex. The findings identified VPL as an appropriate target site for stimulation experiments. Further research should concentrate on replicating these results in awake behaving monkeys in order to assess the degree of perceptual processing associated with the signals recorded in the cortex.

Chronically implanted electrodes in the same sensory areas will aid in the investigation of perceptions evoked by thalamic stimulation. Experiments on awake behaving monkeys trained to discriminate the location of the tactile stimulus will provide a behavioral measure of signal detection and perception. The monkeys will be asked to localize the percept evoked by electrical stimulation of the somatotopically corresponding

location on the skin. The proper somatotopic correspondence will be determined by the neural responses to tactile stimulation recorded through the electrode arrays spanning most hand regions. The main aim would be to optimize the parameters of electrical stimulation so that the correspondence between behavioral responses to tactile and electrical stimulation would be observed. The next stage would be to merge microstimulation paradigm with motor neuroprosthesis in order to obtain a closed loop system.

Appendix A

Psychophysical assessment of signal detection in rats

The feasibility of brain stimulation used to produce cues to guide behavior has been established by several studies conducted in the lab (Talwar et al., 2002; Xu et al., 2004). In these experiments, the barrel cortex of rats was stimulated as a signal that rats were expected to interpret as a cue to move in a specific direction. The success of these experiments supports the view that electrical stimulation of brain regions could be consciously perceived by an animal. Another series of experiments (Rozenboym, et al., 2002) aimed at addressing the psychophysical properties of behavioral responses cued by the SI cortical stimulation. These experiments were conducted on rats.

As a model, rats were trained in a detection task that used SI stimulation as cues and Medial Forebrain Bundle (MFB) stimulation as reinforcement (Olds and Milner, 1954; Olds and Fobes, 1981). Signal detection theory (SDT) was used to analyze the resulting animal behaviors.

Signal Detection Theory (Green and Swets, 1966) seeks to model the decision processes behind making detections of a stimulus signal (S+) against background noise (N). It states that the presentation of either a stimulus or noise causes a sensory state that has a Gaussian distribution. The means of the two distributions are separated by an amount proportional to the "detectability" of the S+ from N. Due to the overlap of these distributions a subjects may be unsure if a signal is present. SDT postulates that a subject detecting S+ from N does so basing decisions on a response criterion that depends on separate behavioral components such as reinforcement. The criterion a subject uses to make decisions is manifested as the subject's "response bias". According to the theory,

even though signal detectability remains unchanged, different hit rates (probability of correct signal identification) and false alarm rates (probability of incorrect identification) can be obtained across experimental sessions if the subjects' response criterion is made to vary.

When hit rates are plotted against false alarm rates these data describe a curve - the receiver operating characteristic (ROC). The shape of such curves is dictated by the underlying signal and noise distributions. The ROC thus represents an isosensitivity condition with all points on the curve representing the same signal detectability without regard for the particular experimental conditions under which the observations were made. The specific location of a point on the curve indicates the response bias of the subject. Signals of different strengths produce different ROCs that are parameterized by the signal's detectability. SDT assumes that the detectability of a signal is independent of the response bias of the subject; its strength is that it provides separate indices to measure both.

Rats were trained to respond to electrical brain stimulation (SI barrel cortex) with the lever press. The parameters of stimulation such as intensity and number of pulses per train were varied systematically. The intensity of the stimulus ranged from 10 to 150microA. Initially, the threshold of detection was established. ROC curves were constructed and decision states were identified. A Variable ratio schedule of reinforcement (1:1 to 4:1) was used in this Go/No-Go task.

Fig.42 is derived from the behavioral measure of the detectability of electrical stimulation. When stimuli of variable intensities are presented within a session– the A' (non-parametric detectability index) corresponding to each such intensity can be derived

from the individual hit rates and the common false alarm rate of the session. The hit rate was defined as a lever press following a cue. These rates were calculated individually for all stimulation intensities. False alarms were defined as lever presses in the absence of a cue. These were calculated separately for each stimulation intensity and summed to obtain overall false alarm rate. The computational formula for A' where h_i = hit rate at a particular stimulation intensity and *fa* = false alarm rate is (Grier, 1971):

$$A'_i = \tfrac{1}{2} + [(h_i - fa)(1 + h_i - fa)] / 4h_i(1 - fa)$$

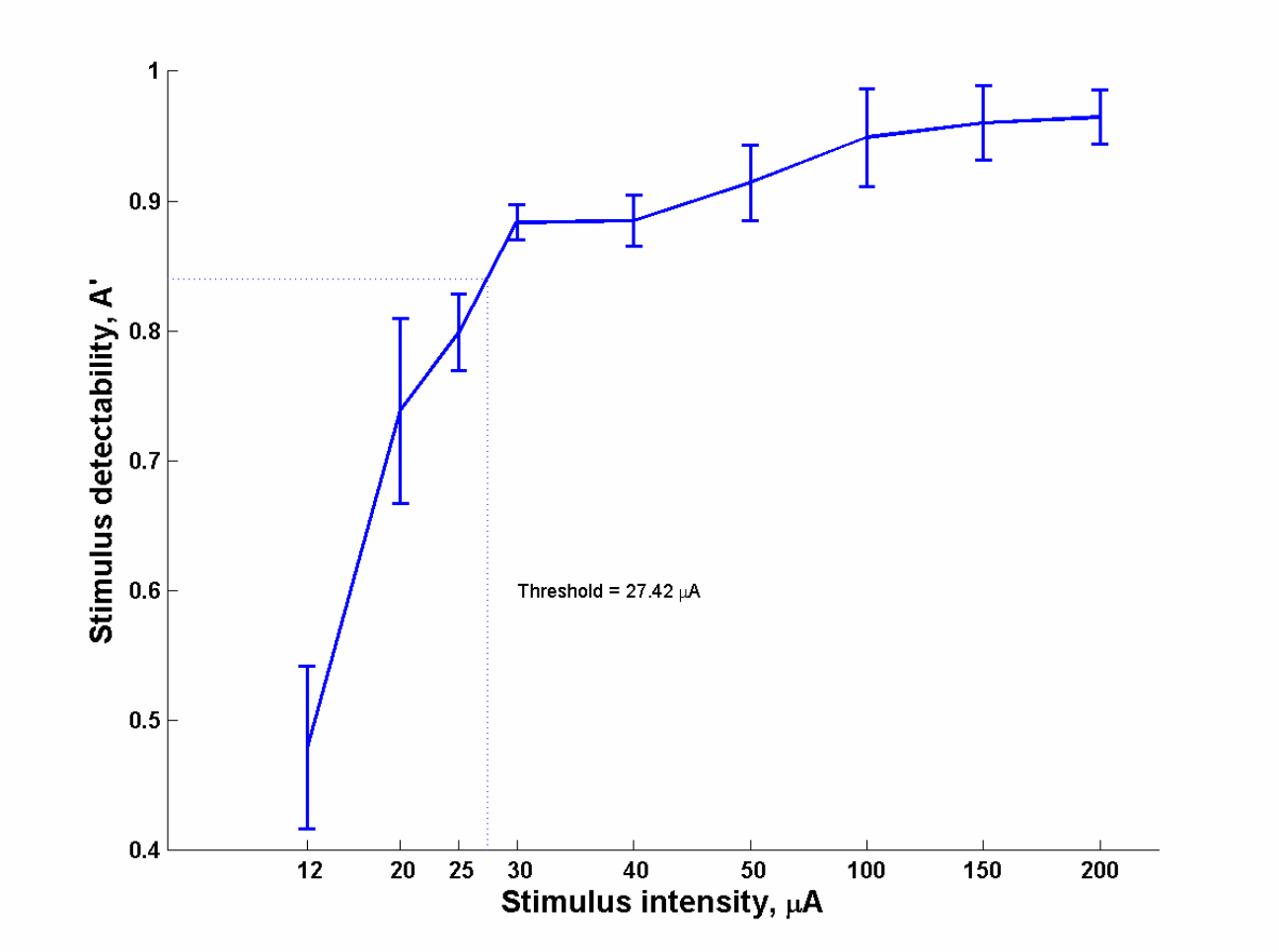

Fig.42. The detectability measure of intracortical electrical stimulation. The stimulus detectability – A' is plotted against the stimulus intensity. The threshold corresponds to stimulation of 27microA. At A' = 0.85 the hit rate equals 50%. Stimulation at higher intensity levels (100-200microA) does not produce marked improvement of performance – the plateau is reached.

Psychometric functions are obtained by plotting A' against stimulus intensity. Values for A' range from 0.4 to 1.0; from chance to perfect performance. A'=0.85 can be taken as representing threshold performance since this corresponds to a conventional threshold hit rate of 0.5 (typically, threshold is established at 50% correct response rate) and false alarm rate around 0.05 (Talwar & Gerstein, 1998, 1999).

Rats were able to identify intracranially delivered cues of intensity higher than 27μA. Overall, threshold intensities for detection of somatosensory stimulation using 2 trains of 10 pulses (delivered at 100Hz) ranged from 25 to 30 μA. At 40 μA the performance was consistently above detectability index of 0.85.

Animals were trained to report presence of a signal appearing randomly (p =.6) over more than 1000 trials. The signal was a train of biphasic pulses given to the SI cortex. Current intensities were either 20 (Fig.43a) or 40μAmps (Fig.43b). The following events were identified: reinforced hits (rh), unreinforced hits (uh), false alarms (fa), correct rejection (cr), and misses (ms). Events on the trials following were then grouped separately to give 5 separate data files. These data were analyzed for hit and false alarm rates and plotted in the ROC plane. While signal detectability (A') remained constant across these data their associated response bias levels (RI) were considerably different from one another giving rise to a spread of data points (hit rates against false alarm rates) that defined a classical ROC curve (fig 43a,b).

Each of the data files was split into 5 different data sets by separating the trials that followed the 5 events. Each set was then tagged with a response bias level. As the Fig.44 shows, response bias levels were different depending on preceding events.

Response bias following a false alarm was greatest; bias levels following reinforced and unreinforced hits were lower. Bias levels following correct rejections and the misses were lowest. Four significantly different ($p<0.001$) response bias states could be detected each of which were associated with unique previous events: false alarms, hits, correct rejection, and misses.

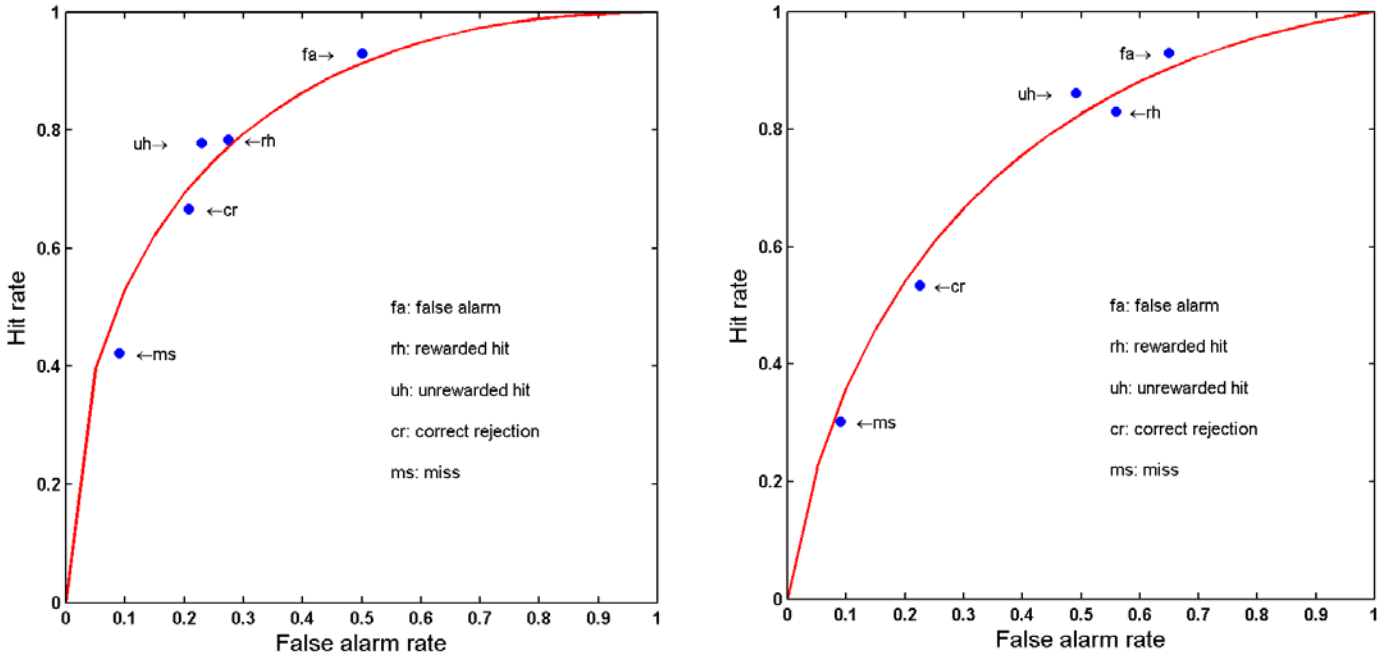

Fig.43a. ROC curve corresponding to responses obtained at 20μA stimulation intensity. Hit rates were plotted against false alarm rates for 5 data sets corresponding to trials following one of 5 events: reinforced hits, unreinforced hits, false alarms, correct rejection, misses. Different hit/false alarm proportions were obtained for most of the conditions. This is interpreted by the presence of underlying behavioral decision states, i.e. after a miss the overall response rate as indicated by the hit and false alarm rates decreases. The animal is not changing the strategy – a miss does not motivate an animal to respond more. Fig. 43b shows similar response pattern for the experiments involving stimulation at 40μA. At 40μA the curve undergoes rightward shift driven by increase in false alarm rates following all 5 events.

Neither reinforced nor unreinforced trials created significantly different decision states. Therefore, the internal state of the organism does not depend on the reinforcement delivery. From reported results it follows that training animals on variable ratio

reinforcement schedules was the optimal paradigm choice for the studies of stimulus detection in monkeys. The interpretation of responses is not confounded by different behavioral states and at the same time high rates of responses are produced. Further because animals are not reinforced on every trial the sessions could run longer, while the interest level of the animal remains almost constant.

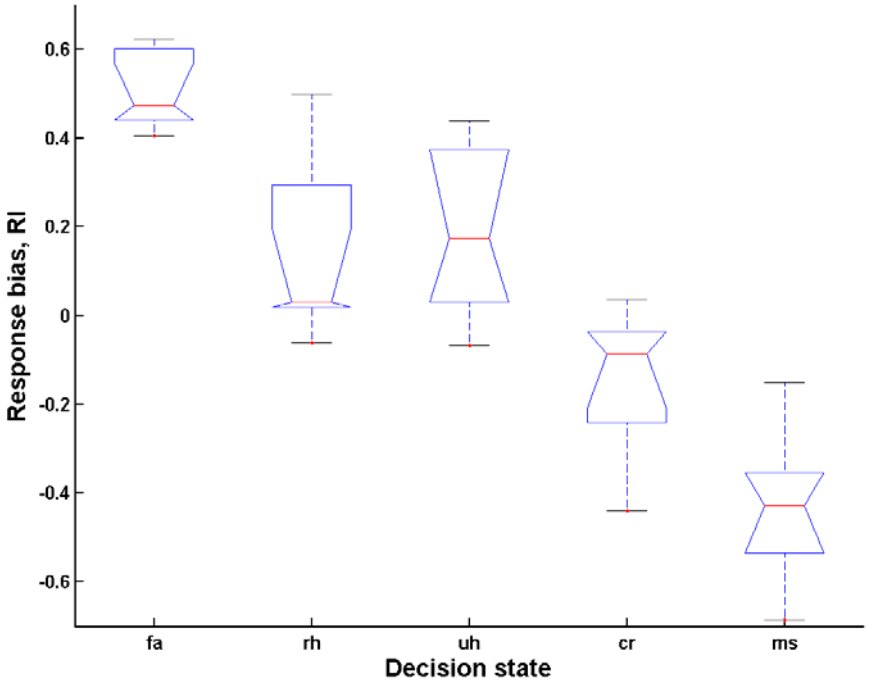

Fig.44. Response bias, RI for 5 decision states. All states were associated with different bias levels, excluding reinforced and unreinforced hits decision states. Unreinforced and reinforced hits were associated with similar decision states.

Performance was analyzed using a parametric detectability index d' (Green & Swets, 1966) and non-parametric detectability indices A' (Grier, 1971; Pollack & Norman, 1964) and SI (Frey & Colliver, 1973). Response bias indices were measured by non-parametric response bias indices B" (Grier, 1971; Hodos, 1970) and RI (Frey & Colliver, 1973). The computation formula for the relevant

indices, where h = hit rate and f = false alarm rate, are:

d' = z(f) – z(h), where z(.) is the z score or the normal deviate. (1)

$A' = 1/2 + [(h-f)(1+h-f)] / [4h(1-f)]$ (2)

$B'' = [h(1-h) - f(1-f)] / [h(1-h) + f(1-f)]$ (3)

$SI = [h-f] / [2(h+f) - (h+f)^2]$ (4)

$RI = [h+f-1] / [1-(h-f)^2]$ (5)

In conclusion, decision states can be identified by events occurring on previous trials. These events are the presence or absence of reinforcement after hits, false alarms, correct rejections, and misses. While reporting a signal, rats appear to make their decisions based on one of four different states as reflected in their associated response bias levels. Over a given session, rats constantly alter their response bias depending on events in their recent history. Response bias levels following reinforced hits are the same as bias levels that follow unreinforced hits. A variable ratio schedule produces high rate of response.

Appendix B

Optimization of running behavior in rats

Another set of experiments, which was termed the virtual learning paradigm, addressed the issue of reinforcement contingency relevant to brain stimulation. The performance of rats on various reinforcement schedules was compared.

The motion of rats under different Medial Forebrain Bundle (MFB – defined in Appendix A) reward schedules and parametric variations was investigated. In a self-stimulation task rats ran on a running wheel to obtain periodic MFB stimulation in the form of 3-pulse trains. The study measured changes in subjects running speed as a response to changing rewarding distances and strengths, to find optimum reinforcement schedules.

The results indicate that training increases speed of running for all conditions, indicating that rats can be trained for both distance and speed running. As was expected in accord with the theory of learning, a variable ratio schedule of reinforcement (reinforcement following 2 to 8 beam breaks) produced the best results. Naïve rats took more that two weeks of regular running to reach satisfactory physical conditioning so that they provided stable running data. Trained rats covered more than a kilometer distance during hour-long sessions.

A Matlab program was designed to deliver stimulation as well as to record all data. Stimulation parameters were set at a level producing clear rewarding effects (typically 10 one-ms pulses, 80μA, delivered at 100 Hz) and kept constant throughout the experiment. Rats were trained to run forward in a wheel under various reinforcement schedules: Fixed Ratio, Fixed Interval, and Variable Ratio. Under FIS rates were

reinforced exclusively when the wheel was turning; if the wheel was not in motion the count was stopped. This led to continuous running of animals. To establish comparable conditions between schedules the time to reward for each condition was established and those intervals were used for the FIS. For schedules FRS and FIS, a number of conditions were established: the minimal distance to reward – 25 cm (coded as 2 beam brakes) and maximal – 1m (coded as 8 beam breaks) with 12.5 cm steps; and the interval to reward which ranged from 1s to 4.25s with 0.25s increments. VR schedule range: 2bb to 10bb. To account for the effect of fatigue, sessions were broken up into periods of 5 min running and 5 min rest. To account for accumulative effect of MFB stimulation, conditions were presented in descending, ascending, and pseudorandom order.

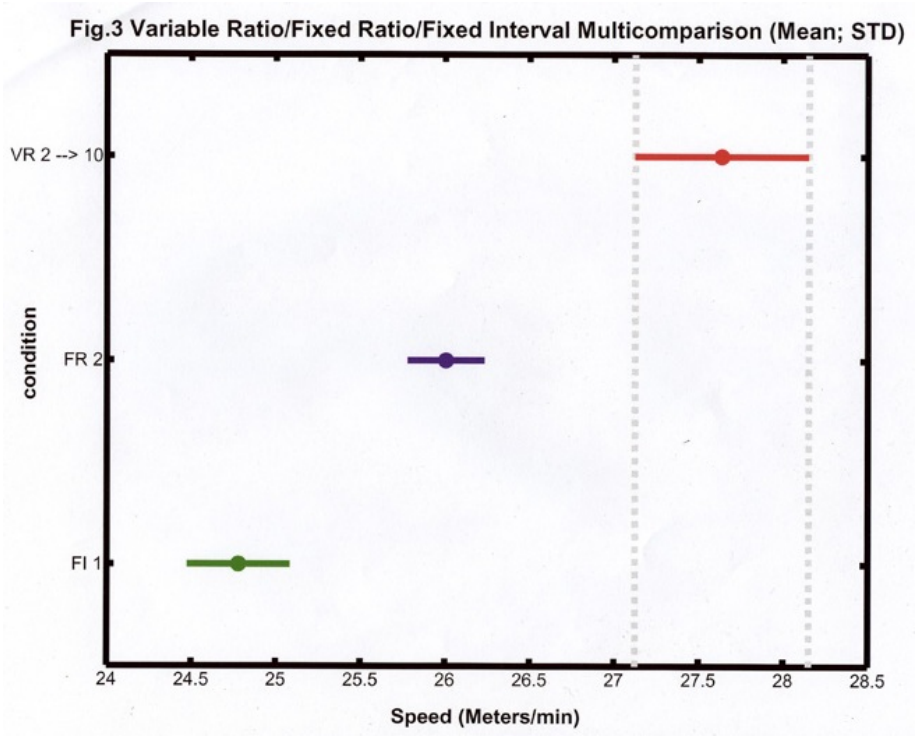

Fig. 45. The running speed of rats was compared across three conditions: Variable ratio, Fixed ratio, and Fixed interval reinforcement schedules. The VR schedule yielded the highest running speeds in all animals. The differences in running speeds between conditions are significant at $p<0.05$ level. The variability of the speed was highest for the VR condition.

Spontaneous running was also recorded.

The average running speed was compared across all 3 schedules, and only conditions producing highest speed were chosen for FRS and FIS (Fig.45). All three groups were tested with ANOVA and Scheffe test. The highest performance was achieved on VRS (Mean = 27.6 m/min; $p<0.05$); FRS was also significantly more efficient (Mean = 26 m/min); $p<0.05$); FIS showed lowest speed (Mean = 24.8; $p<0.05$).

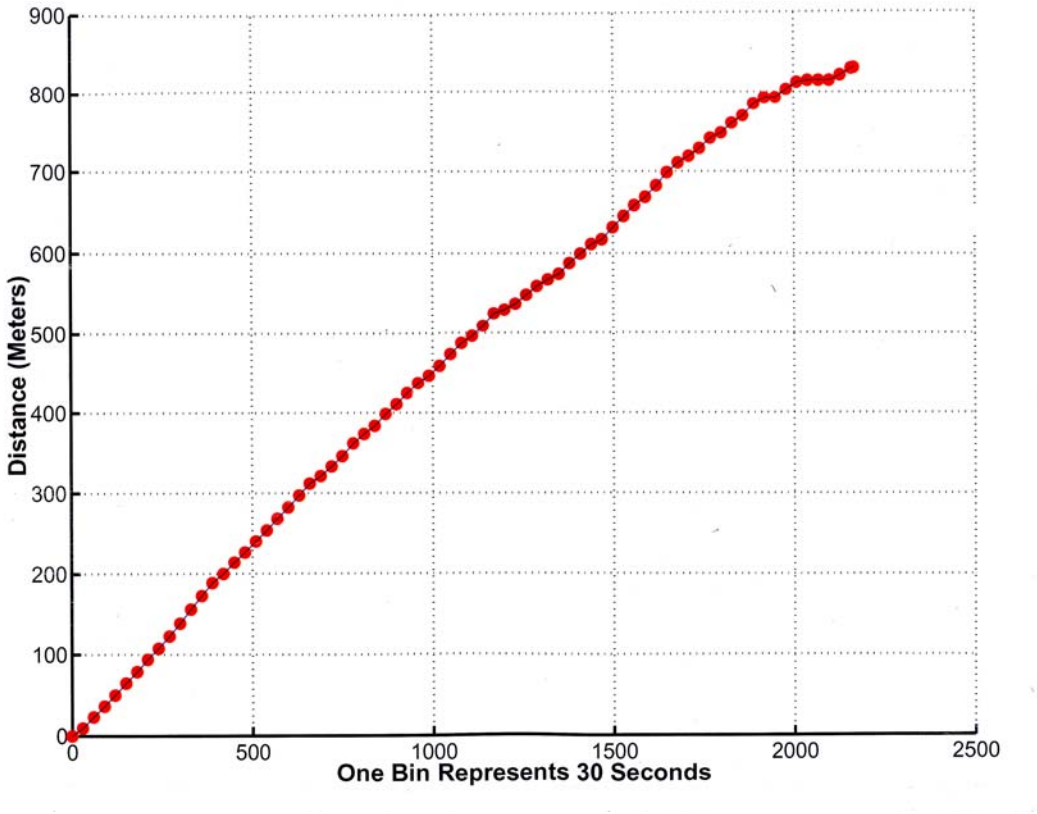

Fig. 46. All rat data for Variable Ratio condition was pooled. Distance was plotted against time. The slope indicates no significant decrease in the speed of running for up to 30 minutes. These results support previously obtained data on the response rates achieved under VR schedule from experiments using natural reinforcement such as food and water.

With training, speed of running increases for all conditions dramatically which indicates that rats can be trained for both distance and speed running. Varying the distance to reinforcement produces the best speed and distance results (Fig.46), as should be expected according to the theory of learning. Although reward density is not high, randomization secures presence of motivation.

These results indicate that Variable Ratio reinforcement schedule is appropriate to utilize in behavioral experiments involving natural and electrical rewarding stimulation (in the form of MFB stimulation). Characteristic properties of VR reinforcement show stability across many conditions.

These findings lend an additional support for the utilization of Variable Ratio schedule in behavioral experiments involving various types of stimulation: mechanical as well as electrical.

References

Agnew, W.F., Yuen, T.G., McCrrery, D.B., and Bullara, L.A. (1986). Histopathologic evaluation of prolonged intracortical electrical stimulation. *Exp. Neurol*., 92, 162.

Albe-Fessard D, Berkley KJ, Kruger L, Ralston HJ 3rd, Willis WD Jr. (1985). Diencephalic mechanisms of a sensation. *Brain Res*., 356(3), 217. Review.

Alegre M, Urriza J, Valencia M, Muruzabal J, Iriarte J, Artieda J. (2006). High-frequency oscillations in the somatosensory evoked potentials of patients with cortical myoclonus: pathophysiologic implications. *J. Clin. Neurophysiol*., 23(3), 265.

Allison T, McCarthy G, Wood CC, Darcey TM, Spencer DD, Williamson PD (1989) Human cortical potentials evoked by stimulation of the median nerve. I., Cytoarchitectonic areas generating short-latency activity. *J Neurophysiol.,* 62, 694.

Alloway KD, Burton H (1985a) Submodality and columnar organization of the second somatic sensory area in cats. *Exp Brain Res.,* 61, 128.

Alloway KD, Burton H (1985b) Homotypical ipsilateral cortical projections between somatosensory areas I and II in the cat. *Neuroscience*, 14, 15.

Alloway KD, Johnson MJ, Wallace MB (1993) Thalamocortical interactions in the somatosensory system: interpretations of latency and cross-correlation analyses. *J Neurophysiol.,* 70, 892.

Alloway KD, Wallace MB, Johnson MJ (1994) Cross-correlation analysis of cuneothalamic interactions in the rat somatosensory system: influence of receptive field topography and comparisons with thalamocortical interactions. *J Neurophysiol.,* 72, 1949.

Alloway KD, Johnson MJ, Aaron GB (1995) A comparative analysis of coordinated neuronal activity in the thalamic ventrobasal complex of rats and cats. *Brain Res.,* 691, 46.

Alloway KD, Zhang M, Dick SH, Roy SA. (2002). Pervasive synchronization of local neural networks in the secondary somatosensory cortex of cats during focal cutaneous stimulation. *Exp Brain Res*., 147(2), 227.

Andersen, R.A., Asanuma, C., Essick, G., and Siegel, R.M. (1990). Corticocortical connections of anatomically and physiologically defined subdivisions within the inferior parietal lobule, *J. Comp. Neurol.,* 296, 65.

Andersen, R.A., Snyder, L.H., Bradley, D.C., and Xing, J. (1997). Multimodal representation of space in posterior parietal cortex and its use in planning movements, *Annu. Rev. Neurosci*., 20, 303.

Anis N.A., Berry S.C., Burton N.R., Lodge D. (1983). The dissociative anesthetics, ketamine and phencyclidine, selectively reduce excitation of central mammalian neurons by N-methyl aspartate. *Br J Pharmacol* 79: 565-575.

Apkarian, A.V. and Shi, T. (1994). Squirrel monkey lateral thalamus. I. Somatic nociresponsive neurons and their relation to spinothalamic terminals, *J. Neurosci*., 14, 6779.

Aston-Jones, G., Rajkowski, J., Cohen, J., (2000). Locus coeruleus and regulation of behavioral flexibility and attention. *Prog. Brain Res*., 126, 165.

Backohja M., Arndt G., Gombar K.A., et al. (1994). Response to chronic neuropathic pain syndromes to ketamine: a preliminary study. *Pain,* 56, 51-57.

Babiloni C, Babiloni F, Carducci F, Cincotti F, Vecchio F, Cola B, Rossi S, Miniussi C, Rossini PM. (2004a). Functional frontoparietal connectivity during short-term memory as revealed by high-resolution EEG coherence analysis. *Behav Neurosci.,* 118(4), 687.

Babiloni C, Brancucci A, Arendt-Nielsen L, Del Percio C, Babiloni F, Pascual-Marqui R, Sabbatini G, Rossini PM, Chen ACN. (2004b). Cortical sensorimotor interactions during the expectancy of a go/nogo task: effects of painful stimuli. *Behav Neurosci.,* 118(5), 925.

Babiloni C, Brancucci A, Capotosto P, Arendt-Nielsen L, Chen ACN, Rossini PM. (2005a). Expectancy of pain is influenced by motor preparation: a high-resolution EEG study of cortical alpha rhythms. *Behav Neurosci.,* 119(2), 503.

Babilini C, Brancucci A, Vecchio F, Arendt-Nielsen L, Chen AC, Rossini PM. (2006). Anticipation of somatosensory and motor events increases centro-parietal functional coupling: an EEG coherence study. *Clin Neurophysiol*., 117(5), 1000.

BairW, Koch C, Newsome W, Britten K (1994) Power spectrum analysis of bursting cells in area MT in the behaving monkey. *J Neurosci.,* 14, 2870.

Barba C, Frot M, Mauguière F (2002) Early secondary somatosensory area (SII) SEPs. Data from intracerebral recordings in humans. *Clin Neurophysiol.,* 113, 1778.

Bennett RE, Ferrington DG, Rowe MJ (1980) Tactile neuron classes within second somato-sensory area (SII) of cat cerebral cortex. *J Neurophysiol.,* 43, 292.

Bentivoglio M, Molinari M, Minciacchi D, Macchi G (1983) Organization of the cortical projections of the posterior complex and intralaminar nuclei of the thalamus as studied by means of retrograde tracers. In: Macchi G, Rustioni A, Spreafico R (eds) *Somatosensory integration in the thalamus.* Elsevier, Amsterdam, pp 337–363.

Berman R.M. et al. (2000). Antidepressant effects of ketamine in depressed patients. *Biol. Psychiatry* 47, 351-354.

Berridge, C.W.,Waterhouse, B.D., (2003). The locus coeruleus-noradrenergic system: modulation of behavioral state and state-dependent cognitive processes. *Brain Res. Brain Res. Rev.*, 42, 33.

Boivie J., Leijon G.,. Johansson I. (1989). Central post-stroke pain: a study of the mechanisms through analysis of sensory abnormalities. *Pain*, 36, 173-185.

Bowsher D., Leijon G., Thuomas K.A. (1998). Central poststroke pain: correlation of MRI with clinical pain characteristics and sensory abnormalities. *Neurology*, 51, 1352-1358.

Britt G.C. and McCance-Katz E.F. (2005). A brief overview of the clinical pharmacology of “club drugs”. *Subs. Use Misuse*, 40, 1189-1201.

Burton H, Kopf EM (1984) Connections between the thalamus and the somatosensory areas of the anterior ectosylvian gyrus in the cat. *J Comp Neurol.*, 224, 173.

Burton H (1986) Second somatosensory cortex and related areas. In: Jones EG, Peters A (eds) *Cerebral cortex: sensory-motor areas and aspects of cortical connectivity*, vol. 5. Plenum, New York, pp 31–98.

Burton H, Robinson CJ (1987) Responses in the first or second somatosensory cortical area in cats during transient inactivation of the other ipsilateral area with lidocaine hydrochloride. *Somatosens Res.*, 4, 215.

Burton H, Fabri M (1995) Ipsilateral intracortical connections of physiologically defined cutaneous representations in areas 3b and 1 of macaque monkeys: projections in the vicinity of the central sulcus. *J Comp Neurol.*, 355, 508.

Burton H, Fabri M, Alloway K (1995) Cortical areas within the lateral sulcus connected to cutaneous representations in areas 3b and 1: a revised interpretation of the second somatosensory area in macaque monkeys. *J Comp Neurol.*, 355, 539.

Burton H, Sinclair R (1996) Somatosensory cortex and tactile perceptions. In: *Touch and pain* (Kruger L, ed.), pp. 105–177. London: Academic Press.

Bushnell MC, Duncan GH, Tremblay N. (1993). Thalamic VPM nucleus in the behaving monkey. I. Multimodal and discriminative properties of thermosensitive neurons. *J Neurophysiol*., 69(3), 739.

Carmena JM, Lebedev MA, Crist RE, O'Doherty JE, Santucci DM, Dimitrov DF, Patil PG, Henriquez CS, Nicolelis MA (2003) Learning to control a brain-machine interface for reaching and grasping by primates. *PLoS Biol*., 1, E42.

Carreras M, Andersson SA (1963) Functional properties of neurons of the anterior ectosylvian gyrus of the cat. *J Neurophysiol.,* 26, 100.

Carpenter W.T.J (1999). The schizophrenia ketamine challenge study debate. *Biol. Psychiatry,* 46, 1081-1091.

Carter A.J. (1995). Antagonists of the NMDA receptor-channel complex and motor coordination. *Life Science*, 57 (10), 917-929.

Cesaro P, Mann MW, Moretti JL, Defer G, Roualdes B, Nguyen JP, Degos JD. (1991). Central pain and thalamic hyperactivity: a single photon emission computerized tomographic study. *Pain*., 47(3), 329.

Chapin JK, Moxon KA, Markowitz RS, Nicolelis MA (1999) Real-time control of a robot arm using simultaneously recorded neurons in the motor cortex. *Nat Neurosci*., 2, 664.

Chapin JK, Nicolelis MA. (2001). Brain control of sensorimotor prosthesis. In *Neural Prosthesis for Restoration of Sensory and Motor Function*, ed. Chapin JK and Moxon KA, pp.235-259. CRC Press.

Chen G. (1965). Arch. Int. Pharmacodyn., 157, 193-201.

Corbetta, M., Shulman, G.L., (2002). Control of goal-directed and stimulus driven attention in the brain. *Nat. Rev., Neurosci.,* 3, 201.

Casey KL, Morrow TJ. (1983). Ventral posterior thalamic neurons differentially responsive to noxious stimulation of the awake monkey. *Science.*, 221(4611), 675.

Chhatbar, P.Y, VonKraus, L., Hawley, E., Francis, J.T., and Chapin, J.K. (2007). An apparatus for punctuate cutaneous stimulation of the arm and fingers of the bonnet macaque: implications for a fully integrated BMI, *Annu. Res Day*, Downstate, Poster.

JM, Lee KH, Surmeier DJ, Sorkin LS, Kim J, Willis WD. (1986). Response characteristics of neurons in the ventral posterior lateral nucleus of the monkey thalamus. *J Neurophysiol*., 56(2), 370.

Craig, A.D., Bushnell, M.C., Zhang, E.T., and Blomqvist, A. (1994). A thalamic nucleus specific for pain and temperature sensation, *Nature*, 372, 770.

Cusick, C.G., Steindler, D.A., and Kaas, J.H. (1985). Corticocortical and collateral thalamocortical connections of postcentral somatosensory cortical areas in squirrel monkeys: a double-labeling study with radiolabeled wheatgerm agglutinin and wheatgerm agglutinin conjugated to horseradish peroxidase, *Somatosens Res.*, 3, 1.

Darian-Smith C, Darian-Smith I, Burman K, Ratcliffe N (1993) Ipsilateral cortical projections to areas 3a, 3b, and 4 in the macaque monkey. *J Comp Neurol.,* 335, 200.

Darian-Smith, C., Darian-Smith, I., Burman, K., and Ratcliffe, N. (1993). Ipsilateral cortical projections to area 3a, 3b, and 4 in the macaque monkey, *J. Comp. Neurol.*, 335, 200.

Davis KD, Kiss ZH, Tasker RR, Dostrovsky JO. (1996). Thalamic stimulation-evoked sensations in chronic pain patients and in nonpain (movement disorder) patients. *J Neurophysiol*., 75(3), 1026.

Destexhe A, Contreras D, Steriade M. (1998). Mechanisms underlying the synchronizing action of corticothalamic feedback through inhibition of thalamic relay cells. *J.Neurophysiol.*,79(2), 999.

Disbrow E, Roberts T, Krubitzer L (2000) Somatotopic organization of cortical fields in the lateral sulcus of *Homo sapiens*: evidence for SII and PV. *J Comp Neurol.,* 418, 1.

Donoghue, J.P., Sanes., J.N., Hatsopoulos, N.G., and Gaal, G. (1998). Neural discharge and local field potential oscillations in primate motor cortex during voluntary movements. *J. Neurophysiol*., 79, 159.

Dougherty PM, Li YJ, Lenz FA, Rowland L, Mittman S. (1996). Evidence that excitatory amino acids mediate afferent input to the primate somatosensory thalamus. *Brain Res*., 29, 728(2), 267.

Downar, J., Crawley, A.P., Mikulis, D.J., Davis, K.D. (2000). A multimodal cortical network for the detection of changes in the sensory environment. *Nat. Neurosci*., 3, 277.

Drake, K.L., Wise, K.D., Farraye, J., Anderson, D.J., and Bement, S.L. (1988). Performance of planar multisite microprobes in recording extracellular single-unit intracortical activity. *IEEE Trans. Biomed. Eng*., 35, 719.

Duffy FH, Burchfiel JL (1971) Somatosensory system: organizational hierarchy from single units in monkey area 5. *Science* 172, 273.

Dykes RW, Gabor A (1981) Magnification functions and receptive field sequences for submodality-specific bands in SI cortex of cats. *J Comp Neurol.,* 202, 597.

Dykes RW, Sur M, Merzenich MM, Kaas JH, Nelson RJ. (1981). Regional segregation of neurons responding to quickly adapting, slowly adapting, deep and Pacinian receptors within thalamic ventroposterior lateral and ventroposterior inferior nuclei in the squirrel monkey (Saimiri sciureus). *Neuroscience*., 6(8), 1687.

Dykes, R.W., Rasmusson, D.D., Sretavan, D., and Rehman, N.B. (1982). Submodality segregation and receptive-field sequences in cuneate, gracile, and external cuneate nuclei of the cat, *J. Neurophysiol*., 47, 389.

Eide P.K., Stubhaug A., Stenehjem A.E. (1995). Central dysesthesia pain after traumatic spinal cord injury is dependant on N-methyl-D-aspartate receptor activation. *Neurosergery*, 37, 1080-1087.

Felleman DJ, Wall JT, Cusick CG, Kaas JH (1983) The representation of the body surface in S-I of cats. *J Neurosci.*, 8, 1648.

Felleman, D.J., Nelson, R.J., Sur, M., and Kaas, J.H. (1983b). Representations of the body surface in areas 3b and 1 postcentral parietal cortex of Cebus monkeys. *Brain Res*., 268, 15.

Ferrington DG, Rowe MJ (1980) Differential contributions to coding of cutaneous vibratory information by cortical somatosensory areas I and II. *J Neurophysiol.*, 43, 310.

Finck A.D., Ngai S.H. (1982). Opiate receptor mediation of ketamine analgesia. *Anesthesiology*, 56, 291-297.

Fisher GR, Freeman B, Rowe MJ (1983) Organization of parallel projections from Pacinian afferent fibers to somatosensory cortical areas I and II in the cat. *J Neurophysiol.*, 49, 75.

Fitzsimmons, N.A., Drake, W., Hanson, T.L., Lebedev, M.A., and Nicolelis, M.A.L. (2007). Primate reaching cued by multichannel spatiotemporal cortical microstimulation. *J. Neurosci.*, 27 (21) , 5593.

Florence, S.L., Wall, J.T., and Kaas, J.H. (1989) Somatotopic organization of inputs from the hand to the spinal gray and cuneate nucleus of monkeys with observations on the cuneate nucleus of humans, *J. Comp. Neurol.*, 286, 48.

Fogassi L, Luppino G. (2005). Motor functions of the parietal lobe. *Curr Opin Neurobiol.*, 15(6), 626.

Forss N, Hari R, Salmelin R, Ahonen A, Hämäläinen M, Kajola M, Knuutila J, Simola J (1994) Activation of the human posterior parietal cortex by median nerve stimulation. *Exp Brain Res.*, 99, 309.

Freitas R.M., Sousa F.C.F., Viana G.S.B., Fonteles M.M.F. (2006). Effect of gabaergic, glutamatergic, antipsychotic and antidepressant drugs on pilocarpine-induced seizures and status epilepticus. *Neurosci. Let.,* 408, 79-83.

Frey, P.W., & Colliver, J.A. (1973). Sensitivity and responsivity measures for discrimination learning. *Learning and Motivation*, 4: 327.

Frot M, Mauguière F (1999) Timing and spatial distribution of somatosensory responses recorded in the upper bank of the sylvian fissure (SII area) in humans. *Cereb Cortex*, 9, 854.

Gage P.W., Robertson B. (1985). Prolongation of inhibitory postsynaptic currents by pentobarbitone, halothane and ketamine in CA1 pyramidal cells in rat hippocampus. *Br J Pharmocol,* 85, 675-681.

Garraghty PE, Florence SL, Kaas JH (1990a) Ablations of areas 3a and 3b of monkey somatosensory cortex abolish cutaneous responsivity in area 1. *Brain Res.*, 528, 165.

Garraghty, PE, Florence SL, and Kaas, JH (1990b). Ablations of areas 3a and 3b of monkey somatosensory cortex abolish cutaneous responsivity in area 1, *Brain Res.*, 528, 165.

Ghosh S, Brinkman C, Porter R (1987) A quantitative study of the distribution of neurons projecting to the precentral motor cortex in the monkey (*M., fascicularis*). *J Comp Neurol.*, 259, 424.

Gomez CM, Vaquero E, Lopez-Mendoza D, Gonzalez-Rosa J, Vazquez- Marrufo M. (2004). Reduction of EEG power during expectancy periods in humans. *Acta Neurobiol Exp* (Wars), 64(2), 143.

Green, D.M., and Swets, J.A. (1966) *Signal Detection Theory and Psychophysics*, John Wiley, New York.

Green S.M. (1998). Intravenous ketamine for pediatric sedation in the emergency department: safety profile with 156 cases. *Acad. Emerg. Med.*, 5, 971-976.

Grier, J. B. (1971). Nonparametric indexes for sensitivity and bias: computing formulas. *Psychological Bulletin*, Vol. 75, (6): 424.

Gynther BD, Vickery RM, Rowe MJ (1995) Transmission characteristics for the 1:1 linkage between slowly adapting type II fibers and their cuneate target neurons in cat. *Exp Brain Res*.,105, 67.

Hanajima R, Chen R, Ashby P, Lozano AM, Hutchison WD, Davis KD, et al. Very fast oscillations evoked by median nerve stimulation in the human thalamus and subthalamic nucleus. *J Neurophysiol* ., 92, 3171.

Hand PJ, Morrison AR (1970) Thalamocortical projections from the ventrobasal complex to somatic sensory areas I and II. *Exp Neurol.*, 26, 291.

Harrison N.L and Simmonds M.A. (1985). Quantitative studies on some antagonists of N-methyl D-aspartate in slices in rat cerebral cortex. *Br. J. Pharmocol*. 84, 381-391.

Heath CJ, Hore J, Phillips CG (1976) Inputs from low threshold muscle and cutaneous afferents of hand and forearm to areas 3a and 3b of baboon's cerebral cortex. *J Physiol* (Lond)., 257, 199.

Hevers W., Hadley S.H., Luddens H., Amin, J. (2008). Ketamine, but not phencyclidine, selectively modulates cerebellar $GABA_A$ receptors containing $\alpha 6$ and δ subunits. *J of Neuroscience*, 28(20), 583-593.

Hirato M, Watanabe K, Takahashi A, Hayase N, Horikoshi S, Shibasaki T, Ohye C. (1994). Pathophysiology of central (thalamic) pain: combined change of sensory thalamus with cerebral cortex around central sulcus. *Stereotact Funct Neurosurg*., 62(1-4), 300.

Hirota K., Lambert D.G. (1996). Ketamine: its mechanisms of action and unusual clinical uses. *Br J Anesth*, 77, 441-444.

Hodos, W. (1970). Nonparametric index of response bias for use in detection and recognition experiments. *Psychological Bulletin*, Vol. 74, (5): 351.

Hoshiyama M, Kakigi R, Koyama S, Watanabe S, Shimojo M (1997) Activity in posterior parietal cortex following somatosensory stimulation in man: magnetoencephalographic study using spatiotemporal source analysis. *Brain Topogr*., 10, 23.

House PA, MacDonald JD, Tresco PA, Normann RA. (2006). Acute microelectrode array implantation into human neocortex: preliminary technique and histological considerations. *Neurosurg Focus*., 20(5), E4.

Huerta, M.F., and Pons, T.P. (1990). Primary motor cortex receives input from area 3a in macaques, *Brain Res.*, 537, 367.

Huffman, K.J., and Krubitzer, L. (2001). Area 3a: topographic organization and cortical connections, *Cereb Cortex*, 11(9), 849.

Hustveit O., Maurset A., Oye I. (1995). Interactions of the chiral forms of ketamine with opiods, phencyclidine, sigma and muscarinic receptors. *Pharmacol Toxicol*, 77, 355-359.

Hyvarinen J, Poranen A (1978) Receptive field integration and submodality convergence in the hand area of the post-central gyrus of the alert monkey. J *Physiol (Lond)*, 283, 539.

Iadarola MJ, Max MB, Berman KF, Byas-Smith MG, Coghill RC, Gracely RH, Bennett GJ. (1995). Unilateral decrease in thalamic activity observed with positron emission tomography in patients with chronic neuropathic pain. *Pain.*, 63(1), 55.

Inui K, Wang X, Tamura Y, Kameoke Y, Kakigi R. (2004). Serial processing in the human somatosensory system. *Cereb Cortex.*,14(8), 851.

Irifune M, Sato T, Kamata Y, Nishikawa T, Dohi T., Kawahar M. (2000). Evidence for $GABA_A$ receptor agonistic properties of ketamine: convulsive and anesthetic behavioral models in mice. *Anesth Analg,* 91, 230-236.

Ishijima B, Yoshimasu N, Fukushima T, Hore T, Sekino H, Sano K. (1975). Nociceptive neurons in the human thalamus. *Confin Neurol.,* 7(1-3), 99.

Iwamura Y, Tanaka M, Hikosaka O (1980) Overlapping representation of fingers in the somatosensory cortex (area 2) of the conscious monkey. *Brain Res*., 197, 516.

Iwamura Y, Tanaka M, Sakamoto M, Hikosaka O (1983) Converging patterns of finger representation and complex response properties of neurons in area 1 of the first somatosensory cortex of the conscious monkey. *Exp Brain Res.,* 51, 327.

Iwamura Y, Iriki A, Tanaka M (1994) Bilateral hand representation in the postcentral somatosensory cortex. *Nature*., 369, 554.

Iwamura Y (1998) Hierarchical somatosensory processing. *Curr Opin Neurobiol*., 8, 522.

Jain, N., Catania, K.C., and Kaas, J.H. (1997). Deactivation and reactivation of somatosensory cortex after dorsal spinal cord injury, *Nature*, 386, 495.

Jain, N., Catania, K.C., and Kaas, J.H. (1997). Deactivation and reactivation of somatosensory cortex after dorsal spinal injury, *Nature,* 386, 495.

Jain, N., Catania, K.C., and Kaas, J.H. (1998). A histologically visible representation of the fingers and palm in primate area 3b and its immutability following long-term deafferentations, *Cereb. Cortex*, 8, 227.

Jain, N., Florence, S.L., and Kaas, J.H. (1998b). Reorganization of somatosensory cortex after nerve and spinal cord injury. *News Physiol. Sci.*, 13, 143.

Jain, N., Qi, H-X., and Kaas, J.H. (2001). Long-term chronic multichannel recordings from sensorimotor cortex and thalamus of primates. In: *Advances in neural population coding,* Nicolelis, M.A.L., Ed., Elsevier, pp. 64-72.

Jain, N., Qi, H.-X., and Kaas, J.H. (2001a) Long-term chronic multichannel recordings from sensorimotor cortex and thalamus of primates, *Prog. Brain Res.,* 130, 64.

Jeanmonod D, Magnin M, Morel A. (1993). Thalamus and neurogenic pain: physiological, anatomical and clinical data. *Neuroreport.,* 4(5), 475.

Johnson MJ, Alloway KD (1994) Sensory modulation of synchronous thalamocortical interactions in the somatosensory system of the cat. *Exp Brain Res.,* 102, 181.

Johnson MJ, Alloway KD (1996) Cross-correlation analysis reveals laminar differences in thalamocortical interactions in the somatosensory system. *J Neurophysiol.,* 75, 1444.

Jones, EG and Powell, TPS (1970) Connexions of the somatic sensory cortex of the rhesus monkey. III. Thalamic connexions. *Brain,* 93, 37.

Jones, E.G. (1975). Lamination and differential distribution of thalamic afferents within the sensorimotor cortex of the squirrel monkey, *J. Comp. Neurol.*, 160, 167.

Kaas, J.H., Nelson, R.J., Sur, M., Lin, C.S., and Merzenich, M.M. (1979). Multiple representations of the body within the primary somatosensory cortex of primates, *Science,* 204, 521.

Kaas, J.H. (1983). What, if anything, is SI? Organization of first somatosensory area of cortex, *Physiol. Rev*., 63, 206.

Kaas, J.H. (1991). Plasticity of sensory and motor maps in adult mammals. Annu. Rev. *Neurosci*., 14, 137.

Kaas, J.H. (1997). Topographic maps are fundamental to sensory processing, *Brain Res. Bull*., 44, 107.

Kaas, J.H., Jain, N., Qi, H. (2002). The organization of the somatosensory system in primates, in *The somatosensory system,* Nelson, R.J., Ed., CRC Press, pp.1-25.

Karhu J, Tesche CD (1999) Simultaneous early processing of sensory input in human primary (SI) and secondary (SII) somatosensory cortices. *J Neurophysiol.,* 81, 2017.

Kazantsev VB, Nekorkin VI, Makarenko VI, Llinas R. (2004). Self-referential phase reset based on inferior olive oscillator dynamics. *Proc Natl Acad Sci.,* 101, 18183.

Kim U, McCormick DA. (1998). Functional and ionic properties of a slow afterhyperpolarization in ferret perigeniculate neurons in vitro. *J Neurophysiol*., 80(3), 1222.

Kiss ZH, Anderson T, Hansen T, Kirstein D, Suchowersky O, Hu B (2003) Neural substrates of microstimulation-evoked tingling: a chronaxie study in human somatosensory thalamus. *Eur J Neurosci.,* 18, 728.

Klimesch W. (1996). Memory processes, brain oscillations and EEG synchronization. *Int J Psychophysiol.,* 24(1–2), 61.

Klimesch W, Doppelmayr M, Schimke H, Pachinger T. (1996). Alpha frequency, reaction time, and the speed of processing information. *J Clin Neurophysiol.,* 13(6), 511.

Klimesch W. (1997). EEG-alpha rhythms and memory processes. *Int J Psychophysiol.,* 26(1–3), 319.

Klimesch W, Doppelmayr M, Russegger H, Pachinger T, Schwaiger J. (1998). Induced alpha band power changes in the human EEG and attention. *Neurosci Lett* .,244(2), 73.

Kohl B.K., Dannhardt, G. (2001). The NMDA receptor complex: a promising target for novel antiepileptic strategies. *Curr. Med. Chem*., 8, 1275-1289.

Kosar E, Hand PJ (1981) First somatosensory cortical columns and associated neuronal clusters of nucleus ventralis posterolateralis of the cat: an anatomical demonstration. *J Comp Neurol.,* 198, 515.

Koyama S, Katayama Y, Maejima S, Hirayama T, Fujii M, Tsubokawa T. (1993). Thalamic neuronal hyperactivity following transection of the spinothalamic tract in the cat: involvement of N-methyl-D-aspartate receptor. *Brain Res*., 28, 612(1-2), 345.

Krubitzer, L.A., and Kaas, J.H. (1990). The organization and connections of somatosensory cortex in marmosets, *J. Neurosci*., 10, 952.

Krubitzer, L.A. and Kaas, J.H. (1992). The somatosensory thalamus of monkeys: cortical connections and redefinition of nuclei in marmosets, *J. Comp. Neurol*., 319, 123.

Krubitzer L, Clarey J, Tweedale R, Elston G, Calford M (1995) A redefinition of somatosensory areas in the lateral sulcus of macaque monkeys. *J Neurosci.,* 15, 3821.
Qi HX, Lyon DC, Kaas JH (2002) Cortical and thalamic connections of the parietal ventral somatosensory area in marmoset monkeys (*Callithrix jacchus*). *J Comp Neurol.,* 443, 168
.

Lamme V.A., Zipser K., Spekreijse H. (1998). Figure-ground activity in primary visual cortex is suppressed by anesthesia. *Proc. Natl. Acad of Sci*., 95, 3263-3268.

Lebedev MA, Nicolelis MA (2006) Brain-machine interfaces: past, present and future. *Trends Neurosci*., 29, 536.

Lee SM, Ebner FF (1992) Induction of high frequency activity in the somatosensory thalamus of rats in-vivo results in long-term potentiation of responses in SI cortex. *Exp Brain Res.*, 90, 253.

Lenz FA, Tasker RR, Dostrovsky JO, Kwan HC, Gorecki J, Hirayama T, Murphy JT. (1987). Abnormal single-unit activity recorded in the somatosensory thalamus of a quadriplegic patient with central pain. *Pain.*, 31(2), 225.

Lenz FA, Kwan HC, Dostrovsky JO, Tasker RR. (1998). Characteristics of the bursting pattern of action potentials that occurs in the thalamus of patients with central pain. *Brain Res.*, 496(1-2), 357.

Lenz, FA, Gracely RH, Baker FH, Richardson RT, Dougherty PM. (1998). Reorganization of sensory modalities evoked by microstimulation in region of the thalamic principal sensory nucleus in patients with pain due to nervous system injury. *J Comp Neurol.*, 399(1), 125.

Levitt M (1991). Chronic dysesthesias of central neural origin in subhuman primates. In: *Deafferentation pain syndromes: pathophysiology and treatment* (Nashold BS, Ovelmen_levitt J, ed), New York: Raven Press., pp 229-238.

Lewis, J.W., and Van Essen, D.C. (2000). Mapping of architectonic subdivisions in the macaque monkeys with emphasis on parieto-occipital cortex, *J. Comp. Neurol*., 428, 79.

Lin, C.S., Merzenich, M.M., Sur, M., and Kaas, J.H. (1979). Connections of areas 3b and 1 of the parietal somatosensory strip with the ventroposterior nucleus in the owl monkey (*Aotus trivirgatus*), *J. Comp. Neurol.*, 185, 355.

Lin L.H., Chen L.L., Zirolli J.A., Harris R.A. (1992). General anesthetics potentiate gamma-aminobutyric acid actions on gamma aminobutyric acidA receptors expressed by

Lockhart E. (2004). Topical combination of amitriptyline and ketamine for postherpetic neuralgia. *J pain*, 5, S182.

Lynch M.E., Clark A.J., Sawyonok J., Sullivan M.J. (2005). Topical amitriptyline and ketamine in neuropathic pain syndromes: an open-label study. *The Journal of Pain*, 6(10), 644-649.

Maeng S., Zarate C.A. (2007). The role of glutamate in mood disorders: results from the ketamine in major depression study and the presumed cellular mechanism underlying its antidepressant effects. *Curr Psychiatry rep*., 9, 467-474.

Maeng S., Zarate C.A., Du J., Schloesser R.J., McCammon J., Chen G., et al (2008). Cellular mechanisms underlying the antidepressant effects of ketamine: role of alpha-amino-3-hydroxy-5-methylisoxazole-4-propionic acid receptors. *Biol Psychiatry*, 63, 349-352.

Maldijian, J.A., Gottschalk, A., Patel, R.S., Detre, J.A., and Alsop, D.C. (1999). The sensory somatotopic map of the human hand demonstrated at 4 Tesla, *Neuroimage.*, 10, 55.

Manji H.K., Moore G.J., Rajkowska G, Chen G. (2000). Neuroplasticity and cellular resilience in mood disorders. *Mol Psychiatry* 5, 578-593.

McCarthy G, Wood CC, Allison T (1991) Cortical somatosensory evoked potentials I., Recordings in the monkey *Macaca fascicularis*. *J Neurophysiol.,* 66, 53.

McCormick, D.A., Pape, H.C.,Williamson, A.(1991). Actions of norepinephrine in the cerebral cortex and thalamus: implications for function of the central noradrenergic system. *Prog. Brain Res.*, 88, 293.

MacDonald J.F., Miljkoviv Z., Pennefather P. (1987). Use-dependent block of excitatory amino acid currents in cultured neurons by ketamine. *J Neyrophysiology*, 58, 251-266.

MacDonald J.F., Bartlett M.C., Mody I., Pahapill P., Reynolds J.N., Salter M.W., Schnederman J.H., Pennefather P.S. (1991). Actions of ketamine, phencyclidine and MK-801 on NMDA receptor currents in cultured mouse hippocampal neurons. *J Physiol* (London), 432, 483-508.

McKenna TM, Whitsel BL, Dreyer DA, Metz CB (1981) Organization of cat anterior parietal cortex: relations among cytoarchitecture, single neuron functional properties, and interhemispheric connectivity. *J Neurophysiol.,* 45, 667.

Merzenich, M.M., Kaas, J.H., Sur, M., and Lin, C.S. (1978). Double representation of the body surface within cytoarchitectonic areas 3b and 1 in SI in the owl monkey (Aotus trivirgatus), *J. Comp. Neurol.*, 181, 41.

Merzenich, M.M., Kaas, J.H., Wall, J., Nelson, R.J., Sur, M., and Felleman, D (1983). Topographic reorganization of somatosensory cortical areas 3b and 1 in adult monkeys following restricted deafferentation. *Neuroscience*, 8, 33.

Metherate R, Dykes RW (1985) Simultaneous recordings from pairs of cat somatosensory cortical neurons with overlapping peripheral receptive fields. *Brain Res.,* 341, 119.

Mima T, Ikeda A, Nagamine T, Yazawa S, Kunieda T, Mikuni N, Taki W, Kimura J, Shibasaki H (1997) Human second somatosensory area: subdural and magnetoencephalographic recording of somatosensory evoked responses. *J Neurol Neurosurg Psychiatry*, 63, 501.

Mogghadda B., Adams B., Verma A., Daly D. (1997). Activatio of glutamatergic neurotransmission by ketamine: a novel step in the pathway from NMDA receptor blockade to dopaminergic and cognitive disruptions associated with prefrontal cortex. *J. Neirosci*, 17, 2921-2929.

Mountcastle, V.B. (2005). *The sensory hand*. Harvard University Press, pp.1-133.
Coq, J.-O., Strata, F., Caroni, P., and Kaas., J.H. (2000) Somatotopic organization of cuneatus and gracilis nuclei in the brainstem of primates, *Soc. Neurosci. Abstrs*., 26, 148.

Moxon KA, Kalkhoran NM, Markert M, Sambito MA, McKenzie JL, Webster JT. (2004). Nanostructured surface modification of ceramic-based microelectrodes to enhance biocompatibility for a direct brain-machine interface. *IEEE Trans Biomed Eng.*, 51(6), 881.

Murthy VN, Fetz EE (1996a) Oscillatory activity in sensorimotor cortex of awake monkeys: synchronization of local field potentials and relation to behavior. *J Neurophysiol.*, 76, 3949.

Murthy VN, Fetz EE (1996b) Synchronization of neurons during local field potential oscillations in sensorimotor cortex of awake monkeys. *J Neurophysiol.*, 76, 3968.

Muthuswamy J, Tran P, Rangarajan R, Lenz FA, Hanley DF, Thakor NV. (1999). Somatosensory stimulus entrains spindle oscillations in the thalamic VPL nucleus in barbiturate anesthetized rats. *Neurosci Lett*., 262(3), 191.

Nelson, R.J., Sur, M., Felleman, D.J., and Kaas, J.H. (1980). Representations of the body surface in postcentral parietal cortex of *Macaca fascicularis, J. Comp. Neurol.*, 192, 611.

Nelson RJ, Kaas JH (1981) Connections of the ventroposterior nucleus of the thalamus with the body surface representations in cortical areas 3b and 1 of the cynomolgus macaque (*Macaca fascicularis*). *J Comp Neurol.*, 199, 29.

Nicolelis, M.A., Lin, R.C.S., Woodward, D.J., and Chapin, J.K. (1993). Induction of immediate spatiotemporal changes in thalamic networks by peripheral block of ascending cutaneous information. *Nature*, 361, 533.

Nicolelis, M.A., and Chapin, J.K. (1994). Spatiotemporal structure of somatosensory responses of many-neuron ensembles in the rat ventral posterior medial nucleus of thalamus. *J. Neurosci*., 14, 3511.

Nicolelis, M.A., Baccala, L.A., Lin, R.C., and Chapin, J.K. (1995). Sensorimotor encoding by synchronous neural ensemble activity in multiple levels of the somatosensory system. *Science*, 286, 1353.

Nicolelis, M.A., Ghazanfar, A.A., Stambaugh, C.R., Oliviera, L.M., Laubach, M., Chapin, J.K., Nelson, R.J., and Kaas, J.H. (1998). Simultaneous encoding of tactile information by three primate cortical areas. *Nat. Neurosci*., 1, 621.

Nicolelis MA, Ghazanfar AA, Stambaugh CR, Oliveira LM, Laubach M, Chapin JK, Nelson RJ, Kaas JH (1998) Simultaneous encoding of tactile information by three primate cortical areas. *Nat Neurosci.*, 7, 621.

Nicolelis MA, Fanselow EE. (2002). Dynamic shifting in thalamocortical processing during different behavioural states. *Philos Trans R Soc Lond B Biol Sci*. 29; 357(1428), 1753. Review.

Nicolelis MA, Dimitrov D, Carmena JM, Crist R, Lehew G, Kralik JD, Wise SP. (2003). Chronic, multisite, multielectrode recordings in macaque monkeys. *Proc Natl Acad Sci U* S A, 16, 100(19), 11041.

Nordhausen, C.T., Maynard, E.M., and Norman, R.A. (1996). Single unit recording capabilities of a 100 microelectrode array. *Brain Res.*, 726, 129.

Normann RA. (2007). Technology Insight: future neuroprosthetic therapies for disorders of the nervous system. *Nat Clin Pract Neurol.*, 3(8), 444.

Nowak LG, Munk MH, Nelson JI, James AC, Bullier J (1995) Structural basis of cortical synchronization. I. Three types of interhemispheric coupling. *J Neurophysiol.*, 74, 2379.

Nunez A, Panetsos F, Avendano C (2000) Rhythmic neuronal interactions and synchronization in the rat dorsal column nuclei. *Neuroscience.*, 100, 599.

Ohara S, Weiss N, Lenz FA (2004) Microstimulation in the region of the human thalamic principal somatic sensory nucleus evokes sensations like those of mechanical stimulation and movement. J Neurophysiol., 91, 736.

Olds, J., and Milner, P.M. (1954). Positive reinforcement produced by electrical stimulation of septal area and other regions of rat brain. *J. Comp. Physiol. Psychol.*, 47, 419.

Olds, M.E., and Fobes, J.L. (1981). The central basis of motivation: intracranial self-

stimulation studies. *Annu Rev. Psychol.*, 32, 523.

Penfield W, Boldrey E (1937) Somatic motor and sensory representation in the cerebral cortex of man as studied by electrical stimulation. *Brain.,* 60, 389.

Perry E.B. (2007). Psychiatric safety of ketamine in psychopharmacology research. *Psychopharmacology*, 192, 253-260.

Petersen, R.S., and Diamond, M.E. (2001). Topographic maps in the brain, In: *Encyclopedia of life sciences,* Macmillan.

Pfurtscheller G, Lopes da Silva FH. (1999). Event-related EEG/MEG synchronization and desynchronization: basic principles. *Clin Neurophysiol.*, 110(11), 1842.

Pinto DJ, Brumberg JC, Simons DJ (2000). Circuit dynamics and coding strategies in rodent somatosensory cortex. *J Neurophysiol*., 83(3), 1158.

Ploner M, Gross J, Timmermann L, Pollok B, Schnitzler A. (2006). Oscillatory activity reflects the excitability of the human somatosensory system. *Neuroimage.*, 32(3), 1231.

Pollack, I., and Norman, D. A. (1964). A non-parametric analysis of recognition experiments. *Psychonometric Science*, 1: 125.

Pons, T.P., Garraghty, P.E., Cusick, C.G., and Kaas, J.H. (1985). The somatotopic organization of area 2 in macaque monkeys, *J. Comp. Neurol*., 241, 445.

Pons, T.P., and Kaas, J.H. (1985). Connections of area 2 of somatosensory cortex with the anterior pulvinar and subdivisions of the ventroposterior complex in macaque monkeys, *J. Comp. Neurol*., 240, 16.

Pons TP, Garraghty PE, Friedman DP, Mishkin M (1987) Physiological evidence for serial processing in somatosensory cortex. *Science.,* 237, 417.

Pons, T.P., Garraghty, P.E., Ommaya, A.K., Kaas, J.H., Taub, E., and Mishkin, M. (1991). Massive cortical reorganization after sensory deafferentation in adult macaques. *Science*, 252, 1857.

Pons TP, Garraghty PE, Mishkin M (1992) Serial and parallel processing of tactual information in somatosensory cortex of rhesus monkeys. *J Neurophysiol*., 68, 518.

Populin L.C. (2005). Anesthetics change the excitation/inhibition balance that governs sensory processing in the cat superior colliculus. *J. of Neurosci*., 25(25), 5903-5914.

Quirk, M.C., and Wilson, M.A (1999). Interaction between spike waveform classification and temporal sequence detection, *J. Neurosci.Methods*, 94, 41.

Rappelsberger P, Petsche H. (1988). Probability mapping: power and coherence analyses of cognitive processes. *Brain Topogr.*, 1(1), 46.

Rausell, E., and Jones, E.G.(1991a). Hisochemical and immunocytochemical compartments of the thalamic VPM nucleus in monkeys and their relationship to the representational map, *J. Neurosci*., 11, 210.

Rausell, E. and Jones, E.G. (1991b). Chemically distinct compartments of the thalamic VPM nucleus in monkeys relay principal and spinal trigeminal pathways to different layers of the somatosensory cortex, *J. Neurosci*., 11, 226.

Rausell E, Bae CS, Vinuela A, Huntley GW, Jones EG. (1992). Calbindin and parvalbumin cells in monkey VPL thalamic nucleus: distribution, laminar cortical projections, and relations to spinothalamic terminations. *J Neurosci.*, 1;12(10), 4088.

Rausell E, Cusick CG, Taub E, Jones EG. (1992). Chronic deafferentation in monkeys differentially affects nociceptive and nonnociceptive pathways distinguished by specific calcium-binding proteins and down-regulates gamma-aminobutyric acid type A receptors at thalamic levels. *Proc Natl Acad Sci.*, 1, 89(7), 2571.

Recanzone, G. H., Jenkins, W. M., Hradek, G. T., and Merzenich, M. M. (1992a) Progressive improvement in discriminative abilities in adult owl monkeys performing a tactile frequency discrimination task. *J. Neurosci*., 67, (5): 1015.

Recanzone, G. H., Merzenich, M. M, Jenkins, W. M., Grajski, K.A., and Dinse, H.R. (1992b) Topographic reorganization of the hand representation in cortical area 3b of Owl monkeys trained in a frequency-discrimination task. *J. Neurosci*., 67, (5): 1031.

Recanzone, G. H., Merzenich, M. M, and Jenkins, W.M. (1992c) Frequency discrimination training engaging a restricted surface results in an emergence of a cutaneous response zone in cortical area 3a. *J. Neurosci*., 67, (5): 1057.

Recanzone, G. H., Merzenich, M. M, and Schreiner, C.E. (1992d). Changes in the distributed temporal response properties of SI neurons reflect improvements in performance on a temporally based tactile discrimination task. *J. Neurosci*., 67, (5): 1071.

Recanzone, G.H., Merzenich, M.M., and Dinse, H.R. (1992e). Expansion of the cortical representation of a specific skin field in primary somatosensory cortex by intracortical microstimulation. *Cerebral Cortex*, 2: 181.

Rennaker R.L., Carey H.L., Anderson S.E., et al. (2006). Anesthesia suppresses nonsynchronous responses to repetitive broadband stimuli. *Neuroscience*, 145, 357-369.

Rodin BE, Kruger L. (1984). Deafferentation in animals as a model for the study of pain: an alternative hypothesis. *Brain Res.*, 319(3), 213. Review.

Rojas M.J., Navas J.A., Rector D.M. (2006). Evoked response potential markers for anesthetic and behavioral states. *Am. J. Physiol. Regul. Integr. Comp. Physiol*., 291, R189-R196.

Romo, R., Hernandez, A., Zainos, A., and Salinas, E. (1998). Somatosensory discrimination based on cortical microstimulation, *Nature*, 392, 387.

Romo, R., Hernandez, A., Zainos, A., Brody, C.D., and Lemus, L. (2000). Sensing without touching: psychophysical performance based on cortical microstimulation, *Neuron*, 26, 273.

Rowe MJ, Turman AB, Murray GM, Zhang HQ (1996) Parallel organization of somatosensory cortical areas I and II for tactile processing. *Clin Exp Pharmacol Physiol.*, 23, 931.

Roy SA, Alloway KD (1999) Synchronization of local neural networks in the somatosensory cortex: a comparison of stationary and moving stimuli. *J Neurophysiol.*, 81, 999.

Roy SA, Alloway KD (2001) Coincidence detection or temporal integration? What the neurons in somatosensory cortex are doing. *J Neurosci.*, 21, 2462.

Roy SA, Dear SP, Alloway KD (2001) Long-range synchronization without concomitant oscillations in the somatosensory system of anesthetized cats. *J Neurosci.*, 21, 1795.

Rozenboym AV, Xu S, Von Kraus L, Semework M, Francis JT, Chapin JK. (2005). Neuronal Ensemble Representation of Cutaneous Stimuli in the Somatosensory Cortex of Awake and Anaesthetized Macaques. *Society for Neuroscience Conference,* Washington DC.

Rozenboym AV, Xu S, Von Kraus L, Semework M, Chhatbar PY, Francis JT, Chapin JK. (2006). Microstimulation in Somatosensory Thalamus Elicits Naturalistic Responses in Cortical Networks. *Society for Neuroscience Conference,* San Diego CA.

Sakata H, Takaoka Y, Kawarasaki A, Shibutani H (1973) Somatosensory properties of neurons in superior parietal cortex (area 5) of the rhesus monkey. *Brain Res.*, 64, 85.

Salvadore G., Cornwell B.R., Colon-Rosario V., Coppola R., Grillon C., Zarate C.A., Manji H.K. (2008). Increased anterior cingulated cortical activity in response to fearful faces: a neurophysiological biomarker that predicts rapid antidepressant response to ketamine. *Biol. Psychiatry*, xx:xxx.

Sanacora S., Zarate C.A., Krystal J.H., Manji H.K. (2008). Targeting the glutamatergic system to develop novel, improved therapeutics for mood disorders. *Nature Reviews*, 7, 426-437.

Saporta S, Kruger L (1979) The organization of projections to selected points of somatosensory cortex from the cat ventrobasal complex. *Brain Res.,* 178, 275.

Schmidt, E.M., Bak, M.J., and McIntosh, J.S. (1976). Long-term chronic recordings from cortical neurons. *Exp. Neurol.,* 52, 496.

Schott G.D. (1995). From thalamic syndrome to central pain poststroke pain. *J Neurol Neurosurg Psychiatry*, 61, 560-564.

Shadlen MN, Movshon JA (1999) Synchrony unbound: a critical evaluation of the temporal binding hypothesis. *Neuron,* 24, 67.

Sheller M., Bufler J., Hertle I., Schneck H.J., Franke C., Kochs E. (1996). Ketamine blocks currents through mammalian nicotinic acetylcholine receptor channels by interaction with both the open and the closed state. *Anesth Analg*, 83, 830-836.

Sherman SE, Luo L, Dostrovsky JO. (1997). Altered receptive fields and sensory modalities of rat VPL thalamic neurons during spinal strychnine-induced allodynia. *J Neurophysiol*., 78(5), 2296.

Singer, W. (1999). Neuronal synchrony: a versatile code for the definition of relations? *Neuron*, 24:49-65, 111-125.

Spreafico R, Hayes NL, Rustioni A (1981) Thalamic projections to the primary and secondary somatosensory cortices in cat: single and double retrograde tracer studies. *J Comp Neurol.,* 203, 67.

Stepniewska I, Sakai ST, Qi H, Kaas JH (2003) Somatosensory input to the ventrolateral thalamic region in the macaque monkey: a potential substrate for parkisonian tremor. *J Comp Neurol.,* 455, 378

Steriade M, Tomofeev I, Grenier F, Durmuller N. (1998). Role of thalamic and cortical neurons in augmenting responses and self-sustained activity: dual intracellular recordings in vivo. *J Neurosci*., 18(16), 6425.

Sur M (1980) Receptive fields of neurons in areas 3b and 1 of somatosensory cortex in monkeys. *Brain Res*., 198, 465.

Sur, M., Nelson, R.J., and Kaas, J.H. (1982). Representations of the body surface in cortical areas 3b and 1 of squirrel monkeys: comparison with other primates, *J. Comp. Neurol.*, 211, 177.

Sur., M., Wall, J.T., and Kaas, J.H. (1984), Modular distribution of neurons with slowly adapting and rapidly adapting responses in area 3b of somatosensory cortex in monkeys, *J. Neurophysiol*., 51, 724.

Sur M, Garraghty PE, Bruce CJ (1985) Somatosensory cortex in macaque monkeys: laminar differences in receptive field size in areas 3b and 1. *Brain Res.*, 342, 391.

Swadlow HA (1995) Influence of VPM afferents on putative inhibitory interneurons in S1 of the awake rabbit: evidence from cross-correlation, microstimulation, and latencies to peripheral sensory stimulation. *J Neurophysiol.,* 73, 1584.

Swadlow HA, Beloozerova IN, Sirota MG (1998) Sharp, local synchrony among putative feed-forward inhibitory interneurons of rabbit somatosensory cortex. *J Neurophysiol.,* 79, 567.

Swadlow HA, Gusev AG. (2001). The impact of 'bursting' thalamic impulses at a neocortical synapse. *Nat Neurosci.*, 4(4), 402.

Talwar, S.K., & Gerstein, G.L. (1998) .Auditory frequency discrimination in the white rat. *Hear. Res*., 126: 135.

Talwar, S.K., and Gerstein, G.L. (1999) .A signal detection analysis of frequency discrimination in the rat. *J. Acoust. Soc. Am*., 105, (3), 1784.

Talwar, S.K. Xu, S., Hawley, E.S., Weiss, S.A., Moxon, K.A., and Chapin, J.K. (2002). Rat navigation guided by remote control. *Nature*, 417, 37.

Tasker RR (1991). Deafferenation pain syndromes: introduction. In: *Deafferenation pain syndromes: pathophysiology and treatment* (Nashold BS, Ovelmen Llevitt J, ed), New York:Raven Press, pp 241-257.

Temereanca S, Simons DJ. (2003). Local field potentials and the encoding of whisker deflections by population firing synchrony in thalamic barreloids. *J Neurophysiol.*, 89(4), 2137.

Tomoffev I, Steriade M. (1998). Cellular mechanisms underlying intrathalamic augmenting responses of reticular and relay neurons. *J Neurophysiol.,* 79(5), 2716.

Tomberg C, Desmedt JE. (1999). Failure to recognize objects by active touch (astereognosia) results from lesion of parietal-cortex representation of finger kinaesthesis. *Lancet*, 354(9176), 393.

Tremblay N, Bushnell MC, Duncan GH. (1993). Thalamic VPM nucleus in the behaving monkey. II. Response to air-puff stimulation during discrimination and attention tasks. *J Neurophysiol*., 69(3),753.

Trivedi M.H., Rush, A.J., Wisniewski S.R., Nierenberg A.A., Warden D., Ritz L., et al. (2006). Evaluation of outcomes with citalopram for depression using measurement-based care in STAR*D: Implications for clinical practice. *Am. J. Psychiatry*, 163:28-40.

Turman AB, Morley JW, Zhang HQ, Rowe MJ (1995) Parallel processing of tactile information in cat cerebral cortex: effect of reversible inactivation of SII on SI responses. *J. Neurophysiol.,* 73, 1063.

Turman AB, Ferrington DG, Ghosh S, Morley JW, Rowe MJ (1992) Parallel processing of tactile information in the cerebral cortex of the cat: effect of reversible inactivation of SI on responsiveness of SII neurons. *J Neurophysiol.,* 67, 411.

Varela F, Lachaux JP, Rodriguez E, Martinerie J. (2001). The brainweb: phase synchronization and large-scale integration. *Nat Rev Neurosci.,* 2, 229.

Vickery RM, Gynther BD, Rowe MJ (1994) Synaptic transmission between single slowly adapting type I fibers and their cuneate target neurons in cat. *J Physiol.,* 474, 379.

Vierck CJ Jr, Hamilton DM, Thornby JI. (1971). Pain reactivity of monkeys after lesions to the dorsal and lateral columns of the spinal cord. *Exp Brain Research,* 13(2), 140.

Vierck CJ Jr, Greenspan JD, Ritz LA. (1990). Long-term changes in purposive and reflexive responses to nociceptive stimulation following anterolateral chordotomy. J Neurosci., 10(7), 2077.

Vierck CJ Jr. (1998). Impaired detection of repetitive stimulation following interruption of the dorsal spinal column in primates, Somatosens Mot Res., 15(2), 157.

Vogt BA, Pandya DN (1978) Cortico-cortical connections of somatic sensory cortex (areas 3, 1 and 2) in the rhesus monkey. *J Comp Neuro.,l* 177, 179.

Warren RA, Agmon A, Jones EG. (1994). Oscillatory synaptic interactions between ventroposterior and reticular neurons in mouse thalamus in vitro. *J Neurophysiol*., 72(4), 1993.

Wehr M., Zador A.M. (2005). Synaptic mechanisms of forward suppression in rat auditory cortex. *Neuron*, 47, 437-445.

Weng HR, Lee JI, Lenz FA, Schwartz A, Vierck C, Rowland L, Dougherty PM. (2000). Functional plasticity in primate somatosensory thalamus following chronic lesion of the ventral lateral spinal cord. *Neuroscience,*101(2), 393.

Weng HR, Lenz FA, Vierck C, Dougherty PM. (2003). Physiological changes in primate somatosensory thalamus induced by deafferentation are dependent on the spinal funiculi that are sectioned and time following injury, *Neuroscience,* 116(4),1149.

Wessberg J, Stambaugh CR, Kralik JD, Beck PD, Laubach M, Chapin JK, Kim J, Biggs SJ, Srinivasan MA, Nicolelis MA (2000) Real-time prediction of hand trajectory by ensembles of cortical neurons in primates. *Nature.*, 408, 361.

Willis W.D. Jr. (1985) The pain system. The neural basis of nociceptive transmission in the mammalian nervous system, *Pain Headache*., 8, 1-346.

Wood CC, Cohen D, Cuffin BN, Yarita M, Allison T (1985) Electrical sources in human somatosensory cortex: identification by combined magnetic and potential recordings. *Science,* 227, 1051.

Woolsey CN. (1958). Organization of somatic sensory and motor areas of cerebral cortex. In *Biological and Biochemical Bases of Behavior*, ed. Harlow HF and Woolsey CN, pp.63-81. Madison: University of Wisconsin Press.
Woolsey CN, Marshall WH, Bard P. (1942). Representation of cutaneous tactile sensibility in the cerebral cortex of the monkey as indicated by evoked potentials. *Bull. Johns Hopkins Hosp.* 70: 399-441.

Xu, S., Talwar, S.K., Hawley, E.S., Li, L., and Chapin, J.K. (2004). A multi-channel telemetry system for brain microstimulation in freely roaming animals. *J. Neurosci.* Methods, 133, 57.

Yamamoto T., Katayama Y., Hirayama T, et al. (1997). Pharmacological classification of central poststroke pain: comparison with the results of chronic motor cortex stimulation. *Pain*, 75, 5-12.

Zachariah MK, Coleman GT, Mahns DA, Zhang HQ, Rowe MJ (2001) Transmission security for single, hair follicle-related tactile afferent fibers and their target cuneate neurons in cat. *J Neurophysiol.*, 86, 900.

Zacksenhause M, Lebedev MA, Carmena JM, O'Doherty JE, Henriquez C, Nicolelis MA. (2007). Cortical modulations increase in early sessions with brain-machine interface. *PLos One*, 2 (7): e619.

Zarate C.A., Quiroz J., Payne J., Manji H.K. (2002). Modulators of glutamatergic system: implications for the development of improved therapeutics in mood disorders. *Psychopharmacol Bull.*, 36, 35-83.

Zarate C.A., et al. (2003). Regulation of cellular plasticity cascades in the pathophysiology and treatment of mood disorders: role of glutamatergic system. *Ann NY Ac. Sci*., 1003, 273-291.

Zarate C.A., et al. (2006). A randomized trial of an N-methyl-D-aspartate antagonist in treatment-resistant major depression. *Arch. Gen. Psychiatry*, 63, 856-864.

Zarate C.A., Charney D.S., Manjii H.K. (2007). Searching for rational anti-N-methyl-D-aspartate treatment for depression. *Arch. Gen. Psychiatry*, 64, 1100-1101.